

**A NUMERICAL AND EXPERIMENTAL STUDY OF
THERMAL PERFORMANCE OF PACKED BED
THERMAL ENERGY STORAGE (PBTES) SYSTEM**

**A Thesis Submitted To The
*University of Petroleum and Energy Studies***

For the award of
Doctor of Philosophy
in
Mechanical Engineering

BY
Ram Kunwer

November 2021

SUPERVISOR
Dr. Shyam Pandey



**Department of Mechanical Engineering
School of Engineering
University of Petroleum and Energy Studies
Dehradun-248007; Uttarakhand**

**A NUMERICAL AND EXPERIMENTAL STUDY OF
THERMAL PERFORMANCE OF PACKED BED
THERMAL ENERGY STORAGE (PBTES) SYSTEM**

**A Thesis Submitted To The
University of Petroleum and Energy Studies**

**For the award of
Doctor of Philosophy
in
Mechanical Engineering**

**BY
Ram Kunwer
(SAP ID 500049712)**

November 2021

Internal Supervisor

**Dr. Shyam Pandey
Professor**

**Department of Mechanical Engineering
University of Petroleum and Energy Studies**



**Department of Mechanical Engineering
University of Petroleum and Energy Studies
Dehradun-248007; Uttarakhand**

November 2021

DECLARATION

I declare that the thesis entitled “**Characteristic analysis of packed bed solar thermal energy storage (TES) system using synthetic oil as a Heat Transfer Fluid (HTF) for concentrated solar power application (CSP)**” has been prepared by me under the guidance of Dr. Shyam Pandey, Professor of Mechanical engineering, University of Petroleum and Energy Studies, Dehradun. No part of this thesis has formed the basis for the award of any degree or fellowship previously.



Ram Kunwer

Department of Mechanical Engineering,
University of Petroleum and Energy Studies
Bidholi Campus, Dehradun

CERTIFICATE

I certify that Ram Kunwer has prepared his thesis entitled “**Characteristic analysis of packed bed solar thermal energy storage (TES) system using synthetic oil as a Heat Transfer Fluid (HTF) for concentrated solar power application (CSP)**”, for the award of PhD degree of the University of Petroleum & Energy Studies, under my guidance. He has carried out the work at the Department of Mechanical engineering, University of Petroleum & Energy Studies.

Supervisor



Dr. Shyam Pandey

Professor

Department of Mechanical Engineering

University of Petroleum and Energy Studies, Bidholi Campus,

Dehradun, Uttarakhand

Date: 16. 11. 2021

ABSTRACT

Concentrated solar power (*CSP*) uses solar insolation to increase the temperature of heat transfer fluid (*HTF*), which can be used in a power block to produce power either by using a steam turbine or gas turbine. In *CSP*, the Levelized cost of electricity is higher than conventional sources due to the intermittent nature of solar energy. The Levelized Cost of electricity can be reduced by integrating *CSP* with thermal energy storage (*TES*) system. This paper provides a comprehensive review of sensible *TES* technologies for *CSP* applications. It includes a brief discussion of various sensible heat *TES* systems, i.e., molten salt *TES* system, single media *TES* system, and *DMT* (Dual-Media-Tank) *TES* systems. Recent advances in the *TES* system show that dual-media thermocline is economically more viable as compared to others. However, it has few technical challenges like a mechanical failure due to thermal ratcheting and varying outlet temperature.

This research work consist of systematic analysis of a dual-media thermal energy storage system consisting of ceramic pebbles as a storage material and high-temperature heat transfer fluid (*HTF*) for 1 MWe National Solar Thermal Power Plant. A numerical model has been formulated to study the thermocline behavior of tanks at different operating conditions. Based on the numerical model, a Lab-scale test facility is developed to validate the numerical model. The main objective of this study is to analyze the formation of the thermocline thickness for various operating parameters such as mass flow rate, void fraction, pebbles diameter, and thermal diffusivity of *HTF* and storage materials, along with a parametric optimization. The numerical result shows that, as the mass flow rate increases, the discharge time can cause the varying temperature at the outlet that is unenviable. The percentage movement of the thermocline layer was observed to be 70.37% with an increase in the mass flow rate of 18.75%. Similarly, it was found that the percentage increase in the volumetric heat transfer coefficient increased by 9.56%, with an increase in mass flow of 18.75%.

The lower pebble diameter gives the superlative results for thermocline thickness, but it causes a great deal of pressure drop, which causes exergy loss.

However, the percentage improvement in volumetric heat transfer coefficient was found to be 80%, with a 33.33% reduction in pebble diameter. It is concluded that a smaller size pebble diameter reduces the thermocline thickness, but it needs to be optimized to counter the problem of pressure drop. Parametric optimization has been done by considering various parameters such as D/L ratio, void fraction, mass flow rate, pebble diameter, thermal diffusivity of solid and HTF. Signal to noise ratio (SNR) has been taken into account to get the optimized value of the parameters. An empirical correlation has been developed to calculate thermocline thickness which is valid for a $D/L > 1$. Further, a Techno-economic cost analysis of the TES (DMT) system for a 1 MW_e CSP plant is done to study the economic facet of the system.

Beside this a heat exchanger design has also been done to integrate TES system with power block. In this research work, to integrate TES system a shell and tube heat exchanger (ST) is analyzed numerically and experimentally using various configurations of baffles. The baffles used are segmental baffle (SB) with baffle cut of 30° (SB-30), 50° (SB-50), Align baffle with baffle cut of 30° (AB-30) and 50° (AB-50). The numerical study of ST with different configurations shows that AB-30 has superior effectiveness than other configurations. The comparison of numerical and experimental results of AB-30 shows a deviation of 10.1%. The study also includes a comparison of the segmental baffle (STs) with continuous helical baffles with a helix angle of 25° (STc) experimentally. The comparative analysis, drawn between STs and STc shows that STs have better effectiveness at all considered mass flow rates varied between 0.00005 to 0.00018 m³/s. Lower mass flow rate had shown better effectiveness than STs by 27.7%. The fixed helix angle of 25° was provided to helical baffles, results in increased heat transfer coefficient (HTC) at the lower pressure drop. The flow pattern in the shell for both STs and STc maintained forced helical and rotational due to the geometry pattern of the baffles, respectively. Based on the experimental data, the non-dimensional parameters for HTC and pressure drop (ΔP_o) is calculated for both the configurations. However, for the optimal design of the heat exchanger, the maximum heat recovery rate has also been computed using the composite hot and cold diagram for different configurations.

An experimental analysis carried out to analyse the thermodynamic behavior of the tank during charging and discharging of the tank. The experimental analysis of DMT shows a 40% drop in the outlet temperature with a mass flow of 0.02 kg/s and 60% with a mass flow of 0.04 kg/s. Additionally the charging efficiency and the energy storage capacity of the system were also examined for DMT tanks. An increasing trend in stored energy was observed during the initial hour, which is later suppressed. At a higher mass flow, however, the stored energy is at its maximum. The experimental results also show a nominal change in charging efficiency for a mass flow rate of 0.01 kg/s and a 40% drop in charging efficiency was observed for a mass flow rate of 0.04 kg/s. In addition, the thermal cycles of the storage material were carried out to analyze the effect of charging and discharging on the physical properties of the material. The result shows a 50% decrease in load-bearing capacity after 8 cycles.

Keywords: *Thermal Energy Storage (TES); Concentrated Solar Power (CSP); Sensible heat; Thermocline; Shell and tube heat exchanger; Helixchanger; Segmental baffles; Align baffle; Heat transfer coefficient; Effectiveness; Process optimization*

ACKNOWLEDGMENT

I would first like to thank my Ph.D. advisors, Dr. Shyam Pandey, for the past five years of great support at UPES. Their passion and persistence in science have always encouraged me during PhD study. In the first year, they spent enormous efforts guiding research and never lost their patience when the experiment was not going well. They would seek every chance to train paper writing and presenting skills that help build confidence and become a qualified researcher. Without their constant support, I would never be able to accomplish a PhD study. All the knowledge and merit that they passed on, has made me today and will continue benefiting my future life.

I am grateful to the R&D team at UPES for their seed support in every manner and further acknowledge the continuous encouragement received from Dr. D.K Awasthi for supporting this work in all its stages. I especially want to thank Mr. Om Prakash Gupta, Thermal lab technician, for helping consistently during my experimentation. I am also grateful to all the lab staff and their support at our Institute (UPES). I also want to express my gratitude to Mr. Arvind Verma, who helped during the manufacturing of energy storage system.

I would like to thank my parents for their constant support and love at every stage of my life. Completing this degree would never be possible without their love and encouragement. Finally, a gratitude to all dear colleagues Dr. Swapnil Bhurat, Prof. Prashant Shukla, and Dr. Abhay Kumar for their continuous help and support.

I would like to thank my wife for consistently, patiently helping and supporting throughout this journey. Her help in my difficult time was always boosted me to complete this work on time. My kids, my stress reliever, are the important contributor to the accomplishment of this thesis work. They took and understand theirs by default duty of keeping me happy and stress-free during this journey.

TABLE OF CONTENTS

LIST OF FIGURES	x
LIST OF TABLES	xiii
LIST OF SYMBOLS	xiv
Chapter 1 - Introduction	1
1.1 Background	1
1.2 Motivation	8
1.3 PROBLEM STATEMENT	9
1.4 Objectives.....	9
1.5 Outlines of The Thesis	10
Chapter 2 - LITERATURE REVIEW	12
2.1 CSP technology	12
2.2 Global status of concentrated solar power	12
2.3 The thermal energy storage system (TES)	16
2.4 Two-tank thermal energy storage system.....	17
2.5 Thermocline tank system	19
2.6 Dual media packed bed thermal energy storage system	21
2.7 Parameter to evaluate performance of TES system	24
2.8 Characterization of Pressure drop in A DMT – TES SYSTEM	25
2.9 Heat Transfer model.....	27
2.10 Continuous Solid Phase Model	27
2.11 Schumann Model.....	28
2.12 Single Phase Model.....	29
2.13 Concentric Dispersion Model (C-D Model).....	30
2.14 Technical challenges of TES for CSP application	31
2.15 Technical challenges of two-tank molten salt TES system.....	36

2.16 Technical challenges of single media thermocline tank.....	38
2.17 Technical challenges of dual media thermocline system (DMT)	39
2.18 Research GAP	42
2.19 Summary of Literature Review	42
Chapter 3 - Numerical and Experimental Methodology.....	45
3.1 Introduction	45
3.2 numerical methodology.....	46
3.3 Experimental Methodology of DMT storage system.....	46
Chapter 4 - Modelling of Dual Media Thermal Energy Storage System..	48
4.1 Introduction	48
4.2 Heat Transfer Model for TES system	50
4.3 Thermal behavior during charging and discharging of tank	52
4.4 Influence of mass flow rate on thermocline behavior	54
4.5 Influence of particle diameter on thermocline behavior	54
Chapter 5 : Development of Dual Media Thermal Energy Storage System	56
5.1 Introduction	56
5.2 Development of LAB scale test facility for the characterization of DMT.....	56
5.3 Heat Exchanger design.....	59
5.4 Numerical study	61
5.5 Performance varying with different baffles configuration.....	62
5.6 Experimental study of the selected configuration	64
5.7 Experimental observation of segmental baffles	65
5.8 Helical Baffle Heat Exchanger.....	66
5.9 Process optimization	68
5.10 Performance Characteristics.....	69

5.11 Thermal Cycling of storage material for TES application	71
5.12 Error Analysis	72
Chapter 6 – Experimental Analysis of Dual Media Tank	73
6.1 Introduction	73
6.2 Temperature variation	73
6.3 Variation of temperature at the outlet of the tank	74
6.4 Energy Stored	75
6.5 Charging Efficiency	76
6.6 Thermal Cycling of storage material.....	77
Chapter 7 – Thermo-Economic Optimization.....	79
7.1 Parametric optimization	79
7.2 Optimum parameters for minimum thermocline thickness.....	81
7.3 Model validation	81
7.4 Techno-economic analysis	82
Chapter 8 - Conclusions and Future Work	86
References	91

LIST OF FIGURES

Figure 1-1: Share of electricity generation by renewable energy in India.....	2
Figure 1-2: Classification of concentrated solar power technology	3
Figure 1-3: Operating temperature and concentration ratio of solar reflector (Barlev et al., 2011)	4
Figure 1-4: Percentage of CSP capacity in different countries by status (operational, under construction, development)	5
Figure 1-5: Concentrated Solar Power (CSP) Technology.....	5
Figure 1-6: CSP in integration with Thermal energy storage (TES)	6
Figure 1-7: TES classification	6
Figure 1-8: Outlines of thesis: Chapter 1 to Chapter 4	10
Figure 1-9: Outlines of thesis: Chapter 4 to Chapter 8	11
Figure 2-1: CSP Global capacity and addition in 2019 (Members, 2020).....	13
Figure 2-2: National status: (A) CSP in integration with TES (B) CSP without TES	14
Figure 2-3: Operating temperature and concentration ratio of solar reflector (Barlev et al., 2011)	15
Figure 2-4: Percentage of CSP capacity in different countries by status (operational, under construction, development)	15
Figure 2-5: Classification of TES system	16
Figure. 2-6: Functionality of TES systems	17
Figure. 2-7: Molten salt <i>TES</i> system	17
Figure. 2-8: Single Media TES system for CSP application	20
Figure. 2-9: Dual media packed bed TES system for CSP application	21
Figure 2-10: Thermocline thickness of various storage material (ELSiHy et al., 2021)	24
Figure 2-11: Thermocline thickness of dual media and single media tank (Mirahern & Flueckiger, 2015).....	25
Figure 2-12: Heat Transfer Model	27
Figure 2-13: Technical challenges of molten salt TES system.....	36
Figure 2-14: Variables in the corrosion mechanism.....	37
Figure 2-15: Major factor influencing corrosion	38

Figure 2-16: Technical challenges of SMT for CSP application.....	38
Figure 2-17: Technological challenges of DMT tank.....	39
Figure 2-18: Method to control temperature degradation.....	40
Figure 2-19: Segmented packed bed storage system [92]	41
Figure 2-20: Temperature in standard and segmented bed(Crandall & Thacher, 2004)	41
Figure 2-21: Thermocline thickness comparison of two tank and dual media tank.....	43
Figure 2-22: Overview of Heat Transfer Model	44
Figure 3-1: Detailed Methodology.....	46
Figure 3-2: Experimental Methodology.....	47
Figure 4-1: Physical model	49
Figure 4-2: Boundary conditions during charging and discharging of tank	52
Figure 4-3: Charging and discharging behavior of DMT	53
Figure 4-4: Effect of mass flow rate on thermocline behavior of DMT	54
Figure 4-5: Effect of pebbles diameter on thermocline behavior of the tank ..	55
Figure 5-1: Experimental setup (A) Charging of Tank and (B) Discharging of Tank	57
Figure 5-2: Experimental Set-up.....	58
Figure 5-3 Oil transfer pump with DC Motor.....	59
Figure 5-4: Ceramic balls with HTF	59
Figure 5-5: Temperature variation across (A) Shell Side and	61
Figure 5-6: Temperature variation across (B) Tube Side	62
Figure 5-7: Effectiveness of different baffles geometries.....	63
Figure 5-8: Effect of Reynold's number on A) friction factor B) Pressure drop C) Nusselt number (D) Heat transfer coefficient	63
Figure 5-9: Validation of the theoretical model.....	64
Figure 5-10: Influence of mass flow rate on LMTD and effectiveness of.....	66
Figure 5-11: Influence of mass flow rate on LMTD and effectiveness	67
Figure 5-12: Comparison of segmental and helical heat exchanger	67
Figure 5-13: Heat recovery analysis of heat exchanger without baffle	68
Figure 5-14: Heat recovery analysis of AB-30	69
Figure 5-15: Heat recovery analysis of SB-30.....	69

Figure 5-16: Colburn factor of helical and Segmental baffle	70
Figure 5-17: Pumping power ratio of helical and Segmental heat exchanger .	71
Figure 5-18 Thermal Cycling of storage material.....	72
Figure 5-19 Compression test of storage material	72
Figure 6-1: Temperature variation along the different section with time	74
Figure 6-2: Variation of outlet temperature with time.....	75
Figure 6-3: Energy stored with time	76
Figure 6-4: Charging efficiency of dual media thermocline tank at varying mass flow rate	77
Figure 6-5: Thermal Cycling (A) Initial (B) After 8 th Cycle	78
Figure 7-1: SNR of control factor	81
Figure 7-2: Validation of numerically predicted thermocline performance with the experimental result.....	82

LIST OF TABLES

Table 2-1: Thermophysical properties of rocks	25
Table 2-2: Technical challenges of TES model	32
Table 2-3: LMP molten salt for CSP application.....	36
Table 4-1: Operating Parameters/ Input parameter for	49
Table 5-1: Operating parameter of LAB scale test facility	58
Table 5-2: Design specifications of heat exchanger	60
Table 5-3: Correlation for friction factor	61
Table 5-4: Correlation for Nusselt number	61
Table 5-5: CFD data for different model	62
Table 5-6: Heat Exchanger data with tube side	64
Table 5-7: Properties of fluid in heat exchanger.....	65
Table 6-1: Physical properties after different thermal cycle.....	78
Table 7-1: Control factors.....	79
Table 7-2: Orthogonal array.....	80
Table 7-3: Validation of developed correlation	81
Table 7-4: Cost assumption for techno-economic analysis of TES system (DMT) (Mostafavi, Taylor, Nithyanandam, & Shafiei, 2017; Nithyanandam & Pitchumani, 2014).....	83
Table 7-5: Cost breakdown of TES (DMT) system for 1 MWe CSP	84
Table 8-1 Thermophysical properties of storage material	87

LIST OF SYMBOLS

Nomenclature

X	Mole Fraction
ε	Void Fraction
V	Volume
κ	Thermal conductivity
C	Specific Heat
d	Diameter of pebbles
R	Radius
H	Convective heat transfer coefficient
D	Diameter of cylinder
Y	Axial length
K	Thermal conductivity
T	Temperature
T	Time
U	Overall heat transfer coefficient
U	Velocity
A	Area
E	Energy
L	Length of tank
M	Mass flow rate
S	Source Term
Re	Reynold Number
Pr	Prandtl Number
N	No of tubes
Q	Volume Flow rate
J	Colburn factor
F	Fanning Friction
η	Efficiency
C	Cost
T	Thickness
SS	Stainless Steel

Greek Symbols

P	Density
A	Thermal Diffusivity
M	Dynamic Viscosity
Φ	Intensive Property

Subscript

<i>t</i>	Tank
<i>p</i>	Pebbles
<i>S</i>	Storage material
<i>C</i>	Cylinder
<i>F</i>	Fluid
<i>V</i>	Volumetric
<i>W</i>	Wall
<i>max</i>	Maximum
<i>E</i>	Void
<i>S</i>	Superficial
<i>Sup</i>	Superficial
<i>I</i>	<i>Inner</i>
<i>O</i>	<i>Outer</i>
<i>hi</i>	<i>Hot Inlet</i>
<i>ci</i>	<i>Cold inlet</i>
<i>ho</i>	<i>Hot outlet</i>
<i>co</i>	<i>Cold Outlet</i>
<i>L</i>	<i>Lowest</i>
<i>i</i>	<i>Insulation</i>
<i>fo</i>	<i>Foundation</i>
<i>pf</i>	<i>Piping and Fitting</i>
<i>EI</i>	<i>Electric and Instrumentation</i>

Abbreviation

<i>PV</i>	<i>Photovoltaic</i>
<i>CSP</i>	<i>Concentrated Solar Power</i>
<i>SHC</i>	Solar Heating and Cooling

<i>HTF</i>	Heat Transfer Fluids
PTC	Parabolic Trough Collector
LFR	Linear Fresnel Reflector
DSG	Direct Steam Generator
<i>TES</i>	Thermal Energy Storage
DMT	Dual Media Tank
LCOE	Levelized Cost of Electricity
MSTES	Molten salt thermal energy storage
DSC	Differential Scanning Calorimeter
PBSS	Packed Bed Storage System
SMT	Single Media Tank
LMP	Low Melting Point
TCC	Thermocline Control
HE	Heat Exchanger
SB	Segmented Baffle
AB	Align Baffle
DOE	Design of Experiment
LMTD	Log Mean Temperature Difference
NTU	Number of Transfer Unit
ST	Shell and Tube
WB	Without Baffle
ST	Stanton Number
NCOTES	Normalized Cost of Thermal Energy Storage System
DNI	Direct Normal Irradiance

CHAPTER 1 - INTRODUCTION

1.1 BACKGROUND

Energy since ages has been mankind's necessity. Humans have always relied upon various sources of energy in order to fulfill their day-to-day needs. Biofuels were the earliest sources of energy. But due to its inefficiency, several other sources of energy saw significant growth. After several years fossil fuels became the primary source of energy. Exploration of fossil fuels led to a remarkable turnaround in the energy sector. It changed the scenario worldwide. Energy now plays an indispensable role in a nation's growth. Growth in economies also leads to an increase in energy demand; hence energy plays a vital role in nation-building. The global energy demand is predicted to rise by 50% by 2050 ("Global energy use projected to nearly double by 2050 - Energy Live News," n.d.). This means the renewable energy sources will play a massive role in maintaining the tradeoff between supply and demand. In the present scenario, over 80% of energy is generated with the help of fossil fuels (Yildiz, 2018). This has led to the fast depletion of these resources with significant global warming and CO₂ emissions. Though fossil fuels remain the major source of energy, countries worldwide are taking steps to reduce their dependencies on fossil fuels. According to the Renewable Energy policy network 2020 global report, renewable energy saw an unprecedented increase of 200GW in 2019 (Members, 2020). The share of renewable energy for producing electricity has seen continuous growth. The two main objectives of renewable energy are: generating power to meet demand and protecting the environment with pollution-free energy (Shouman & Khattab, 2015). We have many alternative and renewable resources that can fulfill our energy requirements if appropriately extracted and utilized. Solar energy alone has the potential to meet the needs and maintain the balance between supply and demand if we have technologies to harness it properly and efficiently. Sun is the

primary energy source emitting nearly 3.86×10^{26} Watt of energy after losing a significant amount due to attenuation caused by the atmosphere and clouds (Tian & Zhao, 2013). Solar energy can be utilized for various purposes such as electricity generation, lighting, and heating water for domestic, and industrial applications. Several techniques are there to straps solar energy like solar photovoltaic (*PV*), Solar heating/cooling and CSP applications. Solar photovoltaic is the conversion of sunlight directly into electricity. It uses a flat plate and concentrator system for this purpose. It consists of a solar cell that generates free electrons with the help of photons by using the photoelectric effect. These free electrons help in generating electricity (Nations, Programme, & Nations, 1973). Many PV cells are grouped together to form a module. This is done because the output from a PV cell is low. This grouping is done on the basis of current and voltage requirements. These systems have an efficiency between 15-20% (Aghaei et al., 2020). Solar PV has seen constant growth over the years because of its constantly expanding demand. It has become one of the most insistent options for the generation of electricity. It is widely being used in residential and commercial applications. This has led to tremendous growth in solar PV technology, and consequently, the prices have also fallen over the years (Kusch-Brandt, 2019; O'Rourke, Kim, & Polavarapu, 2009; Stephanie Weckend, Andreas Wade, & Garvin Heath, 2016). Solar PV prices modules have seen a fall of 12% between 2018-19, costing about 25.2 INR per watt ("Module Price Index – pv magazine International," n.d.). Figure 1-1 shows the share of electricity generation in India. Similarly, solar heating and cooling (SHC) has proved to be a viable alternative. SHC systems are used for space heating, producing hot water for domestic purposes, or used in absorption chillers (Buonomano, Calise, & Palombo, 2018). Solar heating and cooling systems consist of a solar collector loop and a load loop. The solar collector loop performs the function of generating and supplying thermal energy for heating or cooling by focusing the solar radiation onto the receiver and giving heat to the *HTF*. In contrast, the load loop consists of hot and chilled water circuits, which include many heat exchangers (Zheng et al., 2019).

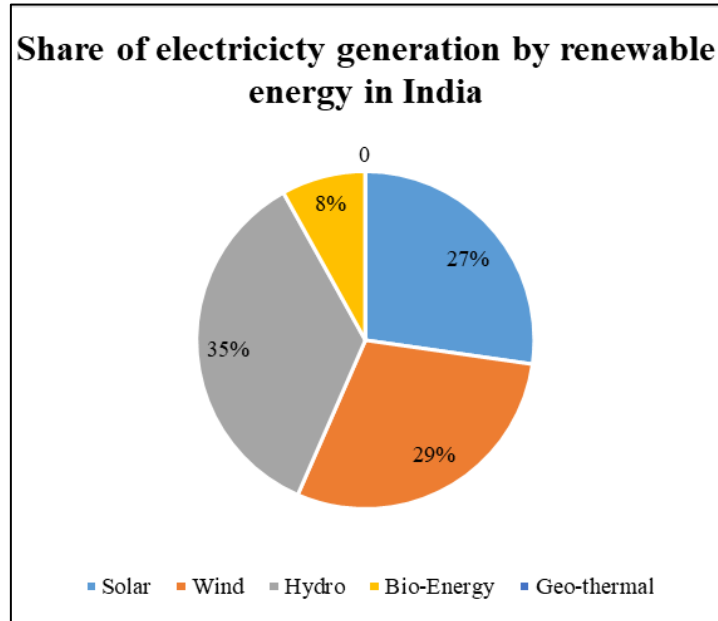


Figure 1-1: Share of electricity generation by renewable energy in India

Various other technologies such as solar air heating, solar photovoltaic plus thermal technology, solar water heating technology under SHC systems are being used for multiple domestic and industrial purposes (“Solar Heating & Cooling | SEIA,” n.d.). The third major technology to harness solar energy is CSP. In CSP solar energy is converted into high-temperature heat with the help of mirrors that concentrate the sun's light onto a receiver. This thermal power can be utilized to convert water to steam which is further used for producing electricity by running a turbine with the help of power cycles like Rankine, Brayton, etc. (Pitz-Paal, 2020). The concentrated solar power consists of three building blocks: Solar field, *TES* and power system. The solar field includes mirrors/reflectors, and storage block consists of storage tanks depending on the storage technique involved while power block is where the power production occurs (Purohit, Purohit, & Shekhar, 2013). Concentrated solar power (CSP) is classified into two major components, i.e. line focus and point focus (Islam, Bhuiyan, & Ullah, 2017). Figure 1-2 shows the classification of CSP technology. In CSP, solar radiation is concentrated on the receiver through several technologies, i.e., PTC, LFR, Solar Tower, and solar dish. However, the solar tower is the most favorable concentrator for CSP applications due to its maximum concentration and maximum temperature. Figure 1-3 compares the concentration ratio and the maximum temperature of the different concentrators.

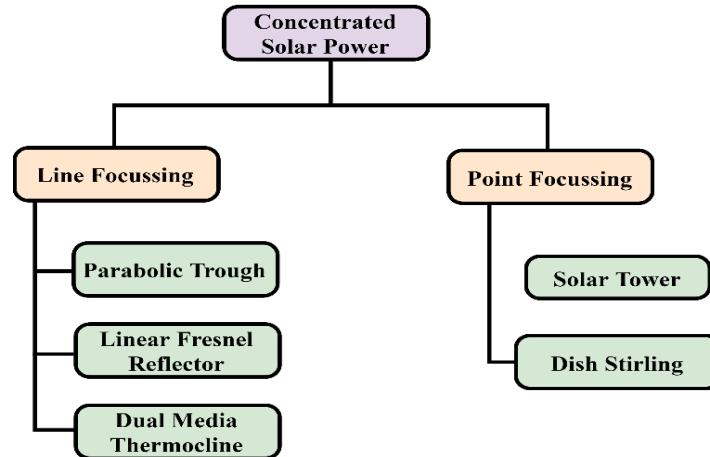


Figure 1-2: Classification of concentrated solar power technology

CSP operates on four other technologies, namely solar tower, dish Stirling, PTC, and LFR. As illustrated in Figure 1-3, the solar tower operates at the highest temperature and has the highest concentration ratio. It is followed by Dish Stirling, which operates in the range of 300°C-1500°C. Both of these technologies have high thermodynamic efficiency. Aforesaid are recent developments in the field of CSP technologies (Moser, Trieb, & Fichter, 2013; Shouman & Khattab, 2015; States, States, & Southwest, 2001; B. Xu, Li, & Chan, 2015; Zhang, Baeyens, Degreève, & Cacères, 2013), while PTC and LFR are mature technologies, but they have relatively low thermodynamic efficiency and operate at lower temperatures (Barlev, Vidu, & Stroeve, 2011). The solar tower can be the best choice for the CSP due to the fact that it can achieve high temperatures with losses that can be minimized. The significant advantage it gives over other technologies is higher steam cycle efficiency, reduced thermal energy storage cost, and the ability to meet peak air conditioning demand in hot arid locations economically (Santos et al., 2018). To make sure that the use of costly and toxic HTF in CSPs are minimized, a new technology named Direct Steam Generation (DSG) was developed. It has been forecasted that CSP based on DSG technology would work on higher temperatures in the coming years. Presently inorganic salts are used as HTF in high-temperature CSPs based on the central receiver (Guillot et al., 2012). According to the REN21 global status report 2018, saw a considerable increase in the CSP technology. Cumulative capacity grew by 11% and approximately, 550MW of concentrated solar thermal power was added.

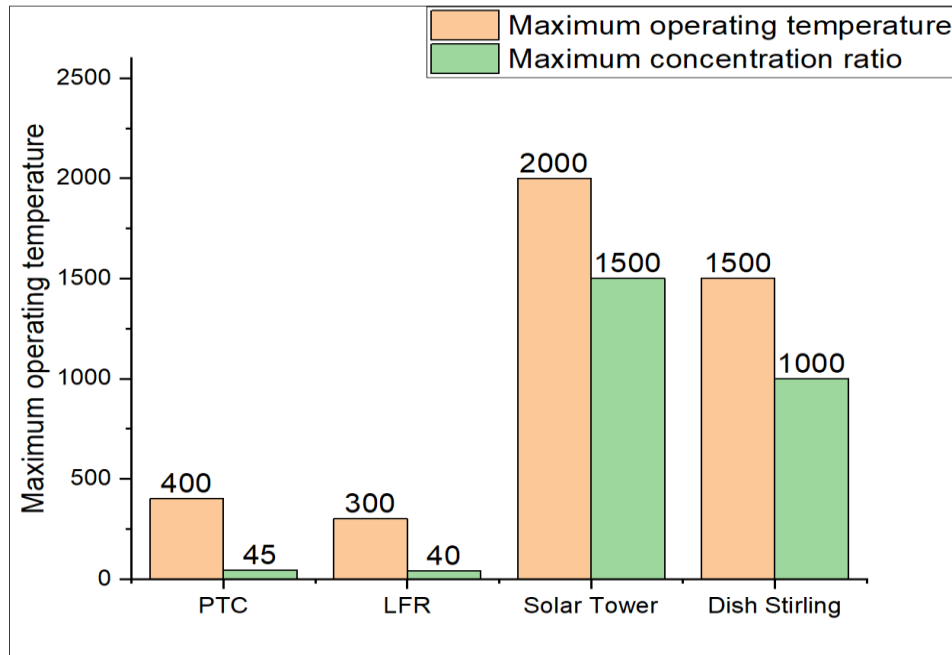


Figure 1-3: Operating temperature and concentration ratio of solar reflector
(Barlev et al., 2011)

Figure 1-4 represents the capacity and addition in each year from 2008 to 2018. Between 2016-18 the capital cost of CSP also fell sharply (Kusch-Brandt, 2019). Though renewable energy is available in abundance, and we have developed several technologies like hydropower, solar power (Photovoltaic and Solar Thermal), wind, and geothermal to utilize it. Still, the primary issue from these resources is their intermittent behavior. Hence, it becomes essential to have storage technologies to store energy and use it whenever needed. Concentrated solar power (CSP) is an encouraging technique for exploiting solar energy in large-scale industrial applications. Figure 1-5 shows the CSP technology to produce power employing a solar field and power block. In 2018, around 12200 GWh of concentrated solar power was produced worldwide, up from 934 GWh in 2009. However, the CSP capacity of the world was nearly 6000 MW till 2019. Among these, the CSP capacity of India was almost 229 MW in 2019 and 226 MW in 2011, which is not recognizable and appreciable growth in this sector.

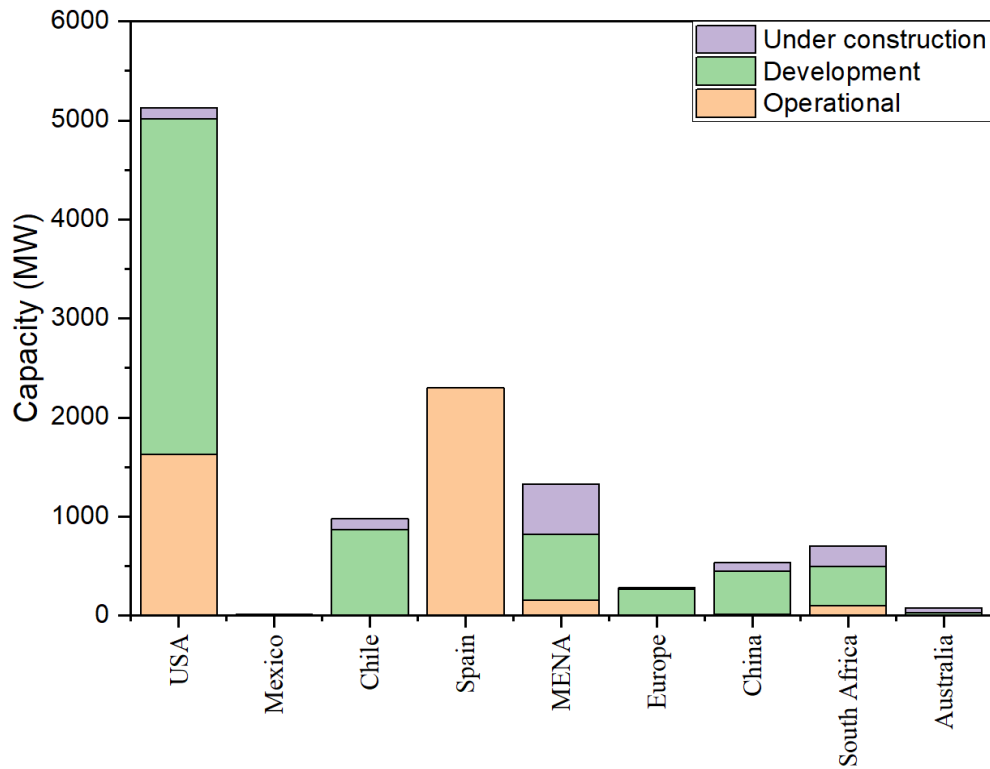


Figure 1-4: Percentage of CSP capacity in different countries by status (operational, under construction, development)

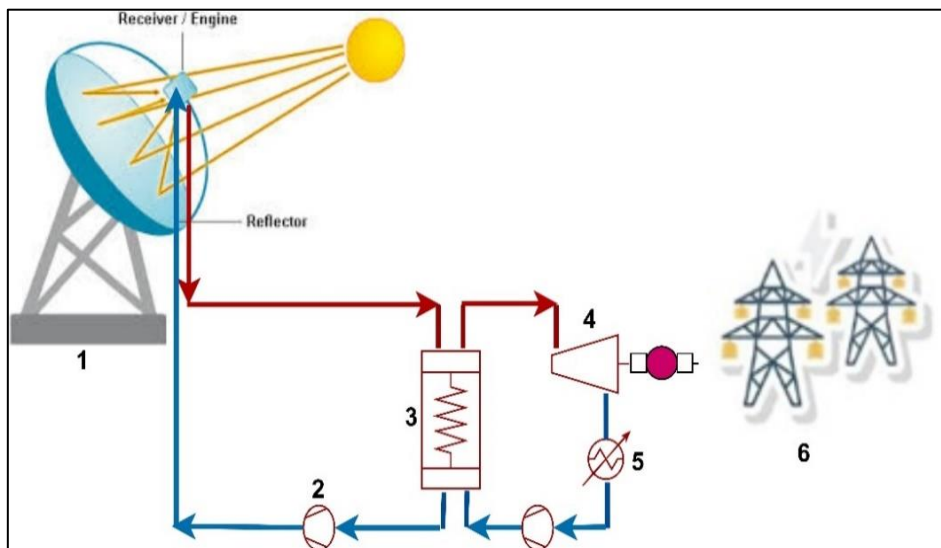


Figure 1-5: Concentrated Solar Power (CSP) Technology

The major issue in the harvesting of solar energy is its intermittent behavior. Hence it becomes essential to have storage technologies to store energy and use it whenever needed. Figure 1-6 shows the CSP in integration with thermal energy storage technology for continuous operation.

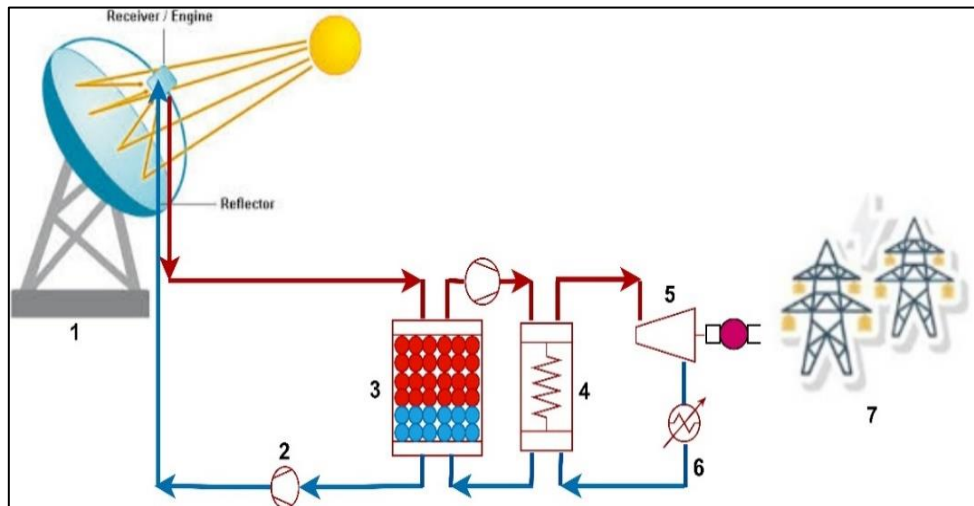


Figure 1-6: CSP in integration with Thermal energy storage (TES)

The integration of the TES system with CSP provides continuous distribution of energy despite its intermittent nature. The TES system is broadly classified into sensible-based TES system, latent-based TES system, and thermochemical-based TES system. Figure 1-7 shows the classification of the TES system for CSP applications.

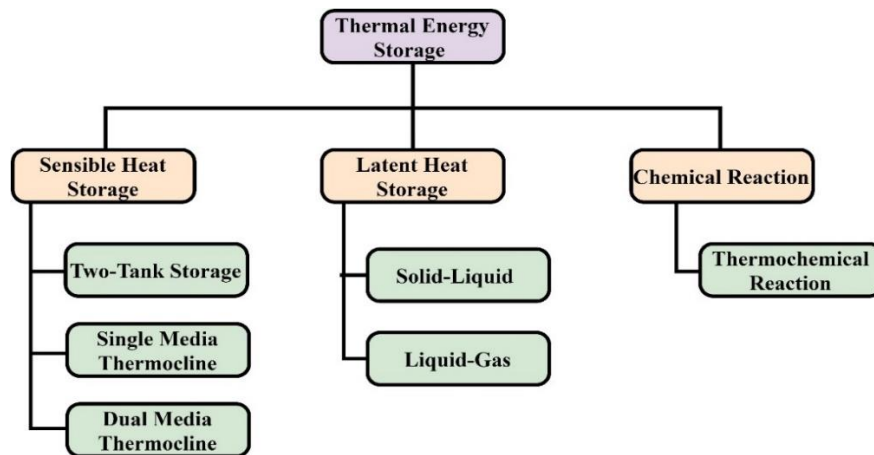


Figure 1-7: TES classification

The sensible-based TES system uses rocks or pebbles to store energy in the form of SH. Similarly, LHTES system uses phase change material to store energy in the form of LH and TCES (Thermochemical energy storage) technology utilize chemical reaction to store energy (Marcot & Kunwer, 2019). The study revealed that sensible heat TES technology is economically more viable than the other storage system (Mira-hern & Flueckiger, 2015). Furthermore, Sensible heat TES systems are classified as single media thermocline TES and dual

media thermocline TES. Single media thermocline TES uses single heat transfer fluid (HTF) to store solar thermal energy. The abrupt temperature gradient inside the storage tank is called the thermocline, and it separates hot and cold fluid, thus maintain the thermal stratification of the tank. In dual media tank (DMT) heat is stored by storage material and HTF. The selection of HTF and storage material is based on the maximum temperature required for CSP operation. The operation of CSP without TES is similar to that of the conventional power cycle. A solar field is added, producing thermal energy and replacing the conventional fuel utilized in producing superheated steam. CSP with TES system includes a storage field, which consists of a storage system of any type. The selection of storage material are based on the structural stability and good thermal properties. Refractories such as aluminium oxide (alumina), magnesium oxide (magnesia) and silicon oxide are suitable for high temperature applications. However, alumina is most widely used storage material due to its availability and low cost. Several authors have developed a wide range of numerical and experimental model to study the thermocline behavior of tank during charging and discharging of tank. Elouali et al. (Elouali et al., 2019) examined the single-phase model (Model 1), continuous solid phase model (Model 1), Schumann model (Model 2), and model with the variation in temperature within the solid particles (model 4) and found model 3 and 4 is in good agreement with the empirical results. The author reported that small solid particles at low mass flow rates are profitable in terms of charging efficiency and pumping power. Doretti et al. (Doretti, Martelletto, & Mancin, 2019) developed a fast and modular lumped capacitance model for the study of charging and discharging of the tank. However, the model accuracy is drastically lower than the CFD/FEM model. Baba et al. (Filali Baba, Al Mers, & Ajdad, 2020) developed a dimensionless model based on dual-phase to study the thermocline behavior of tanks under various operating variables. The proposed model does not require discretization with an accuracy similar to the two-phase model with less computational effort. Bayon et al. (Bayón & Rojas, 2013) investigated the thermal characterization of thermocline tanks using a 1D single – phase model. The author examined the effect of dimensionless

velocity on thermocline thickness and found that thermocline thickness decreases with increasing dimensionless velocity. Zanganeh et al. (Zanganeh, Pedretti, Zavattoni, Barbato, & Steinfeld, 2012) demonstrated pilot-scale and industrial-scale designs to study the performance of a packed bed thermal energy storage system. The author has used a truncated conical shape tank immersed in the ground for studying thermocline behavior of tank. (Pizzolato, Donato, Verda, Santarelli, & Sciacovelli, 2017) analyzed the technical and economic modeling of the thermocline TES system for CSP application. In addition to the techno-economic model, the author also performed the parametric optimization by implementing genetic algorithms (GA) of the MATLAB optimization toolbox.

Most of the above studies focused on the thermocline behavior of DM TES systems under various operating variables such as mass flow rate, pebbles diameter, void fraction, and thermophysical properties of the storage material. However, none of the authors has studied the effect of operating variables on thermocline thickness. This study examines the influence of variables such as void fraction, pebbles diameter, and mass flow rate to close these gaps with thermodynamic modelling and parametric optimization. In addition, an empirical correlation is also developed to evaluate the thermocline thickness under various operating conditions.

1.2 MOTIVATION

TES is a promising area that needs to be elaborated more on the technical point of view. Although CSP technology are more on technical front, but without thermal energy storage system that cannot be further continued. However, more work is going on to integrate CSP with the TES system, but most of the works are limited to the LAB scale. The most significant advantage of CSP over other technologies is its ability to incorporate Thermal Energy Storage systems. Though other storage techniques are available, thermal storage is the most economical option as storing electrical energy is difficult and costly. This could also be one of the reasons for the fall in storage capacity. According to IEA 2019 saw a fall of 30% in storage capacity addition compared to that of 2018, which clearly states that battery storage may not always be the best option.

(“Energy Storage – Analysis - IEA,” n.d.; Languri & Cunningham, 2019; Sarbu, 2018). Thermal energy storage is a system that stocks thermal energy. This provides a CSP plant, a buffering capacity and flexibility of operation. It fills the temporal gap between supply and demand. TES adds better dispatchable qualities to the system. This means whenever power is required; it can be supplied to improve operational characteristics, especially when the sun is not shining. Storing thermal energy storage is a more accessible and economical option as compared to electrical energy storage (Palacios, Barreneche, Navarro, & Ding, 2019; Pelay, Luo, Fan, Stitou, & Rood, 2017; Power, n.d.). The TES system also helps in reducing Levelized cost of energy (LCOE) by shifting the power delivering time and reducing the mismatch between supply and demand (Aneke & Wang, 2016; Kalaiselvam & R.Parameshwaran, 2014; “Thermal Energy Storage - Overview and basic principles,” n.d.).

1.3 PROBLEM STATEMENT

The intermittency of solar energy is a major factor for high levelized cost of electricity based on solar power plant. However, this limitation can be overcome by integrating CSP with TES. The TES system are based on sensible heat are commercially available but still economically not so viable due to high cost. Of all sensible based TES system, dual media tank energy storage system is economically more viable due to its lower cost but still this system is not on commercialized state. However the commercialization is possible by integrating the DMT TES system with CSP plant based on micro grid. The smallest commercial CSP plant, which was operational in 2019, was of a 9 MW capacity with a 36 MWh energy storage system. Therefore, research needs to be done to integrate micro solar power plants with the *TES*.

1.4 OBJECTIVES

The primary objective of this work is:

Characteristic analysis of solar-based packed bed TES system using synthetic oil as a HTF for CSP

- Parametric optimization of TES system using Design of Experiments (DOE)
- Experimental setup: Design and fabrications

1.5 OUTLINES OF THE THESIS

The thesis will be outlined as follow:

Chapter 2 will discuss the technical barrier to integrate TES system with CSP plant. In addition a detailed study of characteristic behavior of DMT for CSP application will be done. In Chapter 3 a methodology to investigate thermal behavior of DMT for CSP application will be done. The Chapter 3 will discuss the numerical and experimental methodology to integrate TES system for CSP applications. In Chapter 4 a mathematical modelling of industrial scale TES system for CSP application will be done. In Chapter 5 based on the mathematical model a LAB scale test facility will be discussed to validate the numerical results and to investigate the thermal performance of DMT TES system. Chapter 6 will present the experimental investigation of DMT for CSP application and Chapter 7 will discuss the techno-economic optimization of DMT. In this the optimum parameter for minimum thermocline thickness will be examined. A detailed outline of thesis is shown in Figure 1-8 and Figure 1-9.

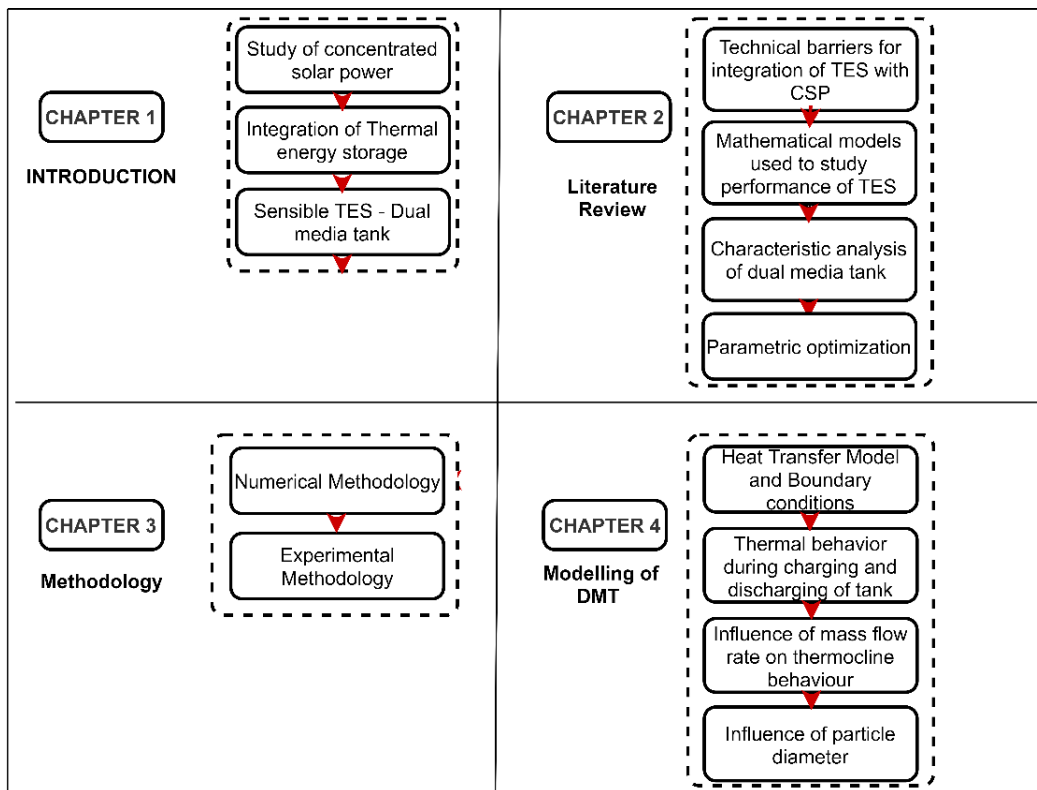


Figure 1-8: Outlines of thesis: Chapter 1 to Chapter 4

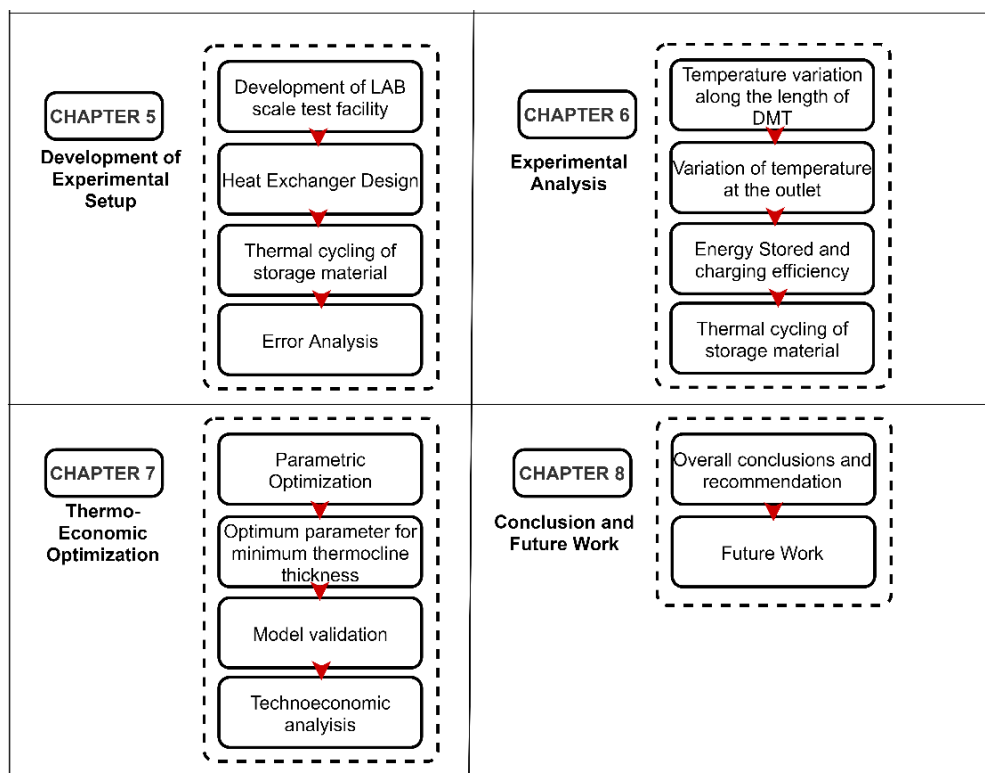


Figure 1-9: Outlines of thesis: Chapter 4 to Chapter 8

CHAPTER 2 - LITERATURE REVIEW

2.1 CSP TECHNOLOGY

Unlike PV, Concentrated Solar Power (CSP) does not convert sunlight directly to electricity; instead works as an interstage step. It consists of a reflector and absorber. The reflector focuses the sunlight on the absorber. Sunlight is converted into heat and absorbed in the absorber. This heat can be utilized to generate steam. It consists of four parts, namely solar field, power block, and Thermal Energy Storage (TES) system (Stekli, Irwin, & Pitchumani, 2013). When TES is combined with CSP, it increases operating capacity, improves the power dispatch of the plant, reduces peak demand and ultimately increases the value of the power produced. The system is most efficient when the energy-carrying material is removed from the system at a temperature, which correspond to its initial value. (P. Li et al., 2012). CSP technology can be classified into two components i.e. point focus concentrator and line focus concentrator. Point focus concentrators achieve high temperatures at the receiver, in the range of 700°C -1000°C. They produce high temperatures due to the high concentration ratio. Line focus based technologies, on the other hand, attain lower temperatures (Bijarniya, Sudhakar, & Baredar, 2016). Electricity generation from CSP grew at a rate of 25 % between 2011 and 2017, in which the total capacity increased to three times. Its demand increases at a rate of 17% in the year 2018. It is forecasted to grow by 3.4 GW from 2019 to 2024 (“Concentrating solar power – Tracking Power – Analysis - IEA,” n.d.).

2.2 GLOBAL STATUS OF CONCENTRATED SOLAR POWER

The CSP global capacity are shown in Figure 2-1. CSP global capacity till 2018 was 5610 GW. The percentage growth of CSP in 2019 was 11.9%, however it is 24% below than the average annual increase from the past decade (Members, 2020).

Five countries come up with the implementation of first commercial CSP plant. The solar field of the majority of the CSP system consists of a parabolic trough collector. Majority of CSP plants are integrated with TES system. China continued with 200 MW capacity in integration with molten salt TES system. The smallest commercial CSP plant of nine MW capacity with 36 MWh energy storage system, it is operational since 2019.

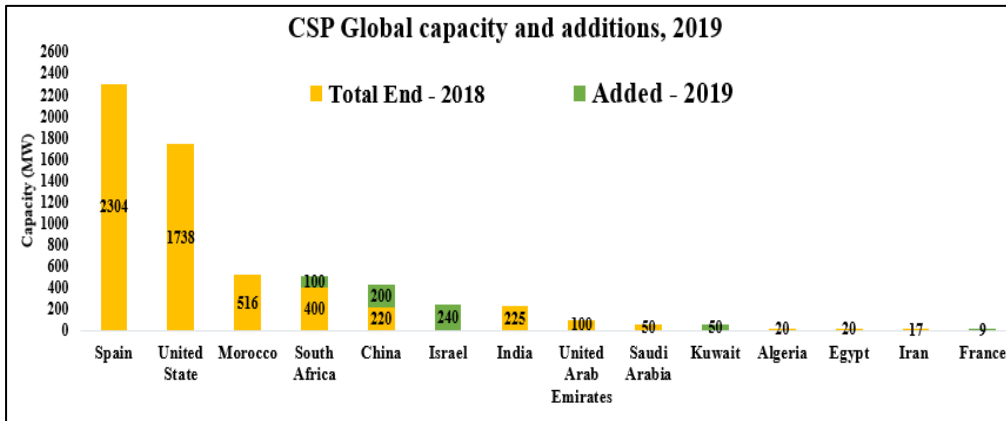


Figure 2-1: CSP Global capacity and addition in 2019 (Members, 2020)

The journey of CSP in India was began in 2010 under Jawaharlal Nehru Solar Mission (JNNSM) with seven projects. Currently, five CSP are operational, and six are under construction. In India, the lack of DNI data is the main reason for the delay in the growing CSP market (“Concentrated solar power (CSP) in India: An outlook to 2024 – HELIOSCSP,” n.d.). The CSP under construction or operational needs to be integrated with the TES system. The CSP in integration with the TES system reduces the per unit of electricity cost by increasing the operational time. Figure 2-2 shows the status of CSP integration with the TES system. In India, only three CSP is integrated with the TES system. In CSP, solar radiation is concentrated on the receiver through several technologies, i.e., PTC, LFR, Solar Tower, and solar dish. However, the solar tower is the most favorable concentrator for CSP applications due to its high concentration and maximum temperature.

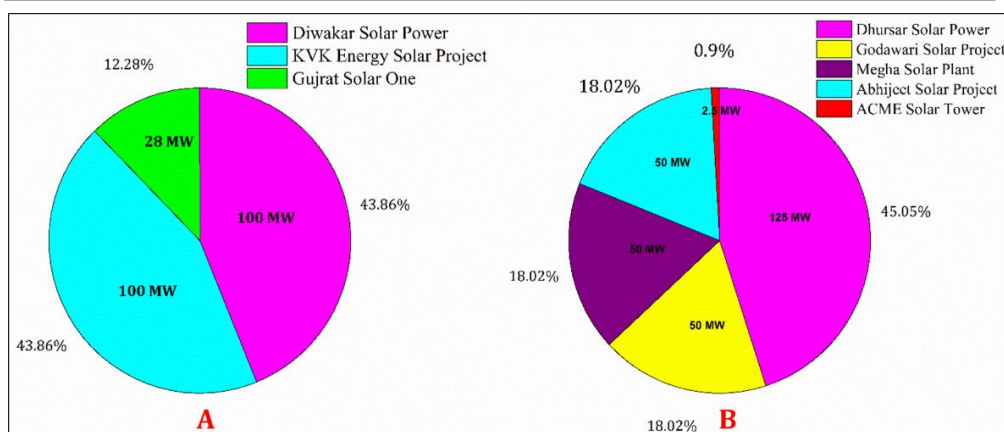


Figure 2-2: National status: (A) CSP in integration with TES (B) CSP without TES

Figure 1-3 compares the maximum concentration ratio and the maximum temperature of the different concentrators. CSP operates on four other technologies, namely solar tower, dish Stirling, PTC (Parabolic Trough Collector), and LFR (Linear Fresnel Reflector). As illustrated in Figure 1-3, solar tower operates at the highest temperature and has the highest maximum concentration ratio. It is followed by Dish Stirling, which operates in the range of 300°C-1500°C. Both of these technologies have high thermodynamic efficiency. They are recent developments in the field of CSP technologies (Moser et al., 2013; Shouman & Khattab, 2015; States et al., 2001; B. Xu et al., 2015; Zhang et al., 2013). While PTC and LFR are mature technologies, but they have relatively low thermodynamic efficiency and operate at lower temperatures (Barlev et al., 2011). The significant advantage it gives over other technologies is the higher efficiency of the steam cycle, reduced thermal energy storage cost, and the ability to meet peak air conditioning demand in hot arid locations economically (Santos et al., 2018). To ensure that the use of expensive and toxic HTF in CSPs is minimized, a new technology called Direct Steam Generation (DSG) has been developed. It was predicted that CSP based on DSG technology would work on higher temperatures in the coming years. Presently inorganic salts are used as HTF in high-temperature CSPs based on the central receiver (Guillot et al., 2012).

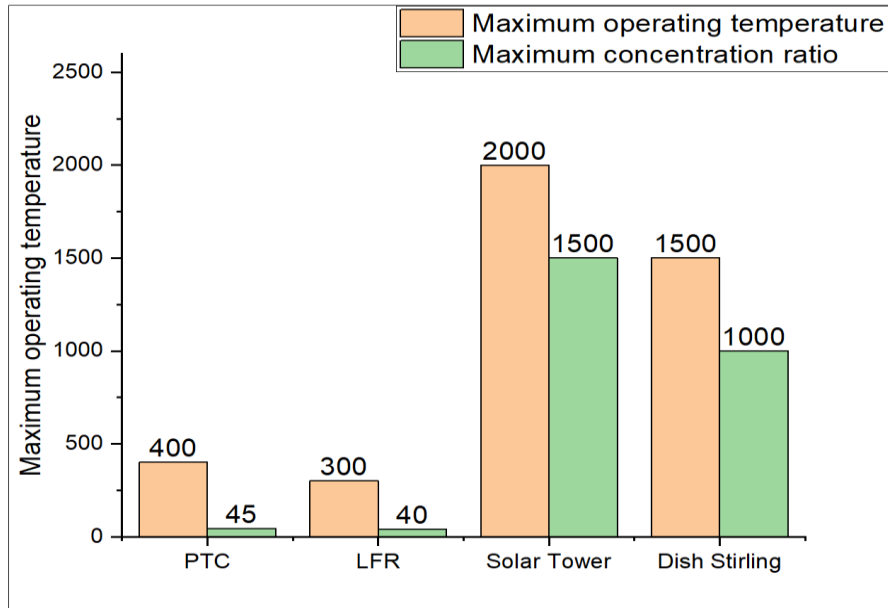


Figure 2-3: Operating temperature and concentration ratio of solar reflector (Barlev et al., 2011)

According to REN21 global status report, 2018 saw a considerable increase in the CSP technology. The cumulative capacity increased by 11% and approximately, 550MW of concentrated solar thermal power was added. Figure 1-4 shows the capacity and expansion in each year from 2008 to 2018. Between 2016-18 the capital cost of CSP also fell sharply (Kusch-Brandt, 2019)

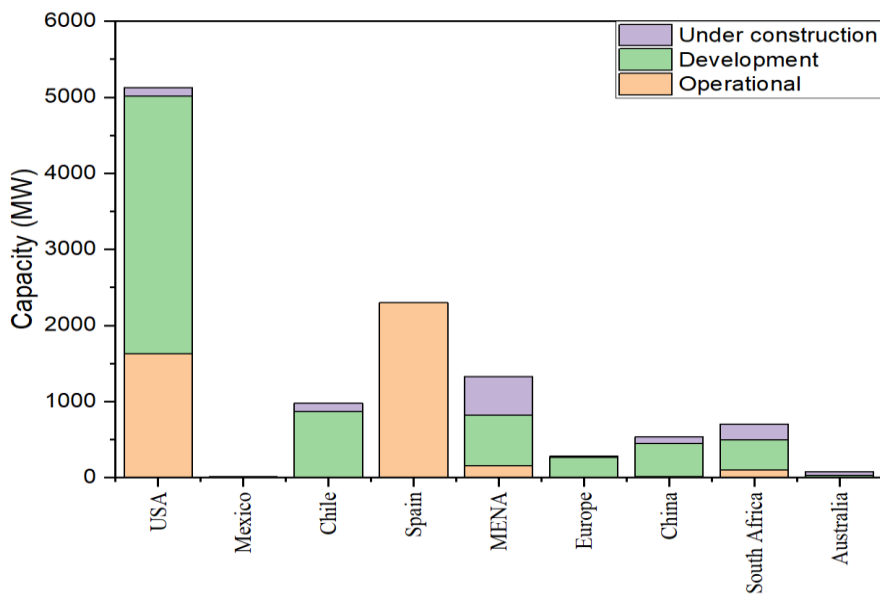


Figure 2-4: Percentage of CSP capacity in different countries by status (operational, under construction, development)

2.3 THE THERMAL ENERGY STORAGE SYSTEM (TES)

Figure 2-5 represents the schematic classification of TES systems. TES systems are classified into active and passive modes. Active TES can be further classified in two systems: Direct and Indirect. The active TES system conventionally uses liquid. This fluid helps in heat transfer through forced convection and heat exchange operation in steam generators. The passive type of TES system is a dual media system (Cabeza, Martorell, Miró, Fernández, & Barreneche, 2015).

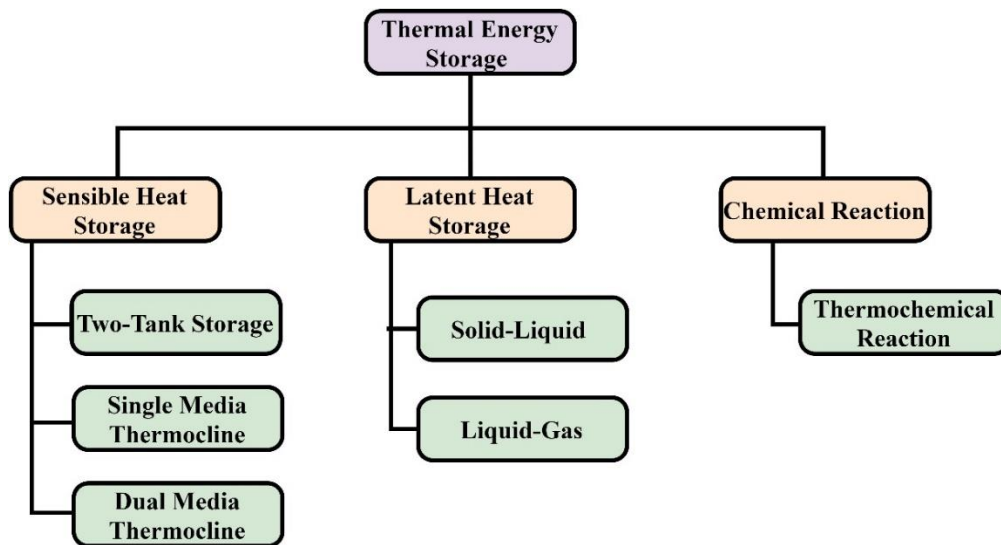


Figure 2-5: Classification of TES system

Thermal storage media itself does not participate in the heat exchange process; instead, charging and discharging takes place through the circulation of heat transfer fluid (Alptekin & Ezan, 2020; Z. Wang, 2019). Figure. 2-6 shows the functional characteristics of the TES system. TES has many advantages over mechanical or chemical storage. The main reasons are the lower capital costs and higher operational efficiency than mechanical or chemical storage systems. A TES system stores the thermal energy in three forms: SH, LHV, and reversible chemical reactions (Chang, Li, Xu, Chang, & Wang, 2015; Kuravi, Trahan, Goswami, Rahman, & Stefanakos, 2013).

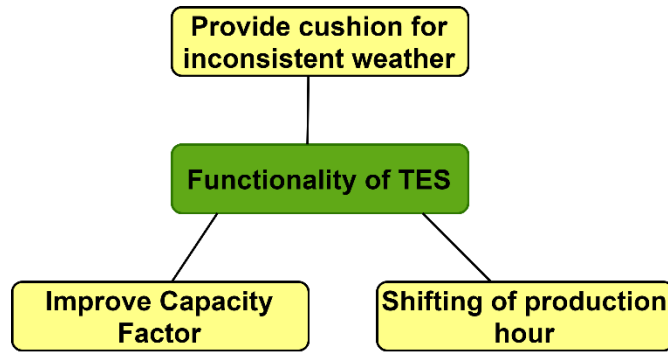


Figure. 2-6: Functionality of TES systems

Aneke et al. (Koller, Hofmann, & Walter, 2019) have illustrated the share of different TES technologies regarding the quantity of energy stored. Molten salts are widely used in CSP's, and account for almost 77% of stored thermal energy. Mehari et al. (Mehari, Xu, & Wang, 2020) has reviewed TES systems based on the absorption cycle. With the absorption cycle based TES, both hot and cold storages are possible. This type of storage system has a high storage density, so the system is usually compact. It is broadly categorized into two types, namely single-stage absorption and double stage absorption TES.

2.4 TWO-TANK THERMAL ENERGY STORAGE SYSTEM

In the two-tank molten salt TES system, solar energy can be stored in the hot and cold reservoirs using molten salt. The MSTES system offers high temperatures when used as receiver fluid instead of thermal oil. High-temperature molten salt provides high-temperature steam and better efficiency (Boretti, Castelletto, & Al-Zubaidy, 2019). The block diagram of molten salt TES system is shown in Figure. 2-7.

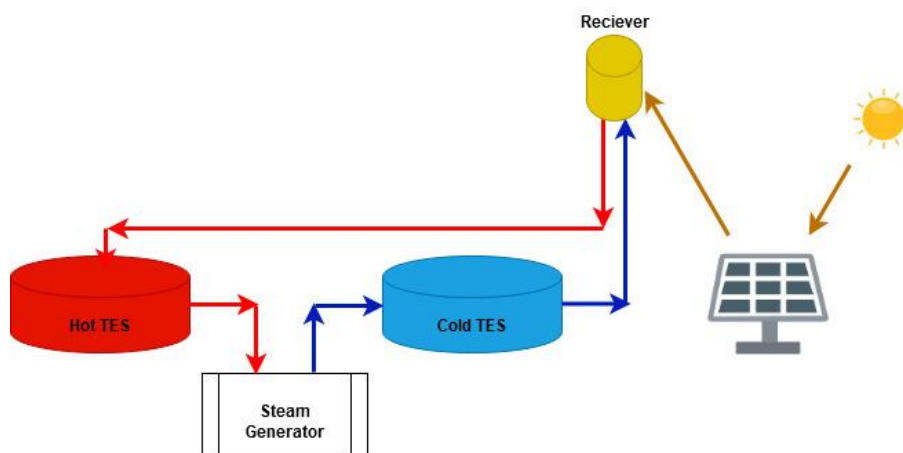


Figure. 2-7: Molten salt TES system

Two tank systems consist of two tanks, namely a hot tank and a cold tank. Hot tank to store the material at a higher temperature and cold tank to store the material at a lower temperature (“Advances in Thermal Energy Storage Systems: Methods and Applications - Google Books,” n.d.; Araújo & Medina T., 2018; Pacheco, Showalter, & Kolb, 2013; Ushak, Fernández, & Grageda, 2015). Most TES systems with two tanks use nitrate salts as a storage material. This type of technology is widely used in parabolic trough collectors and central tower-based solar power plants. All CSP plant operational from year 2014 to 2018 was based on TES, and nearly 17 GWh of the available TES was entirely based on two tanks of molten salt (Kusch-Brandt, 2019). The TES enables CSP as a dispatchable source of power by providing grid flexibility. Solar salt ($\text{NaNO}_3\text{-KNO}_3$: 60-40%) and HITEC ($\text{NaNO}_3\text{-KNO}_3\text{-NaNO}_2$: 7-53-40 wt%) are the most common molten salt used in CSP plant (Nunes, Queirós, Lourenço, Santos, & Nieto de Castro, 2016a). Additionally, Li et al. (X. Li, Wu, Wang, & Xie, 2018) suggested a eutectic ternary mixture of $\text{NaCl-NaF-Na}_2\text{CO}_3$ based on the thermodynamic and experimental approach. The eutectic point of ternary mixture consists of $X_{\text{NaF}} = 21.66$ mol %, $X_{\text{NaCl}} = 41.87$ mol% and $X_{\text{Na}_2\text{CO}_3} = 36.47$ mol% at temperature of 849 K. Furthermore, results were verified experimentally using DSC method. The thermophysical properties of molten salt can be determined specifically using the thermal analysis method. The molten salt with two tanks has a higher melting point and required additional heating to prevent clogging of the flow tubes. Hoffmann et al. (Nunes, Queirós, Lourenço, Santos, & Nieto de Castro, 2016b) developed a low temperature and inexpensive molten salt and reduced the cost of auxiliary heater used to maintain the temperature above the melting point. Peiro et al. (Peiró et al., 2018) conducted an empirical pilot-scale review of the TES system to test the viability of storage material, HTF, and CSP components on the integration of TES with CSP facility. The author recommended uniform heating to avoid any kind of vapor or air along with the thermal stress. Zhu et al. (Zhu, Yuan, Zhang, Xie, & Tan, 2019) carried out numerical investigation to identify the effect on thermocline behavior considering radiative losses. In the high-temperature molten salt TES system, however, the radiative heat transfer increases with an

increasing temperature. In the high-temperature TES system, radiative heat transfer cannot be neglected due to its high proportion of total heat transfer. The radiation model used by the author to investigate thermal performance was a discrete coordinate method. Numerical simulation (Torras, Pérez-Segarra, Rodríguez, Rigola, & Oliva, 2015) based on a modular- object-oriented methodology was carried out to examine critical parameters for the TES system. The parameter investigated are metrological data, insulation thickness, and foundation of the TES system. The thickness of insulation is the important parameter for the design of the tank. However, the foundation of the tank has not a great impact on the TES system. Cocco et al. (Cocco & Serra, 2015) did a numerical investigation to compare the two-tank TES system and thermocline tank for ORC. The result shows that the molten salt *TES* system has high-energy conversion efficiency as compared to the thermocline tank. However, the thermocline tank is economically more viable as compared to the two tank TES systems.

2.5 THERMOCLINE TANK SYSTEM

Two-tank molten salt TES systems are not economically so viable due to their initial cost. To overcome the limitations of TES system uses molten salt, a single tank TES system came into existence. The single media thermocline system consists of high-temperature HTF, which increases its temperature and energy content of working fluid in solar field and power block respectively. The power block generally consists of a vapor power cycle or gas power cycle; the selection is based on requirement and space. In a thermocline tank, hot and cold fluid are stored in the same tank, and hot fluid is always lies above the cold fluid due to the difference in density. The performance of the Thermocline container depends on the thermal stratification of the Thermocline container. However, the thermocline thickness also plays a major role in thermal performance tank. Figure. 2-8 shows the single medium thermocline tank for CSP application. Water-based thermocline tanks operate at lower temperature differences as compared to molten salt-based thermocline tanks.

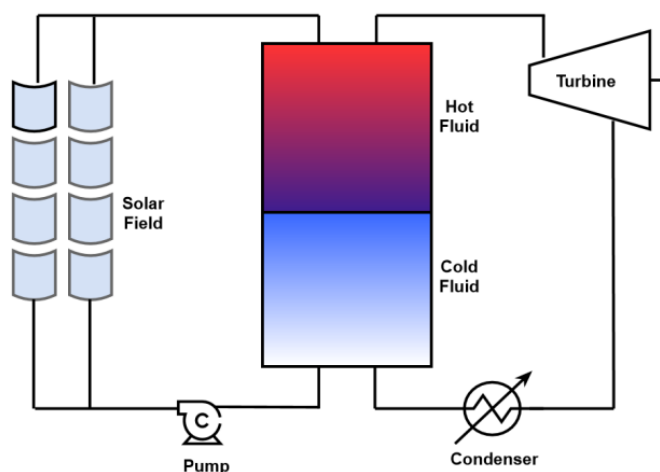


Figure. 2-8: Single Media TES system for CSP application

Thermocline tanks for molten salt have higher thermal stratification forces. In order to ensure a higher degree of thermal stratification in the thermocline system; the distributor is fitted at the top so that the flow is uniform and no mixing of hot and cold fluid can take place. Thermal stratification can be improved by using perforated inlet and a slotted inlet. For the flow rate is 5 L/min , the discharge efficiency is 21% higher than that of the direct inlet, and when the flow rate is increased to 15 L/min , the discharge efficiency is 40% higher than that of the direct inlet (S. Li, Li, Zhang, & Wen, 2013). According to the study carried out by Reddy et al. (Reddy, Jawahar, Sivakumar, & Mallick, 2017) the movement of thermocline thickness is rapid in solar salt as compared to that of HITEC. The author has also studied the effect of porosity on charging and discharging effectiveness. The result shows that discharge effectiveness drops with an increase in voids for all kind of HTFs. As values of porosity increases from 0.1 to 0.7, the discharge effectiveness falls continuously. The most suited HTF for thermocline tanks is Therminol if it is not being subjected to high pressure. Baba et al. (Filali Baba et al., 2020) has estimated the thermal performance of a thermocline TES system using a dimensional model based on the dual-phase approach. Three critical variables were examined namely: thermocline zone thickness, dimensionless discharge time, and discharge efficiency. Gajbhiye et al. (Gajbhiye, Salunkhe, Kedare, & Bose, 2018) used eccentrically mounted vertical porous flow distributor to maintain the tank's thermal stratification. The author has also investigated the effect of Peclet

number on thermocline thickness. It has been found that at a low diffusion rate at a higher Peclet number leads to smaller thermocline thickness.

2.6 DUAL MEDIA PACKED BED THERMAL ENERGY STORAGE SYSTEM

Dual media thermocline tank consists of storage material in the form of small pebbles and HTF, as shown in Figure. 2-9. The storage material reduces the required HTF volume and thus reduces the cost of the TES system. In a single medium thermocline tank, the quantity of HTF needed is considerable. The HTF used in CSP applications are Therminol VP1, Therminol 66, Caloria HT 43, and other synthetic HTFs. The cost of HTF required in a single media TES tank is very high; therefore, it is not so economically viable. The other factor that impedes the commercialization of a single media tank is thermal ratcheting. Thermal ratcheting is mechanical failure due to cyclic heating and cooling, which causes the tank to expand and contract. To overcome the limitation of the tank, a single media tank has been replaced with a dual media tank. The dual media TES system consists of storage material in the form of pebbles. These pebbles are randomly added to the tank, which results drop in the volume of HTF required. The void fraction (ε) of the dual Media TES system can be defined as:

$$\varepsilon = \frac{V_T - V_p}{V_T} \quad \text{Eq.2-1}$$

Here, V_T is the tank volume and V_p is the pebbles volume.

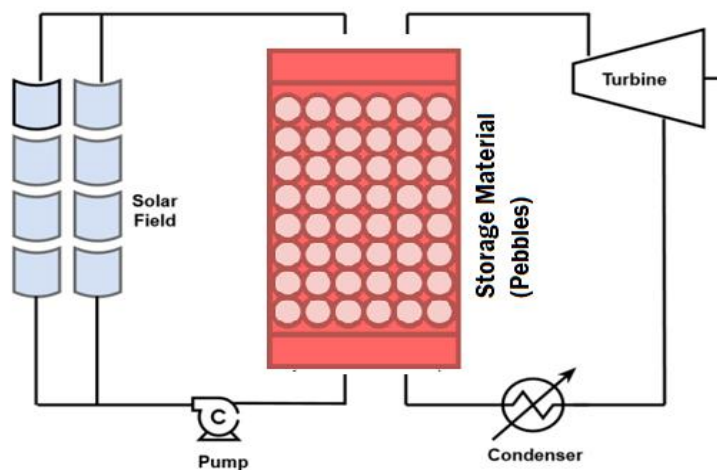


Figure. 2-9: Dual media packed bed TES system for CSP application

The major advantage of packed bed storage system (PBSS) is to reduce storage costs. It can be operated at wide temperature ranges, and it is simple and efficient. PBSS with improved thermal stratification increases the collector efficiency. Unlike other TES systems, PBSS has high chemical stability, high safety and negligible corrosion issues. PBSS consists of a storage medium, and energy exchange system. Storage system stores thermal energy in the form of SH, LH, or in the thermo-chemical form (Erregueragui, Boutammachte, & Bouatem, 2016). The energy transfer mechanism takes the help of HTF, which supplies or extracts energy. PBSS contains packing elements in the form of particles that act as a heat storage medium. There are voids in the bed, HTF occupies these voids, and it exchange heat with the storage material (Gautam & Saini, 2020). Charging and discharging are done by shifting thermocline by circulating *HTF* through the packed bed. The *HTF* fluid is heated through solar radiation and then supplied to storage material, which then takes up the heat. On the other hand, during the discharging operation to extract the stored energy, the flow direction is reversed, low-temperature fluid is passed through the heated bed. Low-temperature fluid gains heat and leaving at a higher temperature, which can be utilized in the power cycle. Charging is done from the top to exploit the buoyancy effect to maintain thermal stratification where the hot *HTF* is at the top and cold *HTF* at the bottom. A higher degree of thermal stratification in a packed bed provides higher efficiency, as higher exergy can be recovered when the mixing of hot and cold zones is minimal (Gautam & Saini, 2020; Haller et al., 2009; Laing & Zunft, 2015; Zanganeh et al., 2012). The particle size in packed bed TES system ranges from few mm to several cm; it is one of the main characteristics of the packed bed. A packed bed with a minimum thermocline thickness contains a high exergy than a well-mixed bed, which has a lower temperature variation in the thermocline region. The dimensioning of the storage tank in PBSS depends on the required load, and is proportional to the collector area. A packed bed has inlet and outlet at top and lower part of the tank to foster thermal stratification (Almendros-Ibáñez, Fernández-Torrijos, Díaz-Heras, Belmonte, & Sobrino, 2019; Lugolole et al., 2019). Air-based solar systems are best suited to packed bed storage system.

The size of storage system depends on variables such as storage temperature, material, losses, etc. Packed beds are compact, simple, and economical. Steel gives the best results as a storage material in packed bed because it has a higher storage rate and higher storage capacity than rock and aluminium (Singh, Saini, & Saini, 2010; L. Wang, Yang, & Duan, 2015). Bruch et al. (Bruch, Fourmigue, Couturier, & Molina, 2014) illustrated by testing that mass flow rate, temperature difference, and partial load affects axial temperature profile. It is also an indication of the fact that dual-media thermocline tanks are robust and controllable and therefore well suited for CSP. Nandi et al. (Nandi, Bandyopadhyay, & Banerjee, 2018) has studied the thermocline system and developed a computational model of the same. It was concluded that aspect ratio and porosity play the most important roles in the design of the thermocline energy storage system. A transient 3D model is developed to predict the thermal behavior of packed bed. Wang et al. (L. Wang et al., 2015) has studied the influence of flow distribution in a dual-media thermocline system. It has been shown that if the flow distribution at the inlet is non-uniform, then the thickness of the thermocline decreases. So the flow distribution does not affect the performance of the tank much. In order to protect the tank from thermal ratcheting, which takes place due to constant thermal expansion and contraction, the tank is given a dodecagon cross-section, the diameter of which decreases from top to bottom. Also, the tank is imbedded in the ground. All of these design factors help to utilize the lateral earth pressure with a higher load-bearing capacity and to reduce the normal force on the tank walls during thermal expansion. Another advantage of a conical-shaped tank over a cylindrical tank is the larger storage volume at the top of the tank where hot fluid rests, which is at a higher temperature. This leads to high V/A_s (Volume-surface area) area ratio. On the other hand, the volume at the bottom is less where cold fluid rests and most of the energy is withdrawn, so that less storage material is required (Zanganeh et al., 2012). Liu et al. (Liu et al., 2016) investigated STHX with various TES media. Oro et al. (Oró, Castell, Chiu, Martin, & Cabeza, 2013) examined the stratification in a packed bed TES system. To study thermal stratification, two methods were discussed, one based on density and other based

on the temperature. A TES system with better stratification and a larger temperature gradient has a higher exergy. Rao et al. (Ravi, Rao, Niyas, & Muthukumar, 2017) performed experimental analysis on LAB scale packed bed model using Hi-tech therm 60 as HTF. The study revealed cast steel prototype give better heat transfer rate as compared to concrete prototype.

2.7 PARAMETER TO EVALUATE PERFORMANCE OF TES SYSTEM

Figure 2-10 shows gradual increase in thermocline thickness with increasing mass flow rate. The thermocline thickness for molten salt is not uniform in the radial direction due to the formation of velocity boundary layer near the wall (ELSiHy, Liao, Xu, & Du, 2021). However, the thermocline thickness for packed bed TES system is uniform along the radial direction.

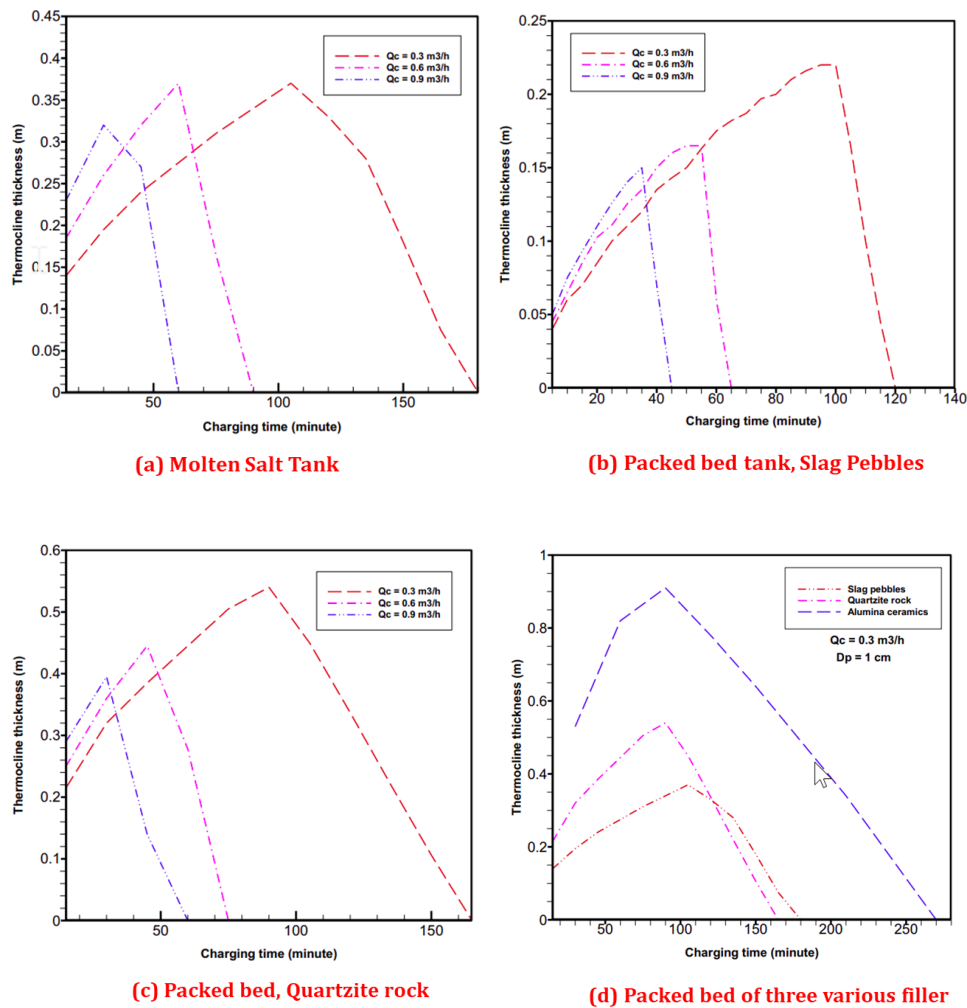


Figure 2-10: Thermocline thickness of various storage material (ELSiHy et al., 2021)

The thermocline thickness of three different filling materials are compared and shown in the Figure 2-10. The thermocline thickness of alumina is greater than that of quartzite rock and slag pebbles. The higher thermocline thickness of alumina is due to its higher thermal diffusivity value. The thermophysical properties of alumina, quartzite and slag pebbles are given in Table 2-1.

Table 2-1: Thermophysical properties of rocks

Pebbles	ρ (kg/m ³)	k (W/mK)	C _p (J/Kg.K)	α (Thermal Diffusivity)
Alumina	3690	30	780	1.04232E-05
Quartzite	2500	5.69	830	2.74217E-06
Slag pebbles	2850	1.66	895	6.50789E-07

The thirmocline thickness of the dual and single media tanks are compared in Figure 2-11. The thirmocline thickness of single media tank is smaller than that of a double media tank due to the low value of thermal conductivity of HTF in single media compared to the equivalent thermal conductivity of HTF and filling media in dual media tanks.

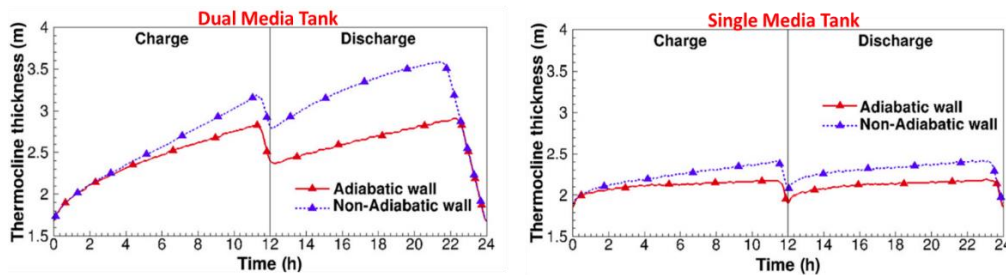


Figure 2-11: Thermocline thickness of dual media and single media tank
(Mira-hern & Flueckiger, 2015)

2.8 CHARACTERIZATION OF PRESSURE DROP IN A DMT – TES SYSTEM

In a packed bed TES system or dual media TES system, heat losses are accompanied by pressure loss, which increases the pumping power of the TES system. In a packed bed, the pressure drop of the TES system is a major as it decreases the storage efficiency (Baghapour, Rouhani, Sharafian, Kalhori, & Bahrami, 2018a). The parameters responsible for various heat and pressure losses are a void fraction, the diameter of storage material, aspect ratio, and temperature. Several correlations have been developed in the literature by

various authors to investigate the pressure drop. The minimization of pressure drop means a reduction in the frictional effect, which can be achieved by increasing the particle diameter (Of, 2016). Theoretically, the pressure drop in packed bed can be calculated by considering parallel conduits and assuming fully developed flow. Pressure drop is due to inertial and viscous effect prevails at different Reynolds number. Inertial effects and viscous effects are dominating at higher and lower Reynolds number respectively. In a packed bed, the relationship between the pressure gradient and superficial velocity ratio is a linear function of the mass flow rate. Ergun et al. (Ergun & Orning, 1949) have given an empirical relationship to find pressure gradient across the packed bed, and a number of authors have largely accepted this empirical relationship. Later on, most of the authors suggested that constants in Ergun equations depend on various parameters like aspect ratio and temperature of HTF (Of, 2016). Ergun equation, Eq. 2-2, is applicable for a wide range of Reynold number, as it is obtained by combining both laminar and turbulent expression (Media, 2019).

$$-\left(\frac{\partial P}{\partial x}\right) = 150 \left(\frac{\mu V_s}{d_p^2}\right) \frac{(1-\varepsilon)^2}{\varepsilon^3} + 1.75 \frac{\rho V_s^2 (1-\varepsilon)}{d_p \varepsilon^3} \quad \text{Eq. 2-2}$$

The Ergun equation was obtained by assuming negligible friction near the wall (Wall effect). Few authors suggested that the inclusion of wall effect is necessary for any packed bed TES system. Modified Ergun equation, Eq. 2-3, can be used to find pressure gradient considering wall effect (Mehta & Hawley, 1969).

$$-\left(\frac{\partial P}{\partial x}\right) = \left(150 \left(\frac{\mu V_s}{d_p^2}\right) \frac{(1-\varepsilon)^2 M}{\varepsilon^3} + 1.75 \frac{\rho V_s^2 (1-\varepsilon) M}{d_p \varepsilon^3}\right) \quad \text{Eq. 2-3}$$

Where, Eq. 2-4, can be used to find parameter M . However, this equation is valid only for $\frac{D_c}{D_p} > 7$.

$$M = 1 + \frac{4D_p}{6D_c(1-\varepsilon)} \quad \text{Eq. 2-4}$$

For, $\frac{D_c}{D_p} > 30$, wall effect can be neglected (Bruch, Fourmigué, & Couturier, 2014).

Moreover, the empirical result published in the literature was based on spherical shape storage material (Baghapour, Rouhani, Sharafian, Kalhori, & Bahrami,

2018b; Erdim, Akgiray, & Demir, 2015; Thabet & Straatman, 2018). However, only a few have considered non-spherical shape with the sphericity of the storage particles (du Plessis & Woudberg, 2008; L. Li & Ma, 2011; Mayerhofer, Govaerts, Parmentier, Jeanmart, & Helsen, 2011; Ozahi, Gundogdu, & Carpinlioglu, 2008; Partopour & Dixon, 2017; Rong, Zhou, & Yu, 2015). Guo et al. (Guo, Sun, Zhang, Ding, & Wen, 2017) did an experimental study to investigate the effect of aspect ratio ($1 < \frac{D}{d} < 3$) on pressure drop across packed bed. The packing arrangement of storage material has noticeable change in the pressure drop for same aspect ratio.

2.9 HEAT TRANSFER MODEL

The thermodynamic modeling of the thermal energy storage system can be subdivided into different groups (Doretto et al., 2019; Elouali et al., 2019; Vigneshwaran, Sodhi, Muthukumar, Guha, & Senthilmurugan, 2019). The modeling of the two-tank TES system, the single media TES system and the dual media TES system can be carried out using a continuous solid phase model, Schumann model, Single-phase model and concentric dispersion model (Ismail & Jr, 1999). The basic heat transfer models used to formulate the thermal energy storage system's transient behavior are shown in Figure 2-12.

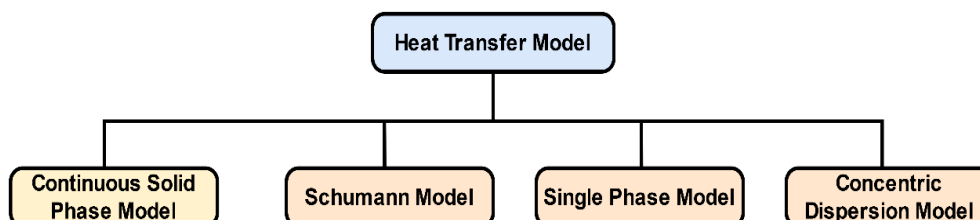


Figure 2-12: Heat Transfer Model

2.10 CONTINUOUS SOLID PHASE MODEL

Continuous solid phase model (CSPM) assumes a continuous storage medium instead of discrete solid particles. The heat transfer in the storage bed is considered to be in the axial and radial direction. The heat transfer equations (Eq. 2-5 & Eq. 2-6) of CSPM are:

$$\varepsilon \left(\frac{\partial T_f}{\partial t} + u \frac{\partial T_f}{\partial y} \right) = \frac{k_{fy}}{\rho_f c_f} \cdot \frac{\partial^2 T_f}{\partial y^2} + \frac{k_f}{\rho_f c_f} \left(\frac{\partial^2 T_f}{\partial r^2} + \frac{1}{r} \frac{\partial T_f}{\partial r} \right) + \frac{h_v}{\rho_f c_f} (T_s - T_f) - \frac{4U}{\rho_f c_f D} (T_f - T_\infty) \quad \text{Eq. 2-5}$$

$$(1 - \varepsilon) \left(\frac{\partial T_s}{\partial t} \right) = \frac{k_s}{\rho_s c_s} \cdot \frac{\partial^2 T_s}{\partial y^2} + \frac{k_s}{\rho_s c_s} \left(\frac{\partial^2 T_s}{\partial r^2} + \frac{1}{r} \frac{\partial T_s}{\partial r} \right) + \frac{h_v}{\rho_s c_s} (T_f - T_s) \quad \text{Eq. 2-6}$$

Here, T_s is the temperature of storage material and T_f is the temperature of HTF. The one-dimensional model of the above equation can be written by ignoring conduction in a radial direction. In this model, thermal diffusion in solid is considered by assuming a continuous solid phase. However, thermal diffusion inside the fluid can be considered in this model. Dispersed plug flow is assumed in this model (Kaguei, Shiozawa, & Wakao, 1976). Torrijos et al. (Fernández-Torrijos, Sobrino, & Almendros-Ibáñez, 2017) formulated the C-S model to study the thermocline behavior of the TES tank for the adiabatic wall and composite cylinder. Moreover, lumped capacitance approximation has been used by the author for $Bi = 0.15$. The study shows that thermal ratcheting can be increased or decreased by changing the heat transfer coefficient. However, the thermal stress studied by the author shows that thermal stress increases and decreases by 10% by doubling and reducing half the convective heat transfer coefficient (Flueckiger, Iverson, Garimella, & Pacheco, 2014). Nunez et al. (Cabello Núñez, López Sanz, & Zaversky, 2019) studied thermocline behavior using steelmaking slag as storage material. This numerical analysis has used a one-dimensional C-S model to investigate the practical viability of slag as storage material.

2.11 SCHUMANN MODEL

In the Schumann model, heat conduction in the radial direction can be neglected for the solid phase and assumes negligible heat conduction in HTF. The heat transfer equation (Eq. 2-7 & Eq. 2-8) for the Schumann model can be written as (Schumann, 1929):

$$\varepsilon \left(\frac{\partial T_f}{\partial t} + u \frac{\partial T_f}{\partial y} \right) = \frac{h_v}{\rho_f c_f} (T_s - T_f) - \frac{4U}{\rho_f c_f D} (T_f - T_\infty) \quad \text{Eq. 2-7}$$

$$(1 - \varepsilon) \left(\frac{\partial T_s}{\partial t} \right) = \frac{h_v}{\rho_s c_s} (T_f - T_s) \quad \text{Eq. 2-8}$$

Agalit et al. (Agalit, Zari, Maalmi, & Maaroufi, 2015) formulated the heat transfer model to investigate the cyclic behavior of the TES tank. The author developed a one-dimensional two-phase dynamic heat transfer model.

Moreover, this heat transfer model integrates temperature-dependent thermophysical properties of both solid and HTF. Modi et al. (Modi & Pérez-Segarra, 2014) studied the cyclic behavior of the storage tank using a one-dimensional Schumann model. The numerical validation of the model shows good agreement with the experimental study. Moreover, temperature-dependent correlation is used to obtain the thermophysical properties. The results also suggest two important properties like cyclic behavior and time required to attain the thermal equilibrium to access the storage tank's thermal behavior. The research shows that the Schumann model is a more accurate and simplified model to access the thermal performance of the TES system. Tigue et al. (Mctigue & White, 2020) studied the thermo-hydraulic behavior of a segmented packed bed using the simplest model (Schumann) and considered a one-dimensional condition. The research shows that losses due to thermal equilibration can be reduced by segmentation of the storage tank. However, the author has also introduced multi-objective optimization for efficiency and capital cost. The thermodynamic analysis based on the modified Schumann model was done by (Mctigue, Markides, & White, 2018). Nevertheless, the effect of cycle duration on the performance of the storage tank was also studied.

2.12 SINGLE PHASE MODEL

The Single-phase model is developed by using a two-phase energy model. This model is more effective in thermal modeling of the TES system with high thermal conductivity and high heat capacity storage material compared to HTF. The energy equation for a single-phase model can be written as:

$$\begin{aligned} & \left[(1 - \varepsilon)\rho_s c_s + \varepsilon\rho_f c_f \right] \frac{\partial T}{\partial t} + \varepsilon\rho_f c_f v_f \frac{\partial T}{\partial y} = \left[\varepsilon k_f + (1 - \right. & \text{Eq. 2-9} \\ & \left. \varepsilon)k_s \right] \frac{\partial^2 T}{\partial y^2} - U_w a_w (T - T_\infty \end{aligned}$$

Bayon et al. (Bayón & Rojas, 2013) developed a single-phase one dimensional model for characterization study of Thermocline in TES tank. The non-dimensional form of the energy equation can be solved numerically, and the effect of non-dimensional velocity on thermocline thickness can be studied. The result shows that efficiency increases an increase in dimensionless velocity.

However, thermocline thickness decrease with an increase in dimensionless velocity.

2.13 CONCENTRIC DISPERSION MODEL (C-D MODEL)

In the C-D model, concentric temperature variation for each particle is considered. This model assumes discrete particles in contrary to the C-S model. The two-phase energy equation (Eq. 2-10, Eq.2-11, Eq.2-12) for the C-D model can be written as (Kaguei et al., 1976):

$$\frac{\partial T_s}{\partial t} = \alpha_s \left(\frac{\partial^2 T_s}{\partial r^2} + \frac{2}{r} \frac{\partial T_s}{\partial r} \right) \quad \text{Eq. 2-10}$$

$$k_s \left(\frac{\partial T_s}{\partial r} \right) = h_p (T_f - T_s), \text{ at } r = R \quad \text{Eq.2-11}$$

$$\frac{\partial T_f}{\partial t} = \alpha_{ax} \frac{\partial^2 T_f}{\partial y^2} - U \frac{\partial T_f}{\partial y} - \frac{h_p a_v}{\varepsilon C_f \rho_f} (T_f - (T_s)_R) \quad \text{Eq.2-12}$$

Odenthal et al.(Odenthal, Steinmann, & Zunft, 2020) Implemented C-D Model in MATLAB/Simulink environment to investigate the thermal performance of the regenerative horizontal flow storage tank. In addition, the author has also considered gaseous flow in a regularly shaped channel. The assumption used in this model was Plug flow, Ideal gas, Incompressible flow, No chemical reaction, and homogenous distribution of storage material. The research also shows that the deviation in temperature distribution without considering the correction factor is 10%. However, through the correction factor, the author wants to show the effect of the plug flow assumption in temperature distribution. Zhao et al. (Zhao, Cheng, Liu, & Dai, 2017) used a dimensional enthalpy based C-D model to study the performance of TES for CSP application. However, the author presented the strategy to estimate the tank size to integrate TES with CSP technology. Niedermeier et al. (Niedermeier et al., 2018) studied the performance of the storage tank under two different heat transfer fluid, i.e., sodium and molten salt using a one-dimensional C-D model. The research shows that smaller size storage material gives better discharge efficiency for sodium. However, larger size storage material is suitable for molten salt. Galione et al. (Galione, Pérez-Segarra, Rodríguez, Torras, & Rigola, 2015) modeled a multi-layered-solid-PCM thermal energy storage system using a one-

dimensional C-D model. The study shows that thermocline degradation can be prevented by using PCM as a dispersed storage material.

2.14 TECHNICAL CHALLENGES OF TES FOR CSP APPLICATION

The technical challenges associated with TES integration with CSP are discussed in Table 2-2. At high temperatures, corrosion is the main problem and most researchers have done several studies to minimize the rate of corrosion at high temperatures. Stress corrosion is a major concern that needs more discussion to make the system more commercially viable. However, intermittent nature and temperature fluctuations at the inlet of TES tank leads to a loss of exergy. Moreover, this problem can be resolved by using phase change material at the inlet and outlet of the tank. Temperature degradation in SMT and DMT tank is another concern that limits the use of SMT tank. Indeed, thermal ratcheting is one of the major concerns, making the system commercially not so viable. As the DMT tank is economically more feasible than other storage systems, and its failure due to thermal ratcheting limits its application in the CSP plant.

Table 2-2: Technical challenges of TES model

Author	Objective	Numerical /Experimental model	Challenges	Outcomes
Johnson et al.(Johnson, Bates, Dower, Bueno, & Anderson, 2020)	To study exergetic efficiency of packed bed TES in integration with sCO ₂ Brayton cycle	One and two-equation numerical model	Temperature degradation	<ul style="list-style-type: none"> Heat loss and thermal diffusion inside the bed is the primary source in the reduction of exergetic efficiency
Ahmed et al. (Ahmed, Elfeky, Lu, & Wang, 2019)	Economic feasibility and performance study of combined sensible and Latent heat TES system	Energy balance coupled with enthalpy method	Mechanical failure due to thermal ratcheting	<ul style="list-style-type: none"> Capacity cost for combined TES system is higher The hybrid configuration has a 26% higher capacity as compared to the sensible based TES system Combine TES system is the most viable configuration
Koller et al.(Koller et al., 2019)	Integration of TES using MILP formulation	Mixed Integer Linear Programming (MILP) model	Saturation of PBR while charging and discharging.	<ul style="list-style-type: none"> Significant increase in the computational effort using MTR formulation Saturation losses should always be considered as it has a notable impact on the performance of the system.
Chang et al. (Chang et al., 2015)	Design of 2 MWh molten-salt thermocline tank and investigation of its heat transfer and fluid dynamics.	Transient two-dimensional and two-temperature model.	Non-uniformity of temperature at the inlet of the TES tank.	<ul style="list-style-type: none"> If solar salt is used as HTF, the thermocline growth is slowest. Non-uniformity in inlet velocity would increase the thickness of the thermocline region because mixing would increase.

				<ul style="list-style-type: none"> • Solar salt has the fastest cooling rate and a sharp temperature gradient.
Yang et al.(Yang & Cai, 2019)	Analysis of a hybrid TES system	One dimensional plug flow.	Heat loss from pipes and valves.	<ul style="list-style-type: none"> • Max temperature difference is observed at the middle of the thermocline. • As the charging time increases, the max temperature difference reduces.
Zaversky et al.(Zaversky, García-Barberena, Sánchez, & Astrain, 2013)	Study of transient molten salt TES system	Transient storage tank model.	Heat loss from tanks outer surface.	<ul style="list-style-type: none"> • Variation in the heat transfer coefficient is negligible • Heat flows within storage tank walls, and temperature distribution are not in steady state.
Grirate et al.(Grirate et al., 2016)	Study and performance analysis of 6 different types of rocks used as storage material in the thermocline tank storage system.	Validated numerical model.	Compatibility of basalt rock with synthetic oil (HTF).	<ul style="list-style-type: none"> • Quartzite and cipolin are the most suitable rocks, which can be used as filler materials. • The best thermal performance was shown by basalt rock.
Gonzalez et al. (González, Pérez-segarra, Lehmkuhl, Torras, & Oliva, 2016)	Analysis of thermo-mechanical properties of a packed bed thermocline storage.	Thermo-Mechanical Model	Energy storage in shorter tanks.	<ul style="list-style-type: none"> • Due to external insulation temperature, difference is minimal • The low-temperature difference in thermocline leads to better storage performance. • If the tanks are taller, performance is better.

Wu et al.(Wu, Li, Xu, He, & Tao, 2014)	Analysis of different structures of concrete tank and studying their thermocline behaviour.	Schumann Model.	Only the lumped capacitance method can be used for the analysis; other methods are time-consuming.	<ul style="list-style-type: none"> • Thermocline thickness at the time of discharge is different for different structures. • On decreasing the inlet fluid velocity from 0.002 m/s to 0.001 m/s the discharging efficiency falls from 83.1% to 60%.
Xu et al.(C. Xu, Wang, He, Li, & Bai, 2012)	Thermal behavior of packed bed	Transient, two-dimensional, two-phase model.	Wall temperature influences the molten salt near it.	<ul style="list-style-type: none"> • During the discharging process, the thermocline region moves upward with little expansion. • The two insulation layers help to achieve uniform temperature throughout the cross-section. • Thermocline thickness increases if: the heat transfer rate between the filler material and fluid is increased or if the thermal conductivity of the filler is increased.
Esence et al.(Esence, Bruch, Molina, Stutz, & Fourmigué, 2017)	Review on the modelling of packed bed thermal energy storage.	One and two-dimensional models.	Preserving thermal stratification during standby periods.	<ul style="list-style-type: none"> • Thermal stratification depends on AR of the tank, charging and discharging conditions, solid filler geometry, fluid, and solid physical properties.
Bayon et al.(Bayón, Rivas, & Rojas, 2014)	Performance analysis of thermocline tanks during dynamic processes and standby period.	Single-phase one-dimensional model.	While extracting thermocline the outlet temperature decreases.	<ul style="list-style-type: none"> • Temperature degradation in molten salt with storage material is more as compared to the molten salt only

				<ul style="list-style-type: none"> • There is an increase in the energy inside the tank after every discharge, while there is a decrease in the energy stored by the tanks.
Lew et al.(Lew, Li, & Stephens, 2011)	Study of dual media TES system	Schumann model.	Heat losses	<ul style="list-style-type: none"> • If the charge time is higher as compared to discharge time, more energy can be stored, and a higher amount of energy can be discharged.
Torras et al.(Torras et al., 2015)	Evaluation and simulation of two-tank TES system for different parameters.	Numerical analysis using Schumann model	Shut down of plant due to salt freezing and heat loss.	<ul style="list-style-type: none"> • Configuration of the base does not have much to do with the heat losses, but it is to be taken into consideration for the design of the tank.
Lu et al.(Lu, Yu, Ding, & Yuan, 2015)	Molten salt storage system with phase change material	Transient and two-dimensional model.	Melting point of PCM	<ul style="list-style-type: none"> • The use of a packed phase change bed increases the discharging efficiency. • An increase in the quantity of phase change material increases effective discharging efficiency.

2.15 TECHNICAL CHALLENGES OF TWO-TANK MOLTEN SALT TES SYSTEM

The TES molten salt storage system is a commercially developed technology and has the potential for CSP integration. However, there are some technical challenges that must be addressed in the future in order to make this system more commercially viable. The technical challenges of the molten salt TES system for CSP applications are shown in Figure 2-13.

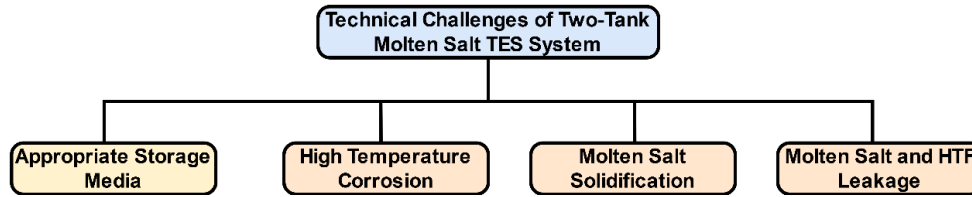


Figure 2-13: Technical challenges of molten salt TES system

The ideal media for MSTES has a liquidus range of 0-1300 °C with little or no vapor pressure. MSTES can work at high temperature leading to the higher thermal efficiency of the power cycle. The temperature range of molten salt is 250 °C to 1000 °C and has a wide variety in this range. Low melting point (LMP) molten salt has a wide range of liquidus temperature and good electrical and thermal conductivity, low viscosity, high chemical, thermal stability, and environmental friendliness. The liquidus range of molten salt varies from 150 to 600 °C and can be increased by mixing different compositions. The main challenge of the molten salt mixture is the high melting temperature, which blocks the pipeline in winter due to low temperature. Therefore, an extra auxiliary heater is required to maintain the melting temperature, which increases the overall cost of the system. However, research is going on to develop low melting range molten salt with a wide range of liquidus temperature, high chemical and thermal stability, and low viscosity (States, Storage, Tes, & Fluid, 2011). LMP molten salt for CSP application is shown in Table 2-3.

Table 2-3: LMP molten salt for CSP application

Property	Solar Salt	Hitech	Hitech XL (Calcium Nitrate Salt)
Composition			
NaNO ₃	60	7	7
KNO ₃	40	53	45
Na NO ₂		40	

Ca(NO ₃) ₂			48
Freezing point (OC)	220	142	120
Upper Temperature (OC)	600	535	500
Density @ 300°C, kg/m ³	1899	1640	1992
Viscosity @300°C, cp	3.26	3.16	6.37
Heat capacity @ 300°C, J /kg. K	1495	1560	1447

Molten salt has low cost and favorable thermophysical properties, which makes the system economically more viable. Salt is a combination of fluoride, chloride, nitrate, carbonate, and sulphates and has a wide range of applicability. However, corrosion of containment due to high temperature is a challenge.

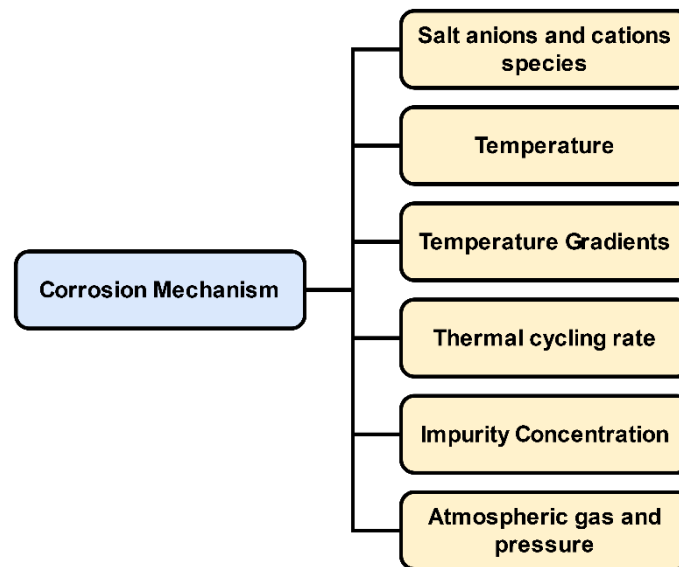


Figure 2-14: Variables in the corrosion mechanism

The corrosion mechanism in the molten salt TES system is very complex and depends on many variables shown in Figure 2-14. To prevent corrosion in chloride and fluoride, the salt must be very pure and free from moisture (Bell, Steinberg, & Will, 2019). Stress corrosion cracking is another phenomenon, which occurs, in the molten salt TES system. Stress corrosion cracking is intergranular corrosion concatenate with mechanical stress and needs to be addressed for life cycle assessment. The major factor influencing corrosion are shown in

Figure 2-15. The other two factors, which usually influence the thermo-economical performance of the MSTES system, are leakage of molten salt through the connection and solidification of molten salt.

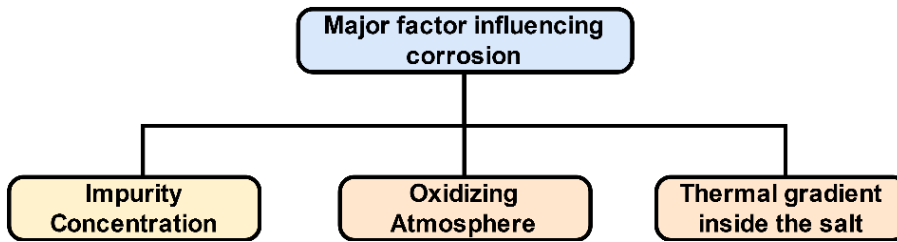


Figure 2-15: Major factor influencing corrosion

It is always recommended to check the connection point to prevent leakage. Spiro-metallic joints can also be used in order to avoid leakage along with continuous monitoring, as suggested. However, solidification is due to the heat loss to the surroundings and can be prevented by proper insulation. The solidification causes blockage in pipe and pumps, leading to the shutdown of the plant (Prieto et al., 2018).

2.16 TECHNICAL CHALLENGES OF SINGLE MEDIA THERMOCLINE TANK

MSTES system requires two-tank and an auxiliary heater to prevent solidification and increase the overall levelized cost of electricity. To overcome this difficulty, single tank thermocline system was developed. In SMT, a single tank is used to store hot and cold fluid, reducing the system's overall cost. The two main problems usually found in the SMT tank are temperature degradation and operational risk mitigation, as shown in Figure 2-16. The temperature degradation destroys the thermal stratification of the tank and reduces the utilization factor.

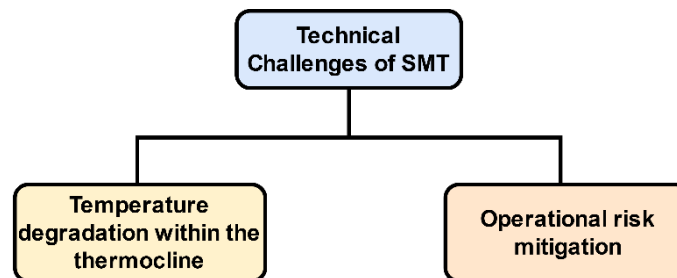


Figure 2-16: Technical challenges of SMT for CSP application

In the thermocline system, temperature degradation is the primary issue that needs to be addressed. Several methods have been developed, i.e., flushing, floating barriers, and active thermocline management, to minimize the effect due to thermal degradation. During flushing, the system operates at diminishing

efficiency, followed by energy loss. The other development to maintain the thermal stratification of the tank is the floating barrier. In this method, a floating insulating material with a density near to hot and cold fluid maintains thermal stratification. In active thermocline management, the HTF is drawn out from the thermocline region rather than the outlet of the tank. This method increases the overall cost of the system due to the need of an extra valve to draw fluid from the thermocline region. SMT tank relies on a single tank, thus increases the risk of a complete shutdown of the plant during failure. Therefore, an extra tank is required for backup for the continuous functioning of the system.

2.17 TECHNICAL CHALLENGES OF DUAL MEDIA

THERMOCLINE SYSTEM (DMT)

To overcome the limitation of increased cost in SMT tank, DMT has come into existence. DMT requires HTF along with storage material to reduce the overall cost incurred due to HTF. DMT tank is economically more viable as compared to other systems. This system also has some technical challenges which already been addressed by several researchers. The technological challenges of the DMT tank are shown in Figure 2-17. In DMT, tank mechanical failure due to thermal ratcheting is the primary issue, which inhibits the application of DMT in CSP plant. Temperature degradation within the thermocline reduces the exergetic efficiency of the system and its effect can be minimized by flushing the thermocline region out of the tank. In DMT, tank use of storage material causes HTF contamination due to the wear of storage material.

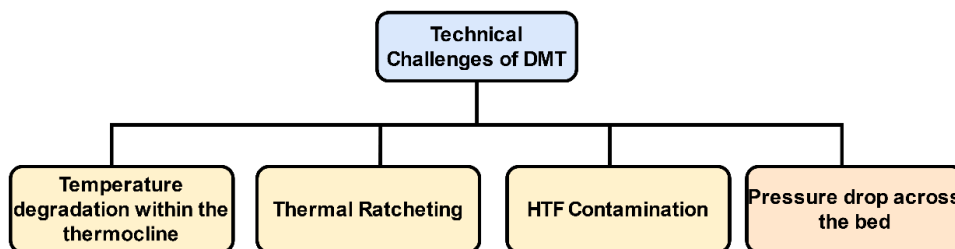


Figure 2-17: Technological challenges of DMT tank

The temperature degradation within the thermocline can be controlled by several methods shown in Figure 2-18. The active method called TCC (thermocline control) includes flushing, segmented storage, sliding flow, extracting, upgrading, and returning (Geissbühler, Mathur, Mularczyk, &

Haselbacher, 2019). Flushing flushes out HTF from the thermocline region, thus reduces the effect of thermal degradation and maintains the thermal stratification of the tank. However, the HTF flushes out has no use in the power cycle due to its low temperature and increases the pumping power. Segmented storage is another method, which inhibits temperature degradation. In segmented storage, the DMT tank is divided into several segments with ports between each segment.

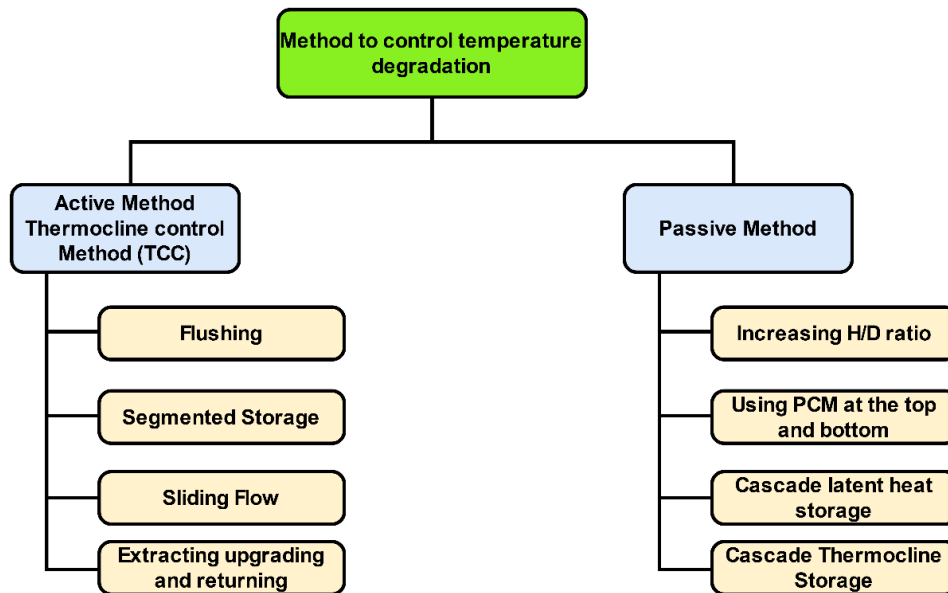


Figure 2-18: Method to control temperature degradation

Segmented storage maintains the thermal stratification of the tank by allowing the flow through multiple ports. There are many ways to segment the packed bed storage system and one possible way is shown in Figure 2-19. However, there is a possible trade-off between heat losses and thermal losses in the segmented packed bed storage system (Crandall & Thacher, 2004; Mctigue & White, 2020). In sliding flow, the multiple segments are charged consecutively. However, in extracting upgrading and returning method, HTF is extracted from intermediate segments, upgraded and returned to the inlet port. In the passive method, increasing H/D ratio increases the convective heat transfer and decreases the axial heat flow, thus diminishing the effect of thermal degradation. However, using PCM decreases the temperature fluctuation near the outlet and maintains constant outflow temperature (Geissbühler, Kolman, Zanganeh, Haselbacher, & Steinfeld, 2016).

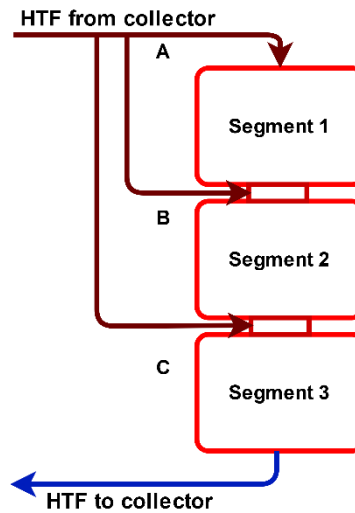


Figure 2-19: Segmented packed bed storage system [92]

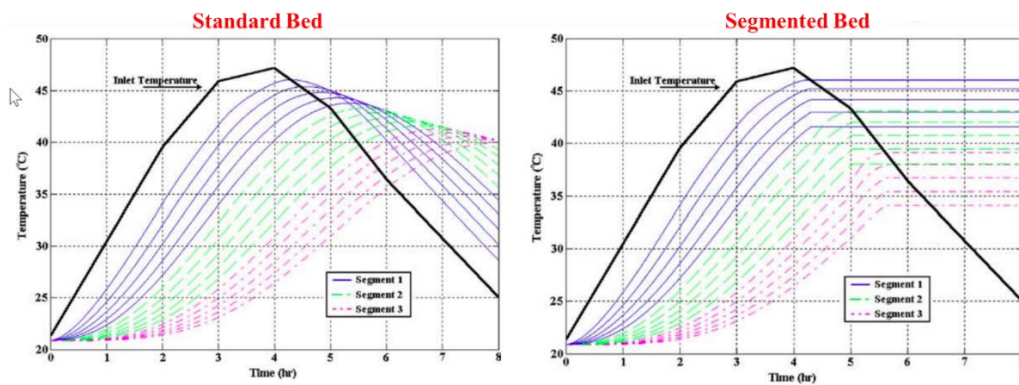


Figure 2-20: Temperature in standard and segmented bed (Crandall & Thacher, 2004)

Figure 2-20 shows the temperature in standard and segmented packed bed TES system. Indeed, the thermal stratification are maintained in segmented bed. The temperature variation up to 4h of charging are same for both standard and segmented bed. However, the outlet temperature at the end of charging is higher for segmented packed bed.

One of the most challenging and potential factors which lead to the failure of the system is thermal ratcheting. Thermal ratcheting is due to the different coefficient of thermal expansion of containment and storage material. Various research has already been done to reduce mechanical failure due to thermal ratcheting. Thermal ratcheting is more common in the DMT tank due to its cyclic operation. González et al. studied stresses in the tank using thermoelastic theory (González et al., 2016). In this, the author has calculated hoop stress to

identify the factor responsible for the yielding of the tank. The failure due to thermal ratcheting can be minimized by considering the factor of safety more than two and having a density of HTF and storage material approximately same.

2.18 RESEARCH GAP

- CSP plant in integration with TES system for Micro Steam Generators used in microgrids has not been studied. The smallest commercial CSP plant, which was operational in 2019, was of a 9 MW capacity with a 36 MWh energy storage system. Therefore, research needs to be done to integrate micro solar power plants with the thermal energy storage system.
- The charging and discharging of the thermal energy storage system (TES) is addressed in the literature. However, the problem of temperature variation as the thermal front approaches the end of the tank is required to be addressed in the literature.
- The parametric investigation to find the optimum parameter for maximum charging/ discharging efficiency is addressed in the literature. However, limited research has been found on the optimum parameter for maximum charging and minimum pressure drop.
- Most of the numerical models are based on assumptions like constant inlet temperature and uniform temperature throughout the tank in literature. Therefore, more research is required to investigate the thermodynamic behavior of tanks at non-uniform temperature and time-dependent inlet temperature.
- Thermocline thickness (temperature gradient along the length of the tank) is the most critical parameter and needs to be discussed in the literature. In most of the research, thermocline thickness at parameters like mass flow rate, granule geometry, and void fraction is discussed, however, none of the authors has done parametric optimization for minimum thermocline thickness.

2.19 SUMMARY OF LITERATURE REVIEW

A systematic review of prospective observational studies showed that the integration of a solar TES system with CSP is an eminent method of power production using solar energy. The levelized cost of electricity using solar

power is more as compared to the conventional power plant due to its intermittent nature. Hence, integration of thermal energy storage system with CSP is required to make the system economically more viable. Currently, molten Salt TES system is operational but economically not so viable due to its high initial cost. Further, various investigators studied the integration of other sensible based storage system with CSP and found dual media single tank (DMT) more economical and competitive as compared to other systems like single media tank and molten salt TES system. The authors throughout the world studied the performance of dual media tank under various operational conditions and found it more effective as compared to other systems. The authors has used the various parameter like thermocline thickness, stratification of tank, temperature variation along the tank, exegetic and energy efficiency during charging and discharging of tank at different input parameters like void fraction, mass flow rate, inlet temperature and D/L ratio of the tank. The study of thermocline thickness shows that two tank molten salt TES system has thinner thermocline thickness as compared to the dual media tank due to low thermal conductivity of molten salt as compared to the thermal conductivity of dual media (HTF and storage material). Figure 2-21, shows the comparison of thermocline thickness of molten salt TES system and Dual Media TES system.

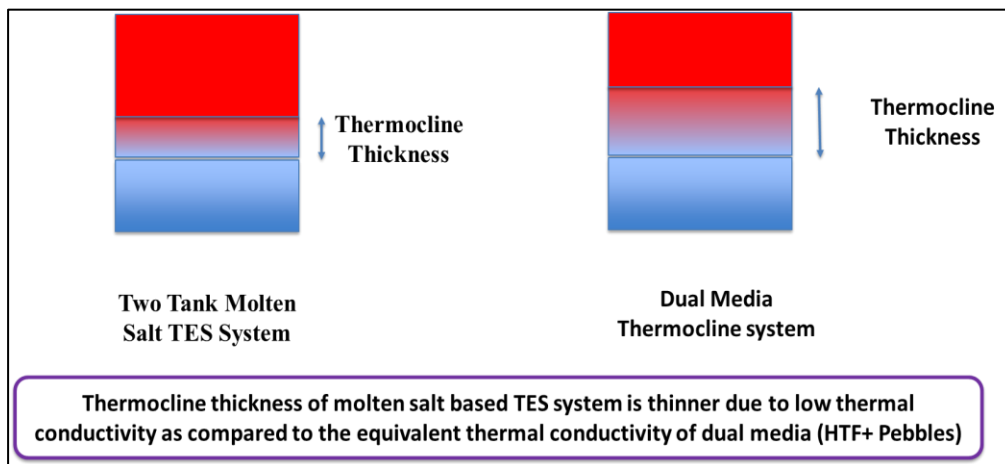


Figure 2-21: Thermocline thickness comparison of two tank and dual media tank

In dual media tank, the effectiveness of storage material has also been studied by the authors to investigate the thermal performance of TES system. The thermocline thickness of storage system depends on the thermal diffusivity of

material and it is higher for maximum thermal diffusivity. The authors has also used different energy model for characteristic analysis of TES system. The characteristic of energy model discussed in this chapter are illustrated in Figure 2-22. Among all energy models, the Schumann model is widely accepted by several authors owing to its simplest formulation and its lower computational time.

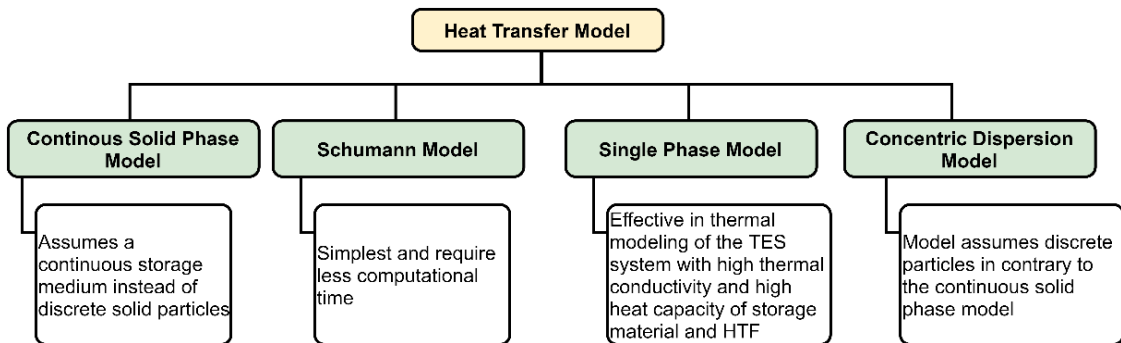


Figure 2-22: Overview of Heat Transfer Model

CHAPTER 3 - NUMERICAL AND EXPERIMENTAL METHODOLOGY

3.1 INTRODUCTION

A dual-media thermocline energy storage system is a cost-effective and viable technique for storing heat in an extended operation of concentrated solar power (CSP) system. Investigating the DMT energy storage system requires thermodynamic modeling of different processes, like charging and discharging of the tank. The charging and discharging of the tank depends on parameters like void fraction, pebbles diameter, L/D ratio, and mass flow rate. This chapter discusses the methodology to study the effect of aforesaid parameters on thermocline behavior of tank under various operating conditions. Figure 3-1 illustrates the numerical and experimental methodology to study the thermo-economic performance of DMT. This research work is divided into four phases. Phase 1 includes the characteristic analysis of dual media tank. This phase consist of effect of pebbles diameter and mass flow rate on thermocline behaviour of tank. Further, in this phase numerical optimization using design of experiment (DOE) has been done to evaluate optimum parameter for minimum thermocline thickness. In phase 2 performance analysis of shell and tube heat exchanger has been done to integrate TES system with CSP plant. In this phase numerical analysis has been done to investigate of effectiveness of shell and tube heat exchanger for different configuration of baffles. In Phase 3 experimental analysis of dual media TES system has been done to investigate the energy storage capability of the system. Further, in phase 4 an experimental analysis on heat exchanger has been done to integrate the system with CSP plant.

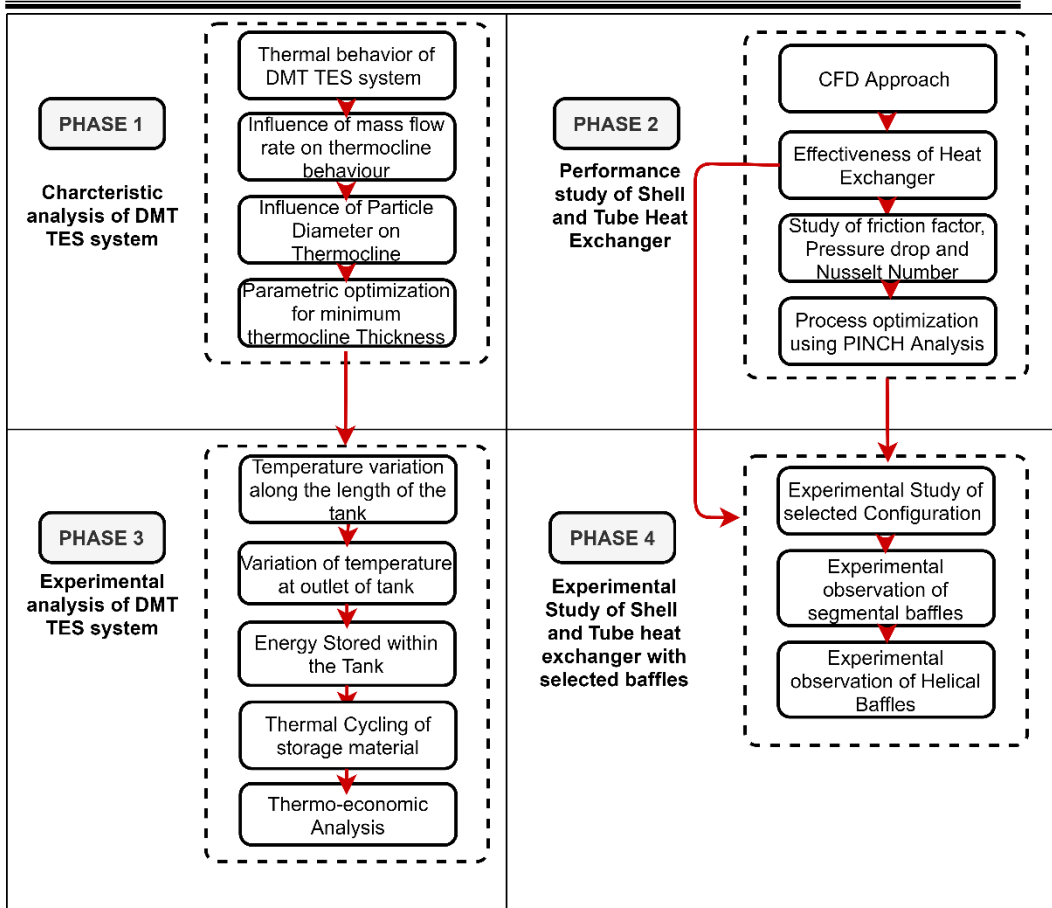


Figure 3-1: Detailed Methodology

3.2 NUMERICAL METHODOLOGY

In the numerical methodology, the Schumann model was used to determine the characteristic behavior of DMT. In addition, parametric optimization was performed to investigate the optimal parameter for maximum efficiency and minimum pressure drop. The numerical model used is based on several assumptions and boundary conditions. The numerical results obtained are validated with experimental data obtained from a test facility on a LAB scale. A 17 kWh_{TH} experimental test facility was developed to study the effect of operating variables on the charging and discharging of the tank.

3.3 EXPERIMENTAL METHODOLOGY OF DMT STORAGE SYSTEM

A LAB scale test facility was developed to study the thermocline behavior of a dual media tank. The experimental study to evaluate the thermocline behavior of the tank has been done in two phases. In phase 1, a 17 kWh_{TH} TES system has been designed to study the various parameter on charging and discharging

of the tank, and, in phase 2, the thermal cycling of the storage material was carried out to investigate the life cycle of DMT. Figure 3-2 shows the experimental methodology to study the thermal behavior of tank under different operating conditions.

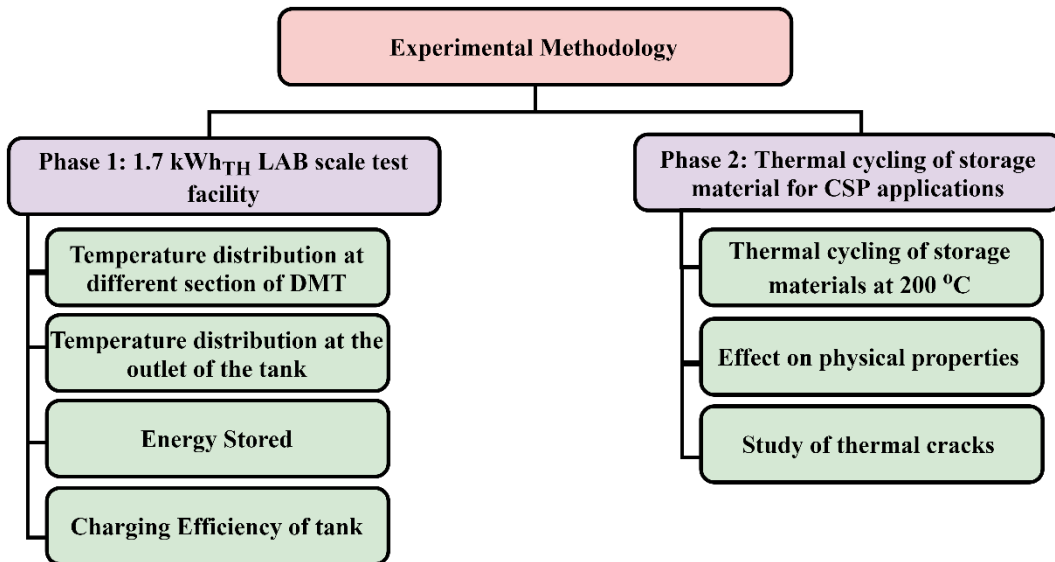


Figure 3-2: Experimental Methodology

CHAPTER 4 - MODELLING OF DUAL MEDIA THERMAL ENERGY STORAGE SYSTEM

4.1 INTRODUCTION

In order to achieve the research goal of numerical analysis, a numerical model is created. In numerical model an industrial-scale design has been done considering the operating parameter of a national solar thermal power plant of 1 MWe capacity. In this dual-media TES system, the thermocline behavior was investigated, taking into account various parameters such as void fraction, pebble diameter, and mass flow rate. The influence of parameters on the thickness of the thermocline is investigated on an industrial scale. In the present work, a model has been developed for 20 MWh_{th} thermal energy storage system to analyze the thermal behavior of a dual media thermocline tank. The numerical model consists of spherical shape storage material filled inside the cylindrical tank. However, the storage material (pebbles) used in packing are either spherical or non-spherical in shape, depending upon the availability and cost. The Therminol VP 1 and granite are used as a Heat Transfer Fluid (HTF) and storage material, respectively for industrial-scale and lab-scale design. The selection of HTF depends on the operating temperature of a concentrated solar power cycle. Therminol VP1 is suitable for high-temperature applications, and its volumetric heat transfer capacity is also very high as compared to other HTF. The maximum and minimum operating temperature of Therminol VP 1 is 12 °C and 400 °C, respectively. The volume of a cylindrical tank was calculated according to (Cascatta, Cau, Puddu, & Serra, 2014) Equation (4-1). Figure 4-1 illustrates the physical model for numerical analysis of DMT.

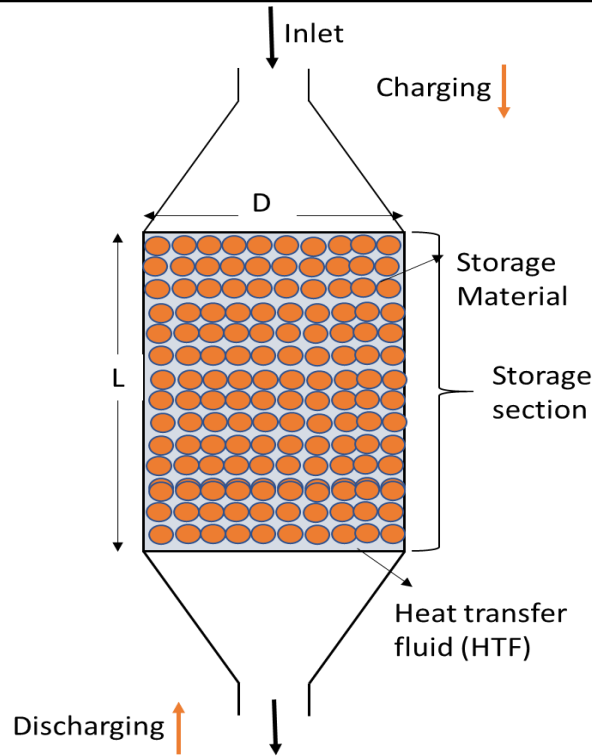


Figure 4-1: Physical model

$$V = \frac{E_{max}}{(\rho_s C_s (1 - \varepsilon) + \rho_f C_f \varepsilon) \Delta T_{max}} \quad (4-1)$$

The void fraction ε , used in Equation (4-1) is the ratio of the volume of voids and total volume of the tank.

$\varepsilon = \frac{V_v}{V_T}$, and $V_v = V_T - V_p$, where, V_p is the total volume of the pebbles.

The operating parameters for 20 MWh_{TH} and 17 kWh_{TH} thermal storage system (TES) are shown in Table 4-1.

Table 4-1: Operating Parameters/ Input parameter for

Operating parameter	20 MWh _{TH}	
	Value	Unit
T _{max}	390	°C
T _{min}	231	°C
Length of tank (L)	6	M
Diameter of tank (D)	7.2	M
Void fraction (ε)	0.33	-
Pebbles diameter (d)	0.04	M
Mass flow rate (\dot{m})	8.53	Kg/s
Density of pebbles	2675 (granite)	Kg/m ³
Specific heat of pebbles	775 (Granite)	J/kg-K
Thermal conductivity	2.85 (Granite)	W/m-K
Density of HTF	858	Kg/m ³

Specific heat of HTF (Therminol VP1)	2.207	kJ/kgK
Thermal conductivity of HTF (Therminol VP1)	0.104	W/mK
Viscosity of HTF (Therminol VP1)	0.272e-03	Pa-sec

4.2 HEAT TRANSFER MODEL FOR TES SYSTEM

A detailed study of heat transfer model has been done in Chapter 2. The heat transfer model used to analyse thermal behaviour of thermocline tank are: Schumann model, Continuous Solid Phase Model, Single Phase Model, Concentric Dispersion Model. Of all these, the Schumann model is simplest and require less computing time. However, concentric Dispersion model is most realistic approach but require more computational time. In this research work, Schumann model is used to study the characteristic behavior of tank. The energy balance equation for a dual media TES system is to set up governing equation for solid and fluid (HTF) individually. The general governing equation for HTF and solid on a unit volume basis is:

$$\frac{\partial(\rho\phi)}{\partial t} + \text{div}(\rho u\phi) = \text{div}(\zeta \text{grad } \phi) + S \quad (4-2)$$

Here, $\frac{\partial(\rho\phi)}{\partial t}$ denotes the rate of change of the intensive property ϕ . The quantity $\text{div}(\rho u\phi)$ is the convection flux, i.e., flux carried away by the flow field and the term, $\text{div}(\zeta \text{grad } \phi)$ is the diffusion flux. Not all diffusion flux is governed by the gradient of specific properties. The term S_v in the governing equation represents volumetric source term due to thermal dissipation or energy generation. The energy equation for fluid flow (HTF) in dual DMT is:

$$\varepsilon \left(\frac{\partial(\rho h)}{\partial t} + \text{div}(\rho u h) \right) = \text{div}(k \text{grad } T) + S_v \quad (4-3)$$

Where, $\phi=h$, and $h = c_f T$ is the specific enthalpy of HTF.

$$\rho_f c_f \varepsilon \left(\frac{\partial T}{\partial t} + \text{div}(uT) \right) = k_f \text{div}(\text{grad } T) + S_v \quad (4-4)$$

There is a volumetric heat transfer rate between the filler material and HTF along with thermal loss in a thermocline tank.

$$\rho_f c_f \varepsilon \left(\frac{\partial T}{\partial t} + \text{div}(uT) \right) = k_f \text{div}(\text{grad } T) + h_v(T_s - T_f) - U(T_f - T_\infty) \quad (4-5)$$

$$\varepsilon \left(\frac{\partial T_f}{\partial t} + u \frac{\partial T_f}{\partial y} \right) \quad (4-6)$$

$$= \frac{k_f}{\rho_f c_f} \cdot \frac{\partial^2 T}{\partial y^2} + \frac{h_v}{\rho_f c_f} (T_s - T_f) - \frac{4U}{\rho_f c_f D} (T_f - T_\infty)$$

The energy equation for filler material is:

$$(1 - \varepsilon) \left(\frac{\partial T_s}{\partial t} \right) = \frac{k_s}{\rho_s c_s} \cdot \frac{\partial^2 T}{\partial y^2} + \frac{h_v}{\rho_s c_s} (T_f - T_s) \quad (4-7)$$

In flow-through porous material average velocity of interstitial velocity u can be determined by:

$$u = \frac{V_s}{\varepsilon} \quad (4-8)$$

Where, V_s is the superficial velocity given by:

$$V_s = \frac{m}{\rho A}, \text{ where } m \text{ is the mass flow rate in Kg/s.}$$

The transient energy equation can be discretized by using the Explicit Method, Implicit Method, or Crank-Nicolson method. In this study, the explicit method is used to discretize energy equations by using well-known stability criteria. The stability criteria can be established as:

$$\Delta t < \frac{\rho c (\Delta x)^2}{2k}$$

If this condition violates, then unrealistic results could emerge. To avoid unrealistic results appropriate time step is chosen as per the criteria given above. The finite-difference equation developed is solved by using the Gauss-Seidel iteration method using applicable boundary conditions and assumptions. The numerical model developed is solved by using the following assumptions:

1. The initial temperature of the tank is assumed uniform throughout the tank
2. Thermohydraulic properties of the fluid are assumed constant
3. There is no temperature variation along the radial direction
4. Uniform velocity and temperature are considered at the inlet of the tank
5. The tank is considered as a uniform and isotropic media.
6. The temperature is uniform throughout the tank

The volumetric heat transfer coefficient between HTF and pebbles is calculated by using the correlation developed by:

$$h_v = \frac{6(1-\varepsilon)k_f[2+1.1Re_{f,sup}^{0.6}Pr_f^{1/3}]}{D_s^2} \quad (4-9)$$

Where, $Re_{f,sup}$ is the superficial Reynold number calculated by:

$$Re_{f,sup} = \frac{4mD_s}{\mu_f \pi D_{tank}^2} \quad (4-10)$$

The boundary condition used to solve the energy equations are shown in Figure 4-2. The finite-difference equation for boundary conditions is based on Euler forward and second-order backward difference methods.

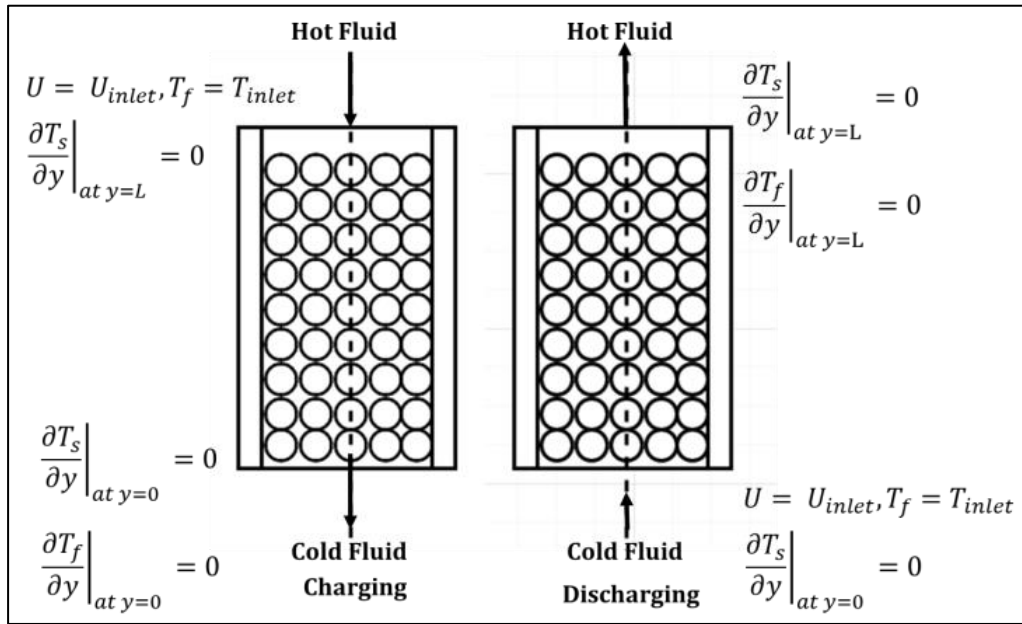


Figure 4-2: Boundary conditions during charging and discharging of tank
The energy equations are solved for multiple cycles. The final temperature of each cycle is considered as an initial temperature in the next coming cycle.

4.3 THERMAL BEHAVIOR DURING CHARGING AND DISCHARGING OF TANK

The analysis of the thermal behavior of the tank is extremely important as it helps to understand the thermal stratification and the thickness of the thermocline. The performance of the tank is dependent on thermal stratification and thermocline thickness. To have better charging and discharging efficiency, the thermocline thickness should be minimum. In an ideal case, the hot and cold fluids are separated by an imaginary baffle. Both the fluids are ideally insulated with each other to avoid mixing. Figure 4-3 shows the thermocline behavior of DMT during the charging and discharging of the tank. A thermocline is dependent on buoyancy, where hot fluid is settled on top and cold fluid on the

bottom to avoid turbulence between hot and cold fluid and disruption in thermocline thickness. When the hot and cold fluids are settled on top and bottom, respectively, the heat transfer medium is conduction as there will be no bulk motion to promote convection. If the hot fluid is on the bottom and the cold fluid at the top, the hot fluid will move upwards due to density difference. This will cause bulk motion of the fluid, causing a disturbance in the thermocline. It is to be noted that the medium of heat transfer between the hot and cold fluid is conduction. But convection takes place between the filler material and the fluid. This study summarizes how thermal stratification is maintained for better charge and discharge performance. It is the utmost priority to keep the thermocline thickness minimum. During discharge, the thermocline zone moves from bottom to top and keeps expanding with time. If the thickness of the thermocline is large, the liquid exiting from the top has a larger temperature fluctuation, and the constant temperature at the exit is not reached. If this variation in exit temperature is utilized in steam generators, the steam of poor quality will be produced. Even if the thickness of the thermocline is large, the discharge time is shortened considerably, limiting the constant temperature of the liquid at the exit. To counter this, it is always recommended to use HTF of low thermal conductivity. The high thermal conductivity of HTF will cause disturbance in thermocline thickness and reduce the discharging time, and consequently, the system will be devoid of fixed temperature at the outlet.

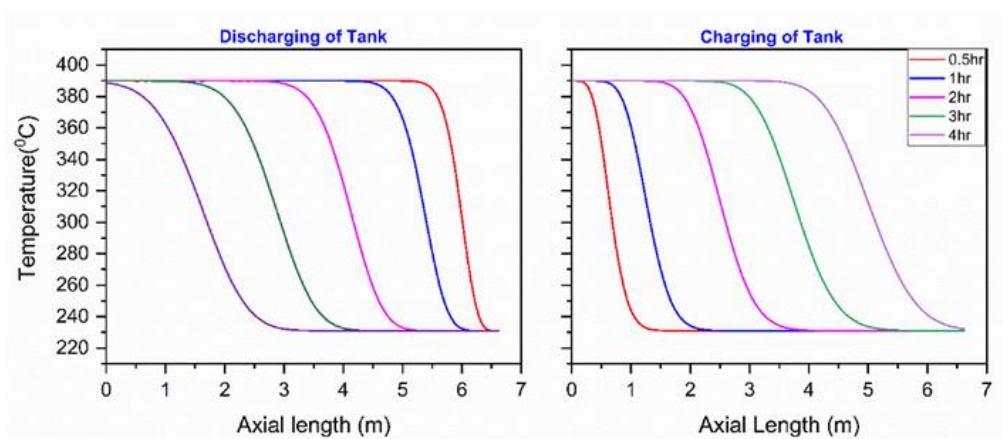


Figure 4-3: Charging and discharging behavior of DMT

4.4 INFLUENCE OF MASS FLOW RATE ON THERMOCLINE BEHAVIOR

Mass flow rate is another parameter that influences thermocline behavior. Figure 4-4 shows the effect of mass flow rate on the thermocline behavior of DMT. It is observed that the discharge time decreases with an increase in mass flow rate, resulting in varying temperatures at the outlet. However, the slope of the thermocline thickness does not show any significant change with the change in mass flow rate. During high mass flow rate, the output power also had a high value, but there is a rapid fall in output power with time. A major disadvantage of lower mass flow rates is heat loss; hence, there is initially reduced power output and temperature. However, an increase in mass flow rates improves the volumetric heat transfer coefficient between pebbles and HTF.

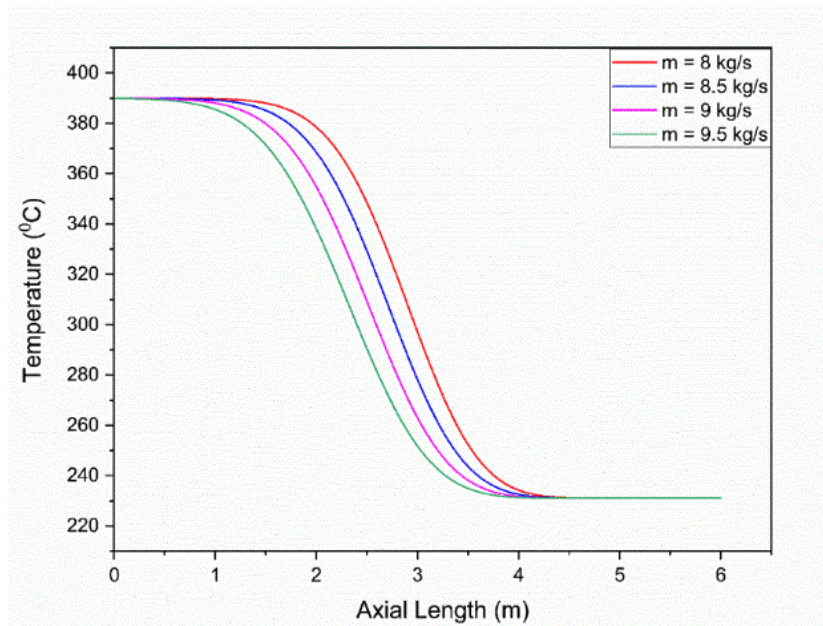


Figure 4-4: Effect of mass flow rate on thermocline behavior of DMT

4.5 INFLUENCE OF PARTICLE DIAMETER ON THERMOCLINE BEHAVIOR

Variation of thermocline with different particle diameters is shown in Figure 4-5. It is observed that the slope of the thermocline region is minimum for smaller diameter pebbles. The results show an improvement in the heat exchange between pebbles and HTF as the diameter of the pebbles decreases. However, decreasing the pebble diameter increases the void fraction resulting

in a greater pressure drop. Pumping power increases with an increase in pressure drop. This leads to loss of exergy.

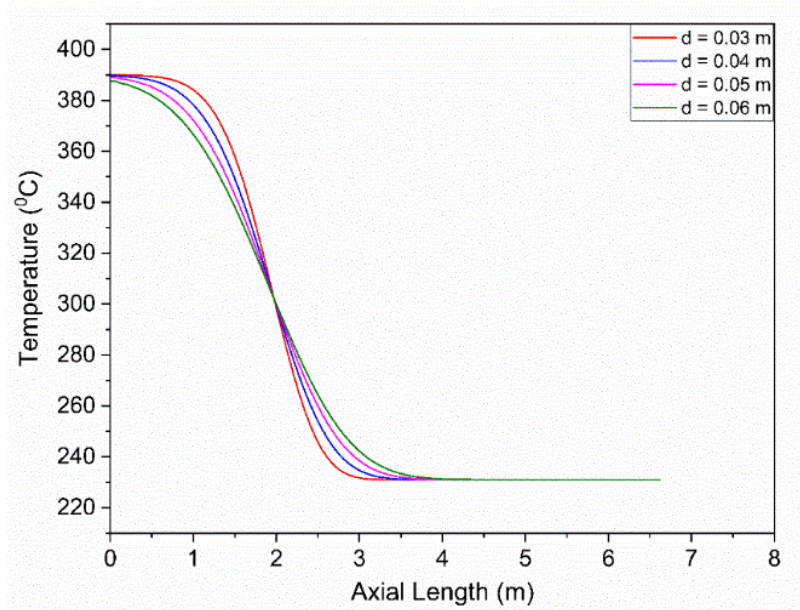


Figure 4-5: Effect of pebbles diameter on thermocline behavior of the tank

CHAPTER 5 : DEVELOPMENT OF DUAL MEDIA THERMAL ENERGY STORAGE SYSTEM

5.1 INTRODUCTION

This chapter includes the design of DMT at LAB scale. A 15.7 kWh_{TH} DMT energy storage system is designed to study the charging and discharging of tank. The discharging of tank has been studied by integrating the system with heat exchanger. This chapter also include the design of shell and tube heat exchanger for TES system.

5.2 DEVELOPMENT OF LAB SCALE TEST FACILITY FOR THE CHARACTERIZATION OF DMT

Based on the analysis carried out, a small-scale test facility is designed and constructed which will be integrated with a parabolic dish in the future. The schematic of the experimental setup is shown in Figure 5-1. The test facility is designed for a 1.57 kW_e solar thermal power plant of 20% thermal efficiency. The high and low fluid temperature required for the power plant is 200 °C and 70 °C respectively. The experimental test facility is shown in Figure 5-2. The test facility consists of a storage tank filled with ceramic balls and HTF. The ceramic balls are used as a storage material, which stores thermal energy during charging and delivers during discharging. A thermocouples tree is used to measure the centerline axial temperature at nine different locations in the cross-section of the storage tank. A PT100-type thermocouples are used to measure the centerline temperature with an accuracy of ± 0.001 °C.

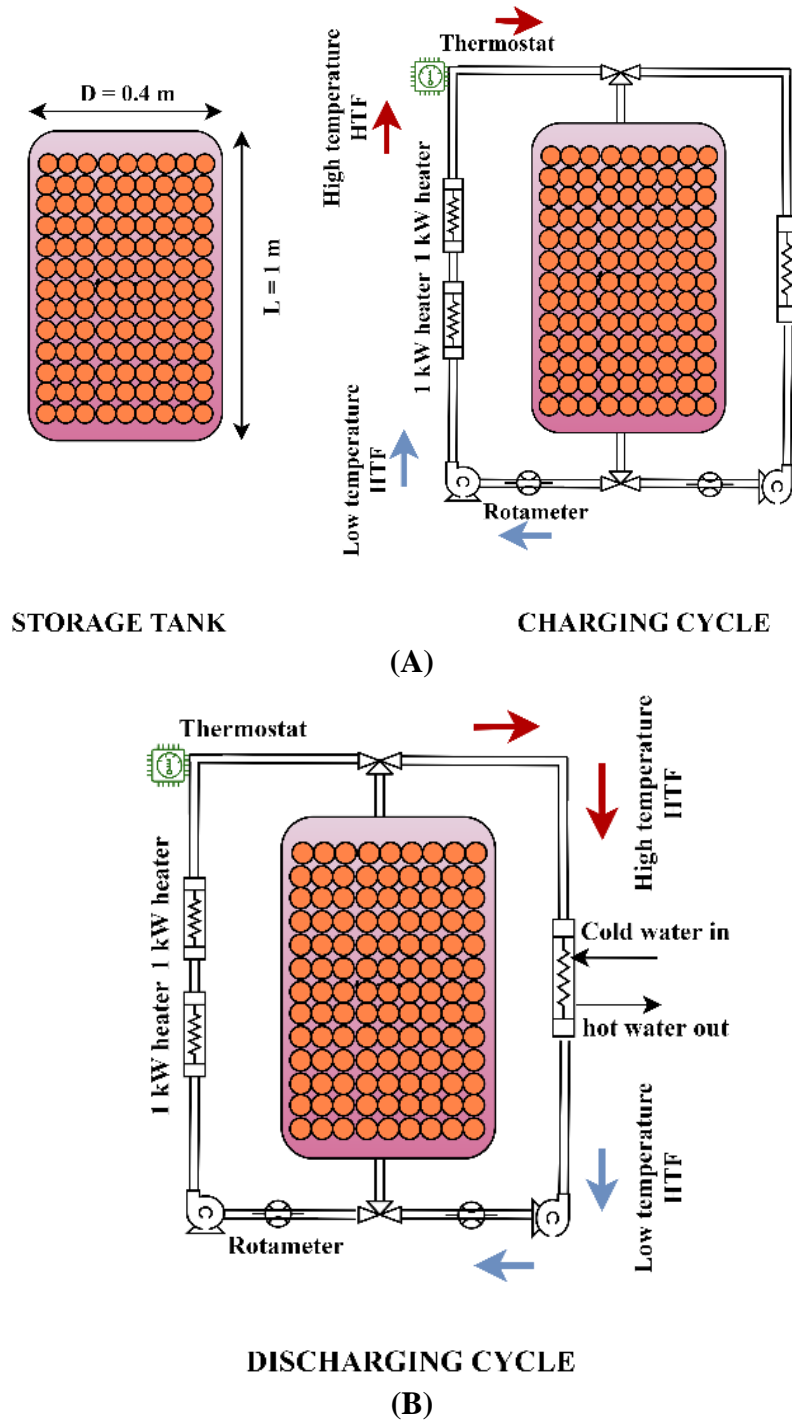


Figure 5-1: Experimental setup (A) Charging of Tank and (B) Discharging of Tank

The thermocouples were connected with the data logger, which converts analog signals to digital signal. Syntherm 1000 (Synthetic oil) is used as an HTF. An oil transfer pump of a capacity of 40 l/min with a maximum operating temperature of 280 °C is used to transfer HTF during the charging and

discharging of the tank. A DC motor (10 A – 12 V DC) shown in Figure 5-3 of a helical gear model is used to run an oil transfer pump. A PID controller of the maximum operating temperature of 400 °C with the least count of 0.1 °C is used to maintain the high temperature at the inlet of the tank. The operational parameters used in a Lab-scale test facility are shown in Table 4-1.

Table 5-1: Operating parameter of LAB scale test facility

Operating parameter	Value	Unit
Power output (Electrical)	1.3	kWe
Power output (Thermal) @ 20% thermal efficiency	15.7	kWh _{TH}
Charging hour	2	Hour
T _{max}	200	°C
T _{min}	70	°C
Length of tank (L)	1	M
Diameter of tank (D)	0.4	M
Void fraction (ε)	0.33	-
Pebbles diameter (d)	75	Mm
Mass flow rate (\dot{m})	0.024	Kg/s
Density of pebbles (Alumina Ceramic)	3200	Kg/m ³
Specific heat of pebbles (Alumina Ceramic)	1070	J/kg-K
Thermal conductivity (Alumina Ceramic)	4.70	W/m-K
Specific gravity (Syntherm 1000) – ASTM D 4052	0.748	Kg/m ³
Specific heat of HTF (Syntherm 1000)	2.291	kJ/kg-K
Thermal conductivity of HTF (Syntherm 1000)	0.12	W/m-K
Viscosity of Syntherm 1000 (ASTM D 445)	22.5	cSt @ 40 °C

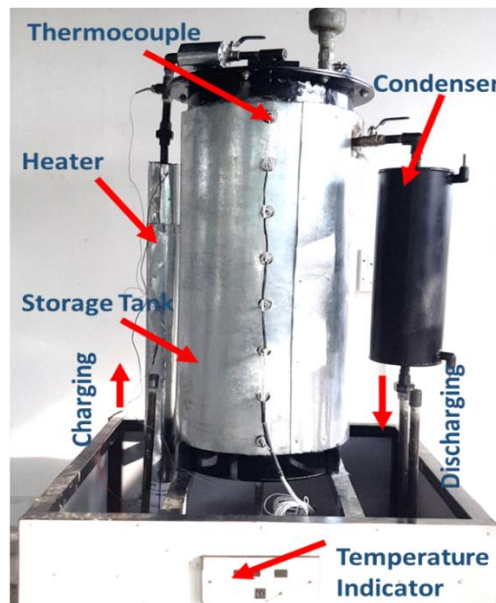


Figure 5-2: Experimental Set-up

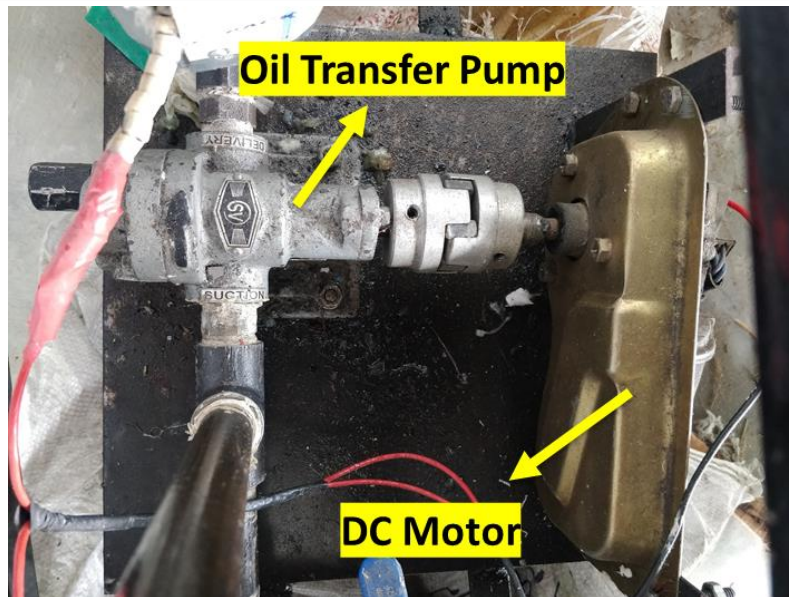


Figure 5-3 Oil transfer pump with DC Motor

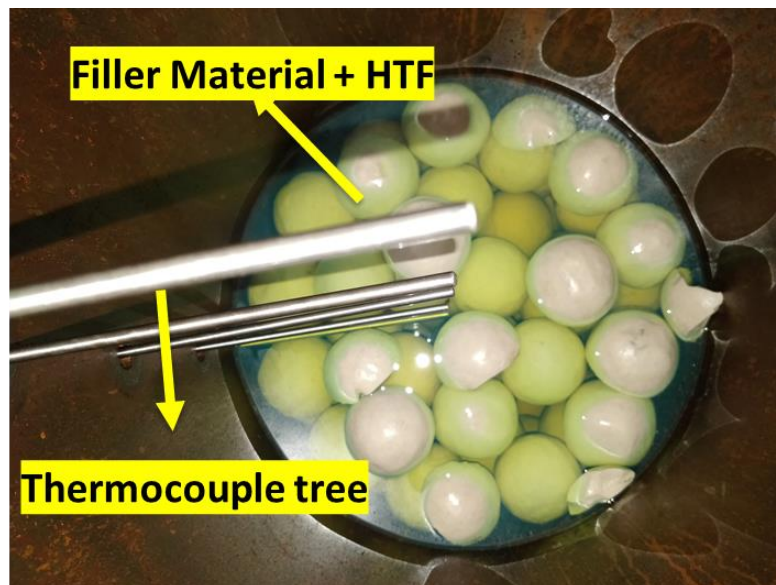


Figure 5-4: Ceramic balls with HTF

5.3 HEAT EXCHANGER DESIGN

In this section numerical and experimental analysis of heat exchanger for CSP applications has been done to integrate TES with power cycle. The effectiveness of heat exchanger for several configurations like segmental and helical baffles has been studied. Initially numerical study of heat exchanger on fluent has been done to investigate the variation of temperature at outlet of heat exchanger. Thereafter effectiveness of heat exchanger has been calculated experimentally for segmental and helical baffles.

The performance of Heat Exchanger (HE) can be increased by providing baffles on the shell side. The baffles can be segmented or continuous based on the pressure drop and effectiveness. In this study, baffles geometry like segmental baffle with 30° cut (SB-30), segmental baffle with 50° cut (SB-50), align baffle with 30° cut (AB-30) and align baffle with 50° cut (AB-50) is taken for performance analysis of HE. Shell and tube HE with different baffle geometries is simulated on FLUENT to select the best possible geometry. The design specification of HE is shown in Table 5-2. The model with 0.48 million-grid number is selected for the computational study. Fine meshing is provided near the wall of the fluid domain with quadrilateral and hexagonal elements. The $k-\epsilon$ method, with a no-slip condition near the wall, is considered for this study.

Table 5-2: Design specifications of heat exchanger

Geometry	Dimensions
Inner diameter of tube (di)	0.018m
Outer diameter of tube (do)	0.02 m
Length of tube (L)	0.4 m
No. of tubes (N)	10
Baffle Thickness	0.01 m
Equally spaced support (measured from centreline of baffl	0.1m
Shell outer diameter (Do)	0.184 m
Shell inner diameter (Di)	0.16 m

The HTC and pressure drop can be calculated by the correlation given by (Q. W. Wang, Luo, Chen, & Zeng, 2015). Eq. (5-1) and (5-2) can be used to find pressure drop and HTC, respectively.

$$f = \frac{\Delta p_0}{\left(\frac{1}{2}\right) \rho u^2} \frac{d_0}{l} \tag{5-1}$$

$$Nu = \frac{h d_0}{k} \tag{5-2}$$

Where ΔP_0 is the pressure drop on the shell side is, ρ is the density of the fluid, d_0 is the outer diameter, and l is the effective length. Friction factor f can be calculated by the correlation obtained by the experimental result of (Ethod, 2012).

$$f = C_1 Re^{m_1} \tag{5-3}$$

Where C_1 is the constant for friction factor and can be selected from Table 5-3, based on Reynold number. The Nusselt number can be calculated by the correlation given below (Q. W. Wang et al., 2015).

Table 5-3: Correlation for friction factor

Heat exchanger	C_1	m_1	Reynold's number
Helical	3.76	-0.578	≤ 1960
	0.316	-0.251	≥ 1960
Segmental	2.79	-0.269	≤ 752
	1.41	-0.167	≥ 752

$$Nu = C_2 Re^{m_2} Pr^{1/3} \quad (5-4)$$

Where C_2 is the constant for Nusselt number and can be selected from Table 5-4, based on the configuration of baffle. The friction factor and heat transfer coefficient can be calculated by the Eq. (5-3) and (5-4), respectively.

Table 5-4: Correlation for Nusselt number

Heat exchanger	C_2	m_2
Helical	0.0599	0.669
Segmental	0.0889	0.717

5.4 NUMERICAL STUDY

In numerical study a CFD (FLUENT) approach has been used to evaluate temperature variation across the shell side and tube side. Figure 5-5 shows the temperature variation for different inlet temperatures for the shell side and tube side.

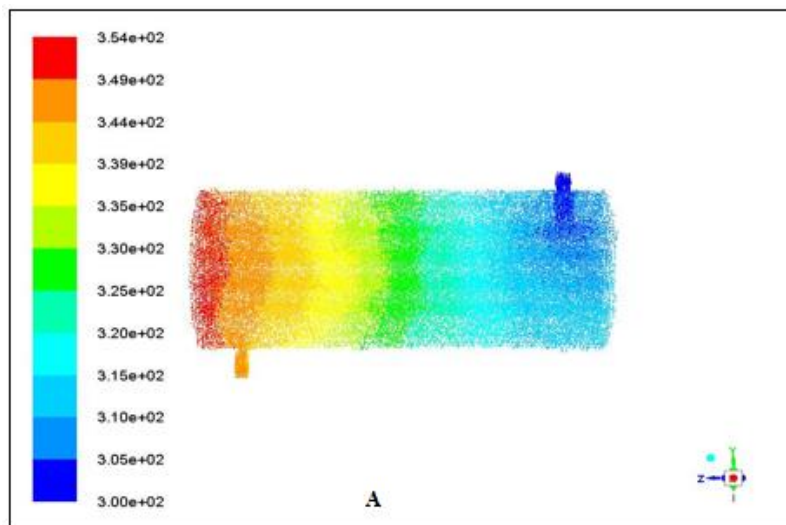


Figure 5-5: Temperature variation across (A) Shell Side and

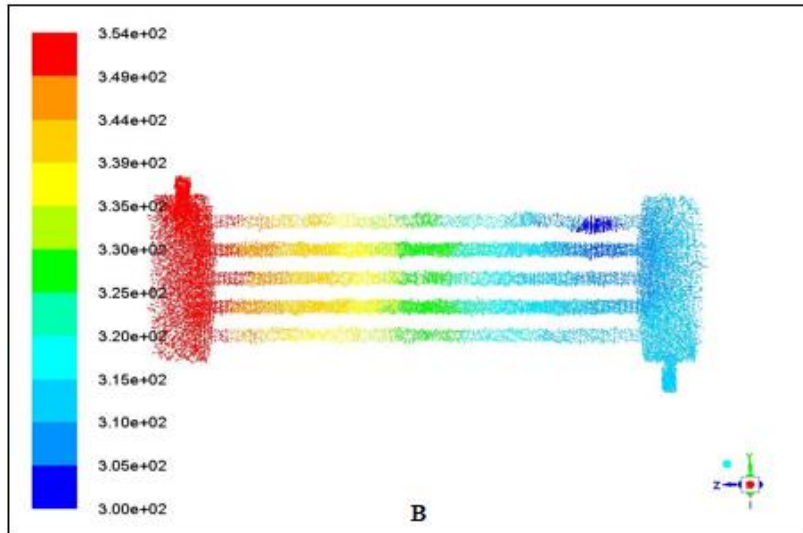


Figure 5-6: Temperature variation across (B) Tube Side

Table 5-5: CFD data for different model

S. No	Model Description	T_{hi}	T_{ho}	T_{ci}	T_{co}	ϵ
1	without baffle	353	312	300	335	0.66
2	Align baffle with baffle cut 30	353	315	300	343	0.81
3	segmental baffle with baffle cut 30	353	313	300	336	0.67
4	Align baffle with baffle cut 50	353	312	300	342	0.79
5	segmental baffle with baffle cut 50	353	318	300	332	0.60

The CFD results for different configuration is shown in Table 5-5. The result shows that align baffle with baffle cut of 30^o is more effective as compared to other models. Based on the result obtained from CFD, an experimental study is done for segmental and helical baffle heat exchangers.

5.5 PERFORMANCE VARYING WITH DIFFERENT BAFFLES CONFIGURATION

In this section effectiveness of HE for different baffles, the configuration has been calculated numerically. The effectiveness of varying models is compared at a mass flow rate of 0.02 kg/s, and the same inlet temperature of 353 K. Result shows that align baffle with baffle cut of 300 (AB-30) is more suitable as compared to other geometries. The effectiveness of different baffles geometries is shown in Figure 5-7.

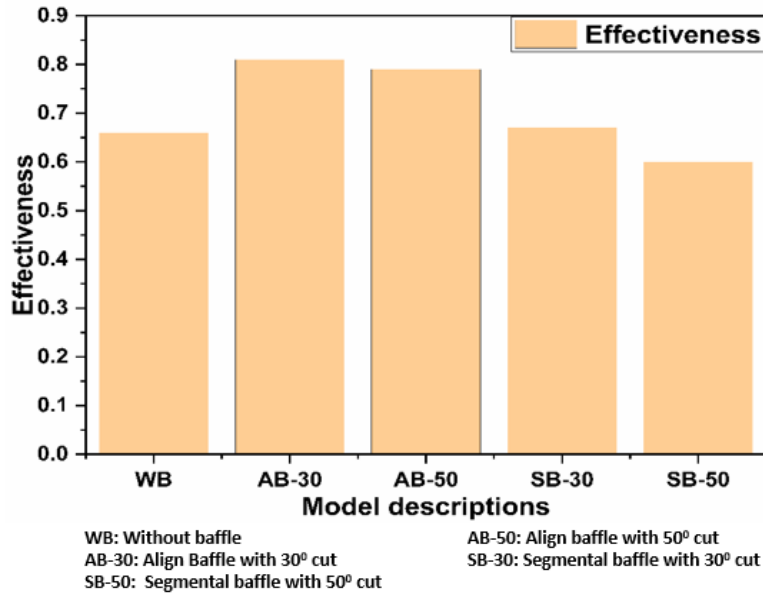


Figure 5-7: Effectiveness of different baffles geometries

The increase in effectiveness is due to the formation of the less dead zone as compared to other geometries. The aligned baffle with baffle cut (AB-30) of 30° is taken for experimental study, and the result obtained from the numerical result is validated with numerical simulation. In this study, the helical and segmental baffle is also compared experimentally. The helical baffle with a helix angle of 25° is taken and compared with the segmental baffle in terms of effectiveness, pressure drop, and Nusselt number.

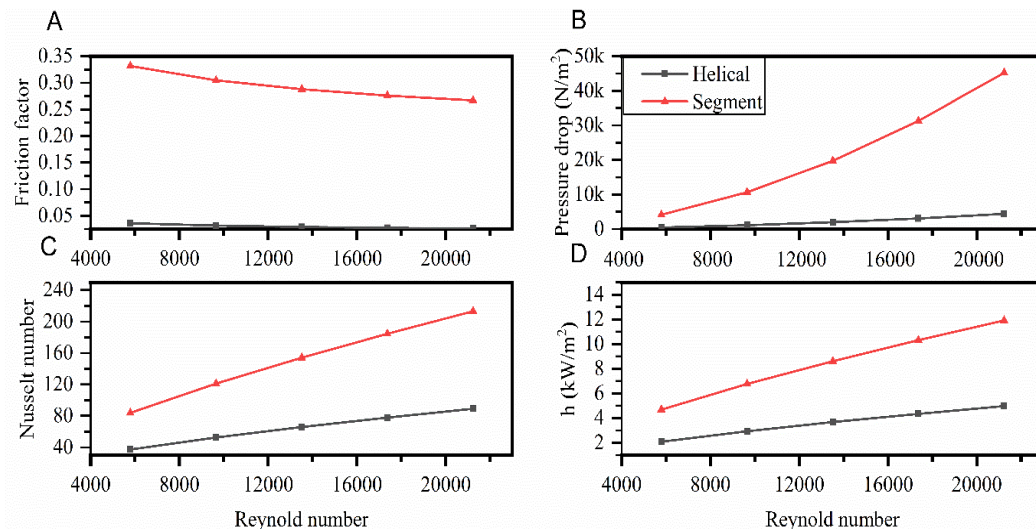


Figure 5-8: Effect of Reynold's number on A) friction factor B) Pressure drop C) Nusselt number (D) Heat transfer coefficient

Figure 5-8 shows that the pressure drop for segmental baffle is more as compared to the helical baffle. Although the heat transfer coefficient for segmental baffle is more as compared helical baffle.

5.6 EXPERIMENTAL STUDY OF THE SELECTED CONFIGURATION

After comparing all the models based on effectiveness, as mentioned in Figure 5-8, the AB-30 baffle is used for the experimentation. In this section, the effectiveness of AB-30 is evaluated analytically to validate experimental values. Comparison, as depicted in Figure 5-9, indicates the small deviation of a maximum of 5.1% between theoretical and analytical.

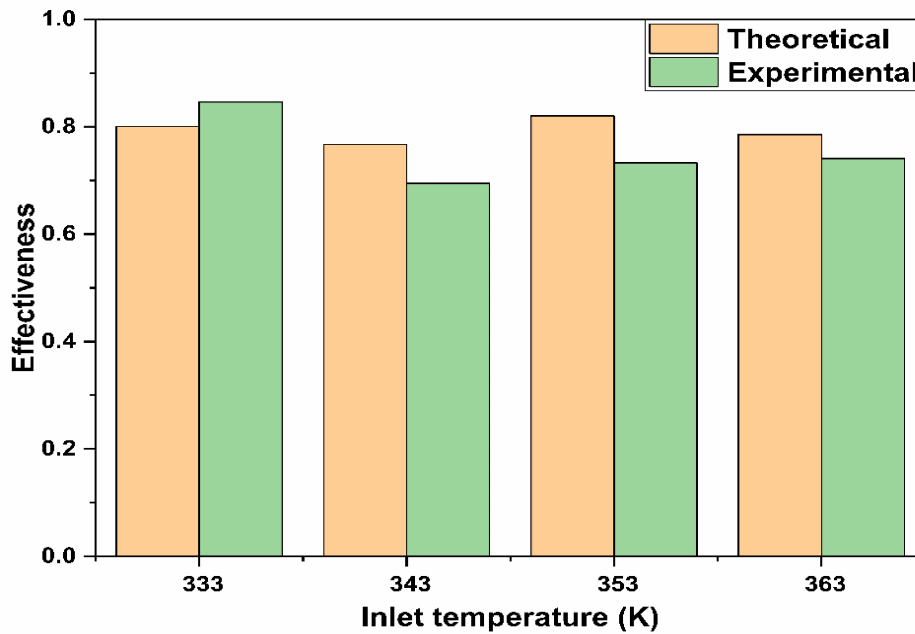


Figure 5-9: Validation of the theoretical model

Table 5-6: Operating variables

S.No	Parameters	Symbol	Value
1	Mass flow rate	\dot{Q}_t	0.00005 – 0.000183 m ³ /s
2	Tube side outer diameter	D_t	0.011 m
3	Thickness of the tube	T	0.00075 m
4	No. of tubes	N	9
5	Mass flow rate (Tube side)	\dot{m}_t	0.05 to 0.183 kg/s

Table 5-7: Thermo-hydraulic properties

S.No	Properties	Symbol	Unit	Cold water	Hot water
1	Specific heat	C p	kJ/kg – K	4.178	4.178
2	Thermal Conductivity	K	W/m – K	0.6150	0.6150
3	Viscosity	μ	Kg/m – s	0.001	0.001
4	Prandlt No	Pr	Dimensionless	5.42	5.42
5	Density	ρ	Kg/m ³	996	996

The geometry of the shell side and the fluid properties used in the shell side are given in Table 5-6 and

Table 5-7. The performance of the heat exchanger can be assessed from the specified flow properties and geometry. In this study, the segmental baffles are used to increase the heat transfer coefficient.

5.7 EXPERIMENTAL OBSERVATION OF SEGMENTAL BAFFLES

The tests are carried out for SB and helical baffle with a helix angle of 25°. The inlet and outlet temperature of the Shell and tube HE is measured with a thermocouple. LMTD and ε-NTU methods are used to design heat exchanger. The temperature has already been measured in an inlet and outlet side of an experimental setup and can be used to calculate LMTD and effectiveness.

$$LMTD = \frac{(T_{HI} - T_{CO}) - (T_{HO} - T_{CI})}{\ln \frac{T_{HI} - T_{CO}}{T_{HO} - T_{CI}}} \quad (5-5)$$

$$\varepsilon = \frac{T_{HI} - T_{HO}}{T_{HI} - T_{CI}} \quad (5-6)$$

Equation (5-5) and (5-6) are used to find LMTD and effectiveness of HE (SB) using counter flow.

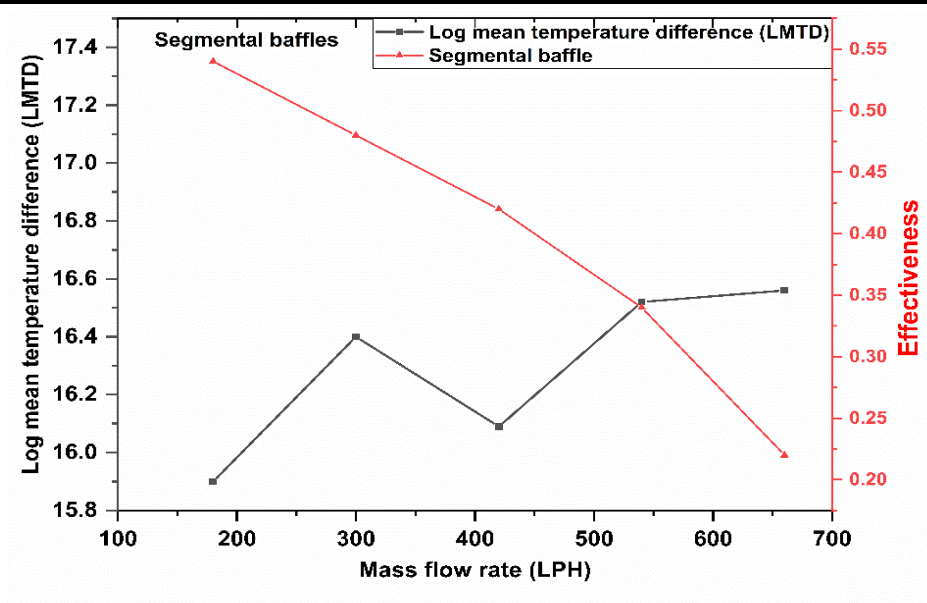


Figure 5-10: Influence of mass flow rate on LMTD and effectiveness of

The effect of mass flow rate on LMTD and effectiveness are shown in Figure 5-10. The result indicates that effectiveness decreases with an increase in mass flow rate. LMTD shows monotonous dependence only when the mass flow rate through the tube is varying with constant flow outside the tube. In this study, the mass flow rate through the tube and shell side both are varying. The decrease in effectiveness is due to the formation of a dead zone, which reduces the heat transfer rate.

5.8 HELICAL BAFFLE HEAT EXCHANGER

The experiments are also carried out for ST with helical baffles. To measure the performance of helical baffles in the HE, LMTD and effectiveness are again measured using the inlet and outlet temperatures of the hot and cold fluids, as shown in Figure 5-11

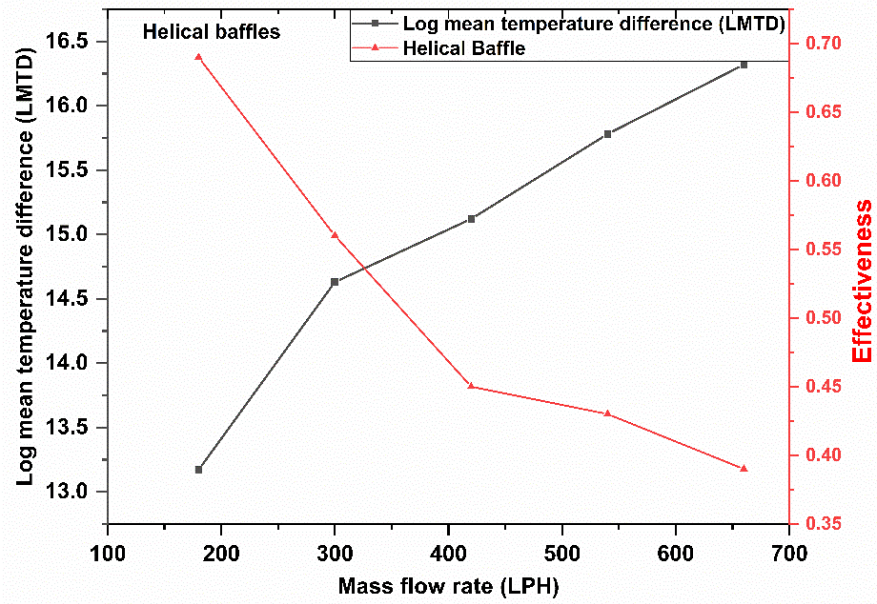


Figure 5-11: Influence of mass flow rate on LMTD and effectiveness

The LMTD and effectiveness of HE (SB) are calculated by using Equation (5-5) and (5-6) for counter flow. With increase in mass flow rate LMTD is increasing, however effectiveness of HE found to be decreasing. In addition, LMTD and effectiveness of helical baffle is same as in the SB. However, helical baffle HE gives the maximum value of effectiveness for the same mass flow rate as shown in Figure 5-12.

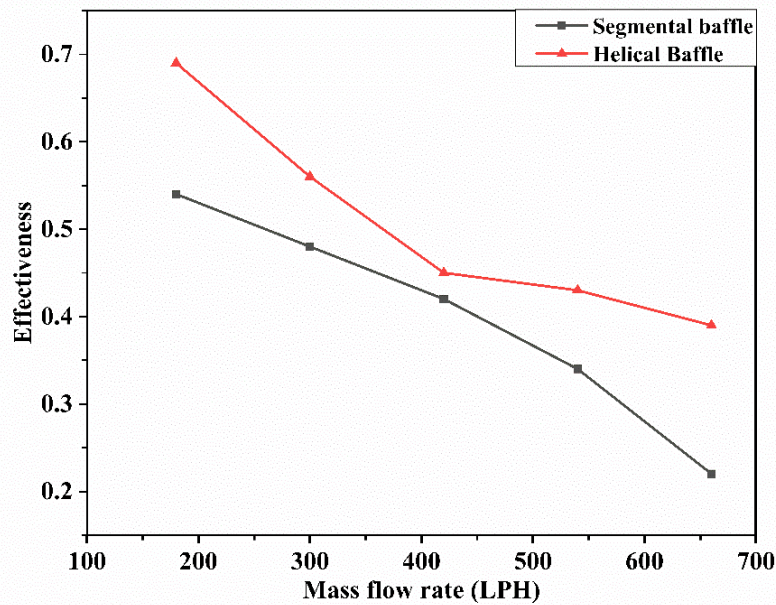


Figure 5-12: Comparison of segmental and helical heat exchanger

5.9 PROCESS OPTIMIZATION

Pinch analysis is a systematic way to identify maximum heat recovery, heating utility, and cooling utility for energy saving and cost. In this section, pinch analysis is used to identify heating and cooling load for optimum heat exchanger design. This analysis is used to compare the heating and cooling utility for WB, AB-30⁰, and SB-30⁰. The composite diagram for WB is shown in Figure 5-13. The composite graph shows that the maximum heat recovery and cooling utility required for the heat exchanger is 6.4 kW and 4 kW, respectively, for optimum design and low cost. However, the maximum heat recovery and heating utility required for AB-30 is 9.5 kW and 1.5 kW, respectively.

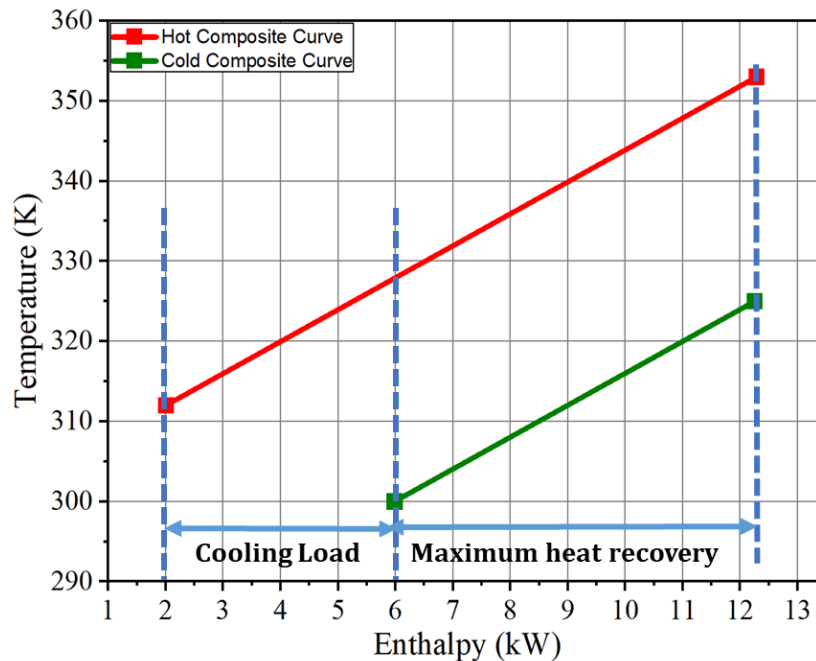


Figure 5-13: Heat recovery analysis of heat exchanger without baffle

Figure 5-14 shows that the size of the heat exchanger for AB-30⁰ is more as compared to WB. However, the heat load required for AB-30 is less as compared to WB. Further, align baffle with baffle cut of 30⁰ is compared with segmental baffle, and the result shows that 9 kW heat recovery is required for segmental baffle with a cooling utility of 1 kW. The composite diagram of the segmental baffle with a baffle cut of 30⁰ is shown in Figure 5-15. This result indicates that the segmental baffle is more suitable for the design of ST for maximum heat recovery and low cost.

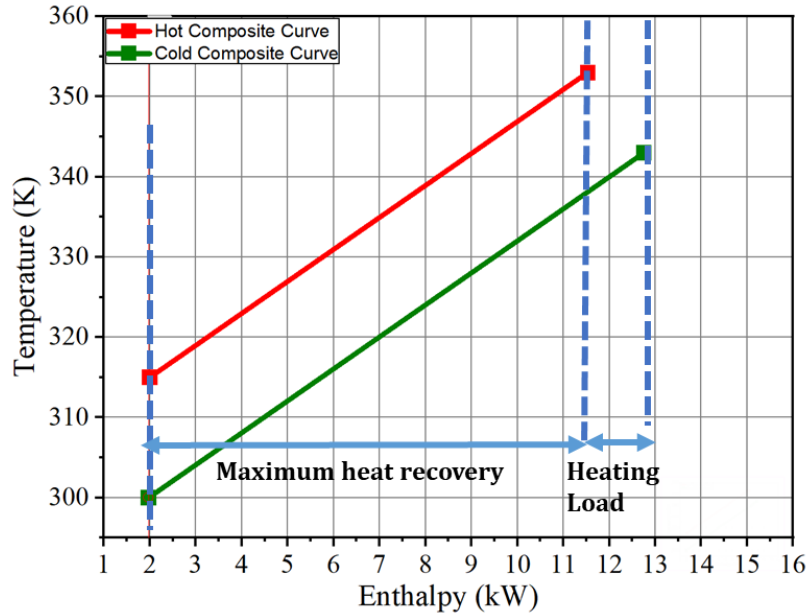


Figure 5-14: Heat recovery analysis of AB-30

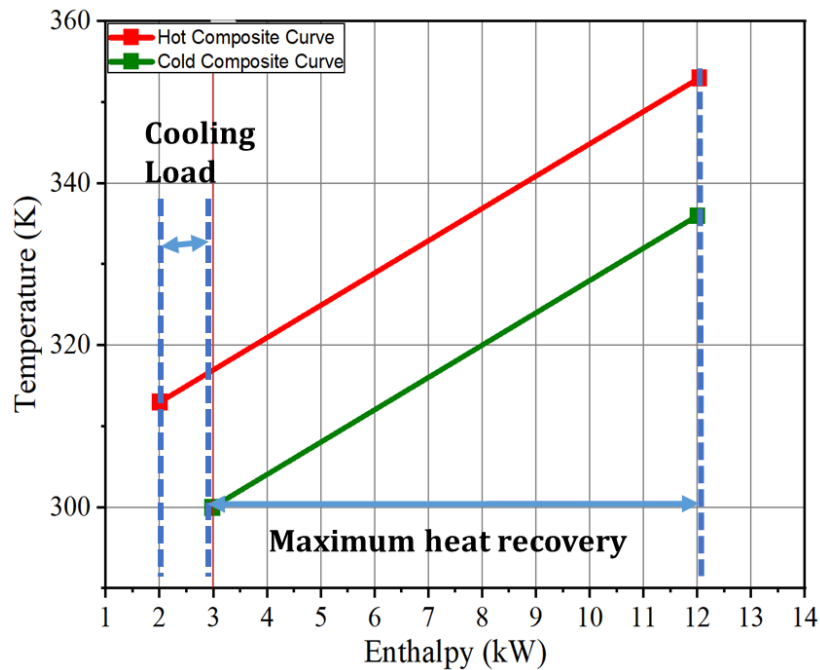


Figure 5-15: Heat recovery analysis of SB-30

5.10 PERFORMANCE CHARACTERISTICS

The performance characteristics of segmental and helical baffle heat exchangers are compared by j (Colburn's) factor and f (Fanning friction) factor. However, j and f factor can be defined as (Webb, 1994):

$$StPr^{1/3} \equiv j = f/2$$

The pumping power of the heat exchanger can be calculated by:

$$P = \left(\frac{fA}{A_c}\right) \left(\frac{G^2}{2\rho}\right) \left(\frac{GA_c}{\rho}\right)$$

Nevertheless, pumping power measures the head loss, and the j factor measures the heat transfer coefficient. Figure 5-16 shows the effect of Reynold number on the ' j ' factor for segmental and helical heat exchangers. The Colburn factor (j) for segmental baffle is more as compared to the helical baffle, and j factor decrease with an increase in the Reynold number.

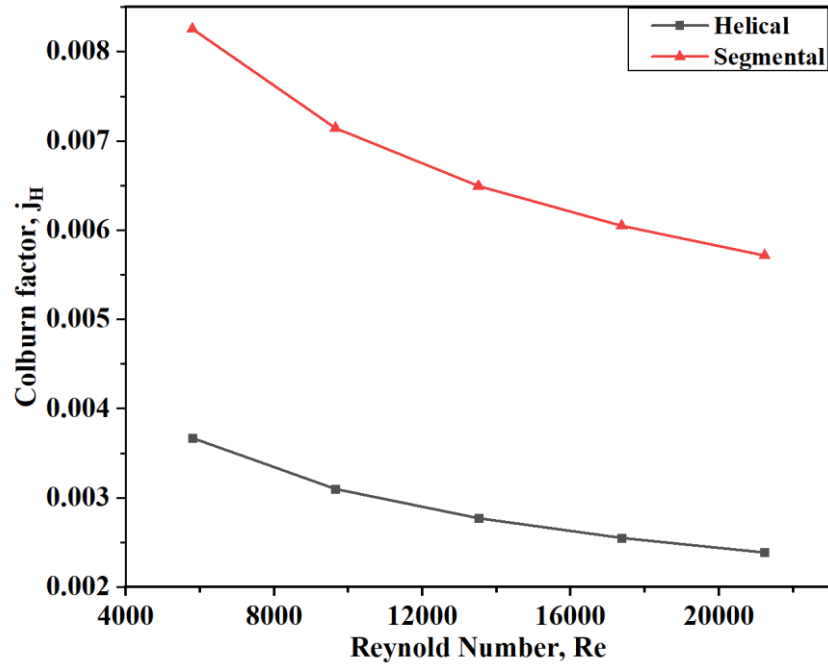


Figure 5-16: Colburn factor of helical and Segmental baffle

As discussed, the heat transfer coefficient for segmental baffle is more as compared to the helical baffle. The same result can also be explained by using ' j ' factor, which is higher for the segmental baffle. However, pumping power for segmental baffle is more as compared to the helical baffle. Figure 5-17 shows the pumping ratio of segmental and helical baffle and result shows that pumping power ratio decrease with increase in Reynold number.

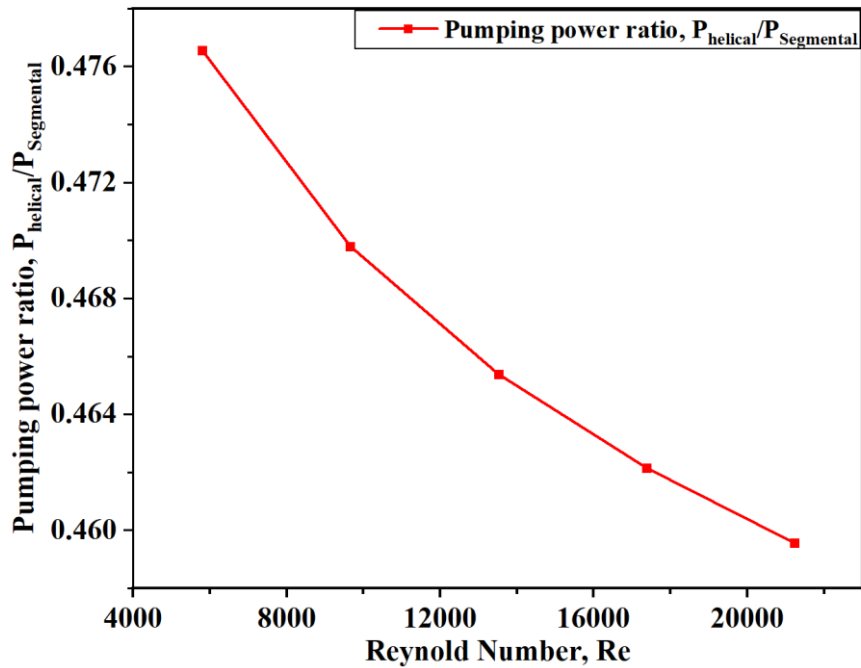


Figure 5-17: Pumping power ratio of helical and Segmental heat exchanger

5.11 THERMAL CYCLING OF STORAGE MATERIAL FOR TES APPLICATION

Thermal cycles of ceramic pebbles used in this research were carried out to analyze the formation of thermal cracks and the change in mechanical properties. In this work a muffle furnace was used to study the effect of cyclic heating and cooling on ceramic balls. Ceramic balls are heated in the muffle furnace to an elevated temperature of 200 °C and left to stand at this temperature for 2 hours and then cooled in the furnace to ambient temperature. Figure 5-18 shows the thermal cycles of storage material.



Figure 5-18 Thermal Cycling of storage material

This process is repeated for 8 cycles and formation of cracks has been studied. Further, mechanical properties before and after thermal cycling has been studied. Figure 5-19 shows the compression test of ceramic pebbles before and after thermal cycling.



Figure 5-19 Compression test of storage material

5.12 ERROR ANALYSIS

The error in measurement is calculated by measuring the error in measurement of temperature and flow rate. The error in measurement of temperature can be calculated by measuring the error in thermocouple and error in measurement of flow rate can be measured by measuring the error in acrylic flow meter. The repeatability of results are calculated by performing the three run test under same operating conditions and same parameter. The percentage repeatability is calculated by measuring the percentage relative standard deviation. The percentage repeatability was found to be within 2.69% based on Gaussian distribution (GD). However for acrylic flow meter the percentage repeatability was found to be within 5.9% based on GD.

CHAPTER 6 – EXPERIMENTAL ANALYSIS OF DUAL MEDIA TANK

6.1 INTRODUCTION

In this chapter numerical and experimental investigations of DMT for CSP applications are carried out. In the numerical study, a physical model of a TES system for a 1 MWe CSP plant is considered. The mathematical formulation of the physical model is carried out using the Schumann model. This section examines the effects of various operational variables such as mass flow, pebble diameter, void fraction, etc. on the thermocline performance of tank. Further experimental results obtained from a LAB scale test facility is used to validate the numerical results obtained from numerical models. With these thermal cycles of the storage material, the life cycle of the material used is also examined. Further work foreseen also includes an extensive study of heat exchanger using different configurations of baffles for further integration of TES system with CSP using shell and tube heat exchanger.

6.2 TEMPERATURE VARIATION

The temperature field of each layer in the dual media tank with time is shown in Figure 6-1. The temperature field consists of three-zone i.e. high-temperature zone, low-temperature zone, and heat exchange zone. In the heat exchange zone, there is a gradual change in temperature due to thick thermocline thickness. The thick thermocline thickness is due to axial conduction along the length of the tank.

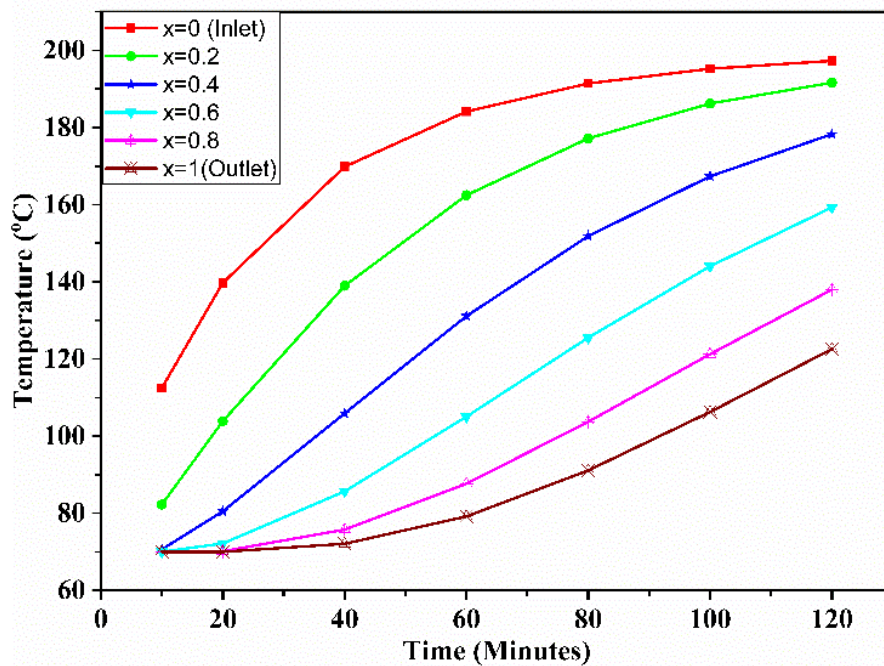


Figure 6-1: Temperature variation along the different section with time

6.3 VARIATION OF TEMPERATURE AT THE OUTLET OF THE TANK

The performance of CSP plants depends on the outlet temperature of the TES tank. The outlet temperature decides the operating hour of CSP plant during cloudy days. The variation in outlet temperature results in fluctuating power supply from CSP plants. The outlet temperature during discharging of the tank at variable mass flow rates is shown in Figure 6-2. The variation in outlet temperature can be minimized by using several techniques, like using Phase change material (PCM) at the outlet. The selection of PCM at the outlet of the tank depends on the cutoff temperature of the TES tank.

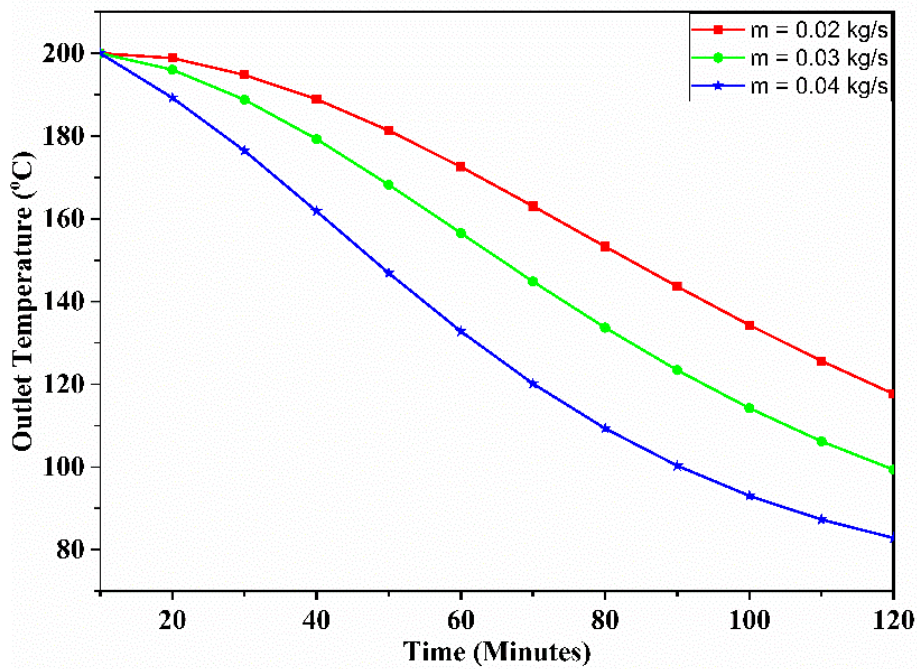


Figure 6-2: Variation of outlet temperature with time

6.4 ENERGY STORED

The energy stored within the storage system at the different instants of time at various mass flow rates is shown in Figure 6-3. The energy stored within the tank increases at a larger rate during one hour and subsequently starts decreasing. The energy stored for a higher mass flow rate is maximum at a particular instant of time. However, at a higher mass flow rate, viscous fingering occurs, disturbing the thermocline stability of the tank.

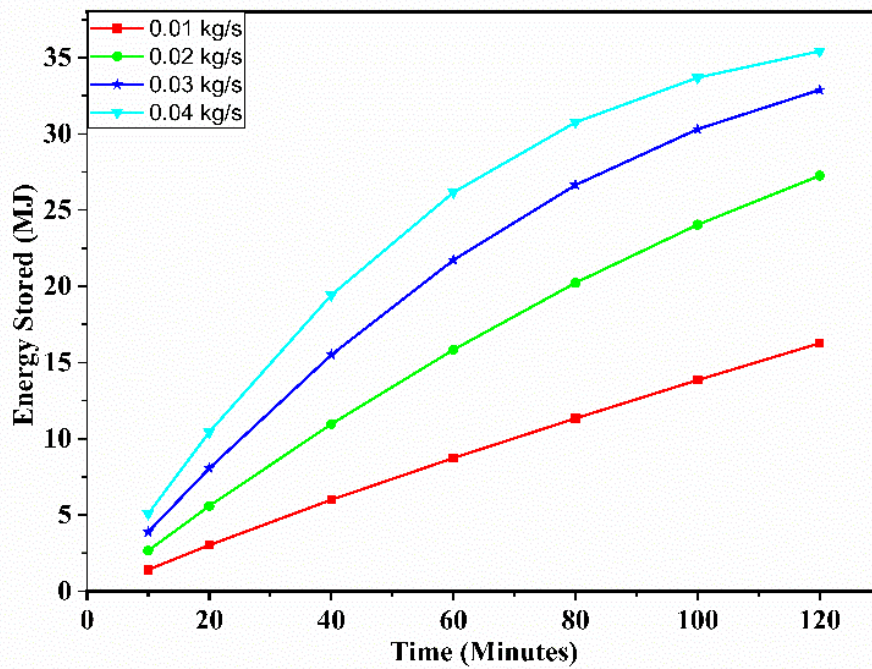


Figure 6-3: Energy stored with time

6.5 CHARGING EFFICIENCY

The charging efficiency of TES system is measured for varying mass flow rate. The result shows maximum charging efficiency for lower mass flow rate. However, charging efficiency increases with time and start decreasing during end of the charging process. The decrease in charging efficiency is due to the formation of thermocline region which keeps on moving as the charging process progresses. The reduction in charging efficiency at lower mass flow rate is nominal. However for higher mass flow rate the reduction is on higher side. The reason for reduction in charging efficiency at higher mass flow rate is mixing of hot and cold fluid which results in thicker thermocline region.

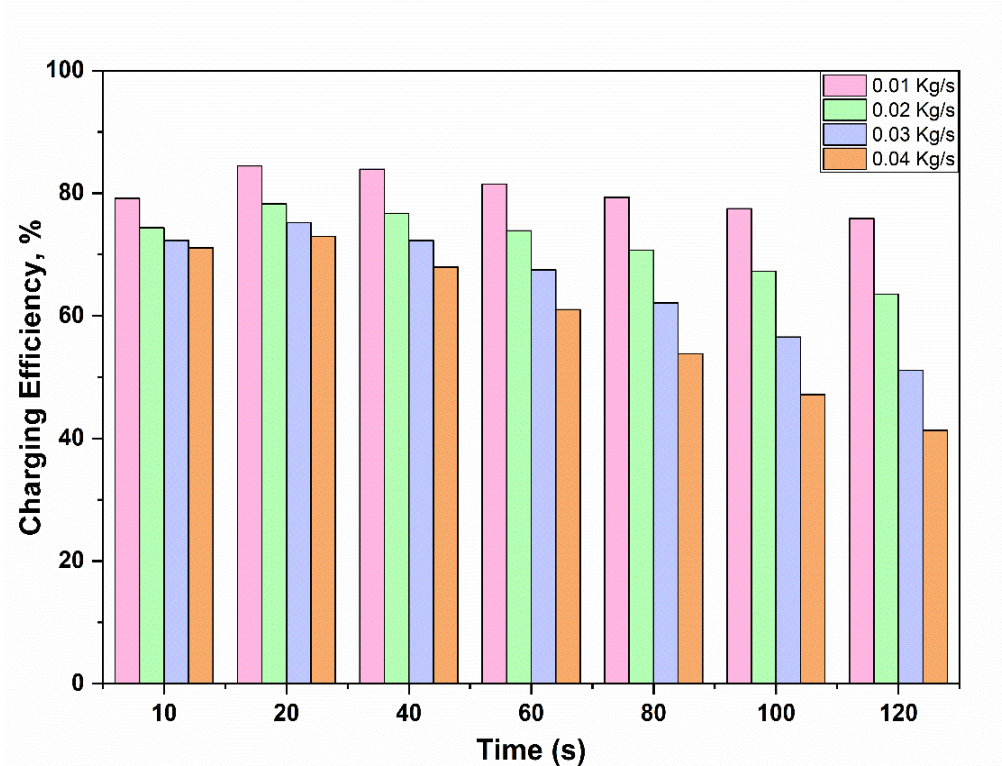


Figure 6-4: Charging efficiency of dual media thermocline tank at varying mass flow rate

6.6 THERMAL CYCLING OF STORAGE MATERIAL

The thermal cycling of ceramic pebbles shows that it is stable over a wide range of temperature. The thermal crack initiation starts after 6th cycle as shown in Figure 6-5. The ceramic pebbles are heated to a temperature of 200 °C and kept at this temperature for 2 h. Thereafter it is cooled to a ambient temperature in furnace. The compressive strength of material is found decreasing during thermal cycling. Initially, ceramic pebbles are found to withstand a pressure of 60.6 kN and after 8th cycle the maximum tolerable pressure was found 30.1 kN. The change in the physical properties during different thermal cycle is shown in the Table 6-1.

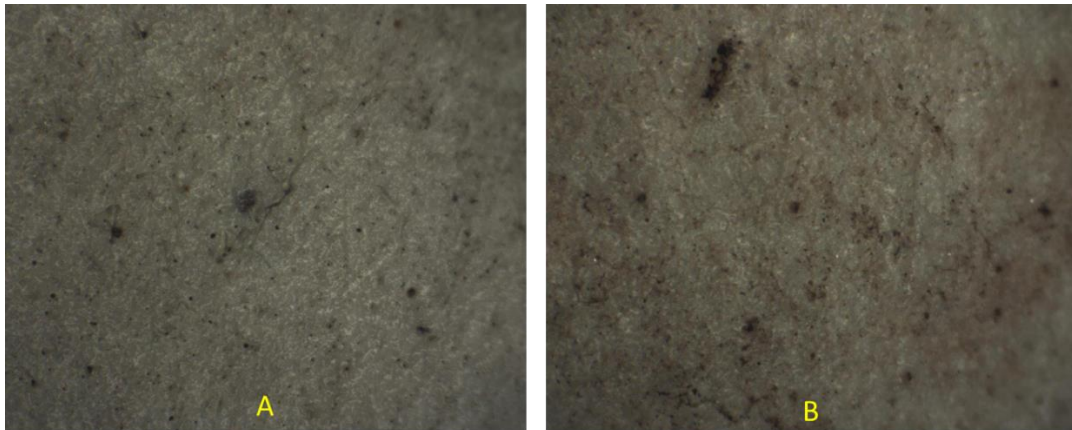


Figure 6-5: Thermal Cycling (A) Initial (B) After 8th Cycle

Table 6-1: Physical properties after different thermal cycle

Thermal Cycle	D (mm)	m (gm)	Density	Load Bearing capacity (kN)
0	75	815	3691.437	60.6
1	75.2	814.8	3661.163	58.2
2	75.5	814.6	3616.805	52.7
3	75.7	814.2	3586.452	46.5
4	75.8	814.1	3571.838	43.2
5	75.9	813.9	3556.865	38.1
6	75.9	813.8	3556.428	36.3
7	75.9	813.6	3555.553	34.2
8	75.9	813.5	3555.116	30.1

CHAPTER 7 – THERMO-ECONOMIC OPTIMIZATION

7.1 PARAMETRIC OPTIMIZATION

The performance of TES is evaluated by performing a numerical simulation based on the Schumann Model. The parametric investigations include parameters like a void fraction, D/L ratio, pebbles diameter, mass flow rate, thermal diffusivity of solid and HTF. The parametric optimization is based on a multilevel parameters approach. The optimization function is to minimize the thermocline thickness for better performance of the TES system. The DOE method has been used to optimize the multi-control parameters. The DOE method using Taguchi is used to avoid multiple simulations. This method examines only a few models using an orthogonal array. In this study, seven control factors are taken to optimize thermocline thickness. The control factors and their level of variations are listed in Table 7-1.

Table 7-1: Control factors

Parameter		Level 1	Level 2	Level 3
A	D/L ratio	1	1.2	1.4
B	Mass flow rate	8	8.5	9
C	Void Fraction	0.3	0.4	0.5
D	Pebbles diameter	0.04	0.05	0.06
E	Thermal diffusivity of pebbles	7.15e-08	1.54e-06	7.02e-07
F	Thermal diffusivity of HTF	7.44e-08	5.26e-08	5.49e-08
G	Time (hr)	2	3	4

The possible combination of control factor and their variation is 7^4 (2401), and require more computational time. The number of simulations can be reduced by using the Taguchi method. The Taguchi method reduces the number of simulations from 7^4 to 27 using the L27 orthogonal array. The parameters in the orthogonal array are listed in Table 7-2.

Table 7-2: Orthogonal array

D/L	Mass flow rate (kg/s)	Void fraction	Pebbles diameter (m)	Thermal diffusivity-Pebbles	Thermal diffusivity-HTF	Discharging Time (Hr)
1	8	0.3	0.04	7.15E-08	7.44E-08	2
1	8	0.3	0.04	1.54E-06	5.26E-08	3
1	8	0.3	0.04	7.02E-07	5.49E-08	4
1	8.5	0.4	0.05	7.15E-08	7.44E-08	2
1	8.5	0.4	0.05	1.54E-06	5.26E-08	3
1	8.5	0.4	0.05	7.02E-07	5.49E-08	4
1	9	0.5	0.06	7.15E-08	7.44E-08	2
1	9	0.5	0.06	1.54E-06	5.26E-08	3
1	9	0.5	0.06	7.02E-07	5.49E-08	4
1.2	8	0.4	0.06	7.15E-08	5.26E-08	4
1.2	8	0.4	0.06	1.54E-06	5.49E-08	2
1.2	8	0.4	0.06	7.02E-07	7.44E-08	3
1.2	8.5	0.5	0.04	7.15E-08	5.26E-08	4
1.2	8.5	0.5	0.04	1.54E-06	5.49E-08	2
1.2	8.5	0.5	0.04	7.02E-07	7.44E-08	3
1.2	9	0.3	0.05	7.15E-08	5.26E-08	4
1.2	9	0.3	0.05	1.54E-06	5.49E-08	2
1.2	9	0.3	0.05	7.02E-07	7.44E-08	3
1.4	8	0.5	0.05	7.15E-08	5.49E-08	3
1.4	8	0.5	0.05	1.54E-06	7.44E-08	4
1.4	8	0.5	0.05	7.02E-07	5.26E-08	2
1.4	8.5	0.3	0.06	7.15E-08	5.49E-08	3
1.4	8.5	0.3	0.06	1.54E-06	7.44E-08	4
1.4	8.5	0.3	0.06	7.02E-07	5.26E-08	2
1.4	9	0.4	0.04	7.15E-08	5.49E-08	3
1.4	9	0.4	0.04	1.54E-06	7.44E-08	4
1.4	9	0.4	0.04	7.02E-07	5.26E-08	2

The thermocline thickness is calculated for each combination of control factors in the orthogonal array. Additionally, a correlation has been established to determine the thermocline thickness using regression analysis.

$$x_{Th} = -2.955A + 0.2266B - 0.144C + 24.944D - 5947D + 6484041.606E + 0.266F + 1.74699 \quad (7-1)$$

Where, x_{Th} = Thermocline Thickness, A = D/L ratio, B = Mass flow rate (kg/s), C = Void fraction, D = Pebble's diameter (m), E = Pebbles thermal diffusivity, F = HTF Thermal diffusivity. The developed correlation was validated with numerical and experiment results of Hoffmann et al. (Hoffmann,

Fasquelle, Goetz, & Py, 2016) and found to be in reasonable agreement for a D/L ratio greater than 1. Table 7-3 shows the validation of developed correlation with the results obtained for the Solar One plant.

Table 7-3: Validation of developed correlation

Thermocline Thickness, x_{Th}	Solar One, Pilot	Correlation	% Error
x_{Th} at t = 4 h	5.1	4.18	18%
x_{Th} at t = 8h	5.5	5.25	4.5 %

7.2 OPTIMUM PARAMETERS FOR MINIMUM THERMOCLINE THICKNESS

In this study, the Taguchi method is used to find the optimum parameter for minimum thermocline thickness. This analysis calculates the SNR ratio to find the most favorable control factor for minimum thermocline thickness.

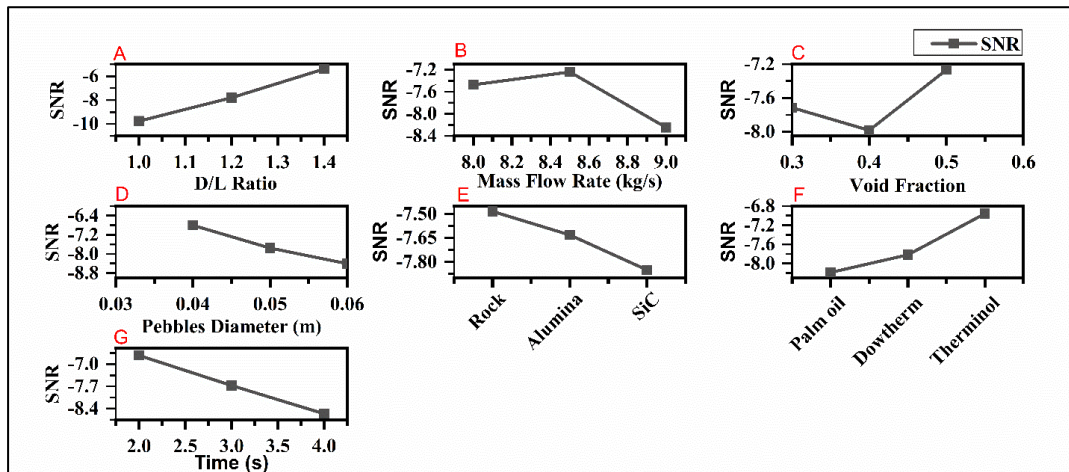


Figure 7-1: SNR of control factor

The level of control factor for minimum thermocline thickness is shown in Figure 7-1. The optimal parameter for the minimum thermocline thickness is the D / L ratio of 1.4, the mass flow rate of 9 kg / s, the void fraction 0.4, the diameter of the pebbles 0.06, the lower thermal conductivity of the pebbles, and the higher thermal conductivity of HTF.

7.3 MODEL VALIDATION

The LAB scale test facility is used to validate the numerically predicted thermocline behavior of the tank. In the numerical simulation, maximum and minimum temperatures are fixed as 200 °C and 70 °C. The mass flow rate is maintained at 40 lit/min for both numerical model and experimental setup. Figure 7-2 illustrates the experimental validation of the developed numerical

model, and numerically predicted results are found very close to the experimental results within the error of 13%. However, the percentage error keeps on decreasing with time.

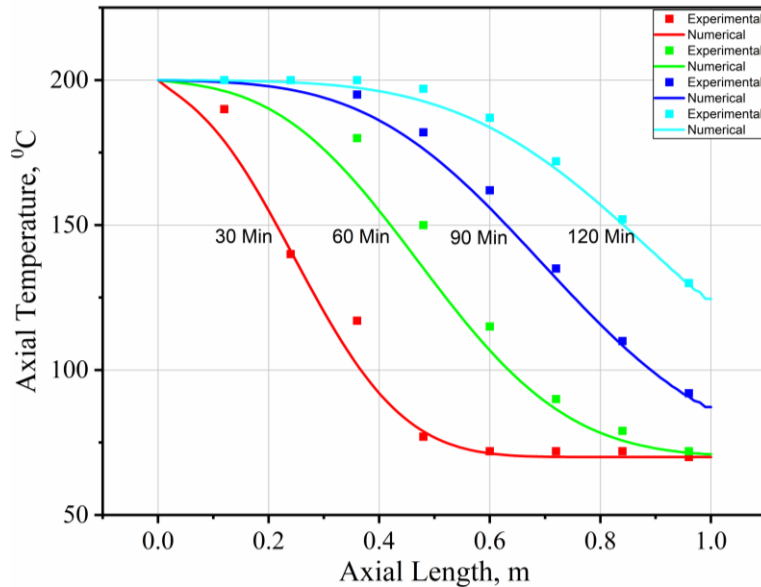


Figure 7-2: Validation of numerically predicted thermocline performance with the experimental result

The proposed model has certain limitations in terms of numerical and experimental methodology such as uniform inlet temperature, limited to $Bi < 0.1$ and uniform pebbles diameter. However, these limitations can be overcome by modelling energy equations for variable temperature and variable pebbles diameter. In addition, the LAB scale test facility developed is limited to a uniform temperature. As we know, solar energy is intermittent and this intermittency of solar energy is missing in the test facility. To get the intermittency nature and seasonal variation, the test facility can be integrated with solar collector.

7.4 TECHNO-ECONOMIC ANALYSIS

The cost analysis of the TES (DMT) system for 1 MW_e CSP requires filler material cost, HTF cost, storage tank cost, and another miscellaneous cost. The miscellaneous cost includes piping, fitting, and electrical and instrumentation cost. The 1 MW_e CSP plant of efficiency 20% requires 20 MWh_{Th} storage system for 4h charging and discharging duration.

$$Q_t = V(\rho_f C_{pf})(T_h - T_L) \quad (7-2)$$

Here, Q_t is the total energy required, V is the volume of the tank, ρ_f is the density of HTF, C_{pf} is the specific heat of the HTF, T_h is the maximum temperature of HTF and T_L is the lowest temperature of HTF.

$$Q_t = \frac{P}{\eta} \Delta t \quad (7-3)$$

Here, P is the capacity of the power plant, η is the thermal efficiency of the plant, and Δt is the charging and discharging duration.

The mass of filler material and HTF required for the DMT tank can be calculated by the definition of void fraction. The void fraction is the ratio of the volume of voids and total volume. The volume of voids is equivalent to the volume of HTF required for the DMT tank. The cost assumption of various TES components for techno-economic analysis is shown in Table 7-4.

Table 7-4: Cost assumption for techno-economic analysis of TES system (DMT) (Mostafavi, Taylor, Nithyanandam, & Shafiei, 2017; Nithyanandam & Pitchumani, 2014)

Components	Unit	Cost
C_{HTF}	US\$/kg	1.15 US\$/kg
C_{filler}	US\$/kg	1.3
C_{SS}	US\$/kg	4.5
$C_{insulation}$	US\$/m ²	230
$C_{foundation}$	US\$/m ²	1210
$C_{pipe\ and\ fitting}$	US\$/kWh _{TH}	0.39
$C_{electric\ and\ instrumentation}$	US\$/kWh _{TH}	0.9

The total cost of TES (DMT) can be expressed as:

$$C_T = C_s + C_{tank} + C_i + C_{fo} + C_{pf} + C_{EI}, \quad (7-4)$$

where C_T is the total cost of the TES system, C_s is the storage material cost (includes HTF and filler material for DMT tank), C_{tank} is the cost of the stainless steel tank, C_i is the cost of insulation, C_{fo} is the foundation cost, C_{pf} is the piping and fitting cost and C_{EI} is the electric and instrument cost. The cost of storage material can be calculated as:

$$C_s = [\rho_f C_{HTF} \varepsilon + \rho_s C_{filler} (1 - \varepsilon)] \times \frac{\pi D^2}{4} \times L. \quad (7-5)$$

Here, ρ_f is the density of the fluid, C_{HTF} is the cost of HTF, ρ_s is the density of filler material, C_{filler} is the cost of filler material, ε is the void fraction, D is the diameter of the tank, and L is the length of the tank.

The cost of a stainless-steel tank can be calculated as:

$$C_{tank} = \rho_{SS}L[\pi(R + t_h)^2 - \pi R^2]C_{SS} \quad (7-6)$$

Where, t_h is the thickness of the storage shell, ρ_{SS} is the density of stainless-steel tank, L is the length of the tank, R is the radius of tank and C_{SS} is the cost of stainless-steel tank. The thickness of the storage tank is considered relatively thick to avoid mechanical failure of the storage tank caused by thermal ratcheting. In this analysis thickness of the shell is considered as 0.06 m to avoid thermal ratcheting as suggested by (González et al., 2016). Similarly, foundation and insulation cost can be calculated as:

$$C_{fo} = \frac{\pi D^2}{4} C_{foundation} \quad (7-7)$$

$$C_i = \pi D L C_{insulation} \quad (7-8)$$

Based on the various cost estimates, the NCOTES system is calculated for 1 MWe CSP with a maximum and minimum temperature of 390 °C and 290 °C, respectively, and 4 h charging and discharging duration. Table 7-5 shows the cost breakdown of DMT for 1 MWe CSP plant.

Table 7-5: Cost breakdown of TES (DMT) system for 1 MWe CSP

Cost Break down	Unit	DMT
HTF cost	US\$	70256.71
Filler material cost	US\$	20158.42
Cost of storage tank	US\$	197820
Insulation cost	US\$	33672
Foundation cost	US\$	36880.8
Piping, valve, and fitting cost	US\$	7800
Electric and Instrumentation cost	US\$	18000
Overhead cost	US\$	38458.79
Installation Cost	US\$	84609.35
Total Cost	US\$	507656.1
Specific Cost	US\$/kWh _{TH}	25.38
NCOTES @ 3h peak sunshine	US\$/ MWh _e	463

The specific cost of the TES system does not indicate the performance of the TES system, including cost. Thus, the specific cost is not the correct indicator of techno-economic analysis. Therefore, the normalized cost of the thermal energy storage system (NCOTES) has been taken into account to evaluate the techno-economic analysis of various alternatives of the TES system. NCOTES is defined as the ratio of the overall capital cost of the TES system and gross

annual electricity generation of the CSP plant. The annual electricity generation of the TES system depends on the region and DNI value. However, peak sunshine duration is an essential parameter to evaluate the operating hour of the CSP plant.

CHAPTER 8 - CONCLUSIONS AND FUTURE WORK

Aim of this research work was to investigate the characteristic behaviour of DMT thermal energy storage system for CSP applications with focus on development of experimental test facility to integrate system with power cycle.

Chapter 1 introduced thermal energy storage system for concentrated solar power applications and described how the TES system integration with CSP could be used to overcome the intermittent nature of solar energy and high levelized cost of electricity. This research work is set out to investigate the effect of operating variables on thermal performance of TES system. The primary objective of this research work was to investigate the thermo-economic model of solar thermal energy storage system for CSP application and to use the optimization technique to identify the optimum variables for maximum charging and discharging efficiency of TES system. This research work is also focusses on the parametric optimization for minimum thermocline thickness under wide range of operating variables.

Chapter 2 comprises of detailed study of Dual media Tank along with its technical barrier and their solution in integration of TES system with CSP application. In this chapter, DMT is compared with other storage technology in terms of commercialization and technology advancement and DMT is found more economical as compared to other technologies. In spite of economical, this technology is still not commercially available. Additionally, comparative study of thermocline thickness for DMT and molten salt tank is studied and it was found that Two-Tank molten salt TES system has minimum thermocline thickness as compared to Dual media tank. DMT uses storage material (rock pebbles etc.) and HTF in a single tank and hot and cold fluid are thermally stratified within the tank. The selection of storage material and HTF is also discussed in Chapter 2 and it was found that higher thermal diffusive material

has higher thermocline thickness. The comparison of few storage materials for DMT is given in Table 8-1 Thermophysical properties of storage material

Table 8-1 Thermophysical properties of storage material

Pebbles	Density (kg/m³)	Thermal conductivity (W/mK)	Specific Heat (kJ/kg K)	Thermal diffusivity
Alumina	3690	30	780	1.04E-05
Quartzite	2500	5.69	830	2.74E-06
Slag	2850	1.66	895	6.50E-07

Beside this, heat transfer model for TES systems is also studied and it was found that Schumann model is simplest energy model and requires less computational time as compared to other models. However, Single phase model is effective for TES system with high thermal conductivity and high heat capacity storage material. Contrary to this, concentric Dispersion model is most realistic model and requires more computational time as compared to other models. Further a detailed methodology is discussed in Chapter 3 to study the thermocline behaviour of tank under various operating conditions.

In Chapter 4 the DMT TES system is modelled using Schumann Energy model. Additionally, an empirical correlation was developed and validated with numerical and experiment results were found to be in reasonable agreement for a D/L ratio greater than 1. Based on the numerical results the following conclusion is summarized.

- The high thermal conductivity of HTF will cause disturbance in thermocline thickness and reduce the discharging time
- No significant change has been found in the thermocline thickness of DMT with an increase in the mass flow rate. The percentage movement of the thermocline layer was observed to be 70.37% with an increase of 18.75% in the mass flow rate. This shows that the mass flow rate has a greater influence on the discharge time.
- The percentage increase in volumetric heat transfer coefficient was found to be 9.56% with an increase of 18.75% in the mass flow rate. This shows that

an increase in mass flow rate improves the volumetric heat transfer coefficient between pebbles and HTF.

- A decrease in pebbles diameter increases the void fraction resulting in a greater pressure drop. However, improvement in thermal exchange has been found with the decrease in pebble's diameter. The percentage improvement in volumetric heat transfer coefficient was found to be 80% with a 33.33% decrease in pebble diameter.

In Chapter 5 an experimental setup is developed to study the characteristic behavior of DMT for CSP applications. The experimental setup is designed for 1.2 kWe solar thermal power plant with 20% thermal efficiency. The system designed can give 17.3 kWh_{Th} thermal power for 2h charging and discharging. A ceramic pebble is used as a storage material due to its higher heat and wear resistance. The HTF used was Synthrm due to its lower thermal conductivity and wide operating range. Further, the design of heat exchanger has also been done to integrate the system with CSP and to study the discharging behavior of tank. In this the effectiveness of shell and tube heat exchanger without baffle (WB), with segmented baffle with baffle cut of 30⁰ and 50⁰ (SB-30 and SB-50) and align baffle with baffle cut of 30⁰ and 50⁰ are compared numerically.

- A numerical result shows that effectiveness is nearly 22% higher than WB (Heat exchanger without baffle) and 2.5 % than align baffle with baffle cut of 50⁰. The effectiveness decreased with an increase in baffle cut for both segmental and aligned baffle.
- The numerical result of AB-30 is validated with experimental setup consist of the same baffle design for different inlet temperatures in the range of 333 K to 363 K. The deviation of 10.1% was observed in the numerical and experimental models.
- Pressure drop and Nusselt number are compared numerically using empirical correlation for helical baffle with a helix angle of 25⁰ and segmental baffle at Reynold's number varied between 5000~2100 in the turbulent zone. The result shows that for helical baffle (25⁰ helix angles),

the pressure drop is nearly 89 % lower than the segmental baffle at Reynold number of 5790.38.

- For maximum heat recovery rate and the low-cost segmental baffle is the most preferred configuration
- The Colburn factor for segmental baffle is higher as compared to helical baffle. However, the pumping power of helical baffle is less as compared to segmental baffle

It is observed that align baffle with baffle cut of 30^0 is more effective as compared to other configurations like align baffle of 50^0 , Segmental baffle of 30^0 and 50^0 cut and can be recommended for industrial use. Other than baffle, cut, the segmental and helical baffle is also compared, and comparison shows that helical baffle is more effective and can be recommended for industrial use.

In Chapter 6 an experimental analysis has been done to study the validate the numerical model and to study the thermal behavior of TES system for CSP applications. Based on the experimental analysis carried out following conclusions are summarized.

- Thermocline thickness is due to the axial conduction along the length of the tank
- The percentage drop in outlet temperature was found 40% for a mass flow rate of 0.02 kg/s and 60% for a mass flow rate of 0.04 kg/s. However, the duration of discharging time for higher mass flow rate was found less.
- An increasing trend of energy stored was observed during the initial hour and later on it is suppressed. However, the energy stored is maximum for higher mass flow rate.
- A nominal change in charging efficiency was observed for a mass flow rate of 0.01 kg/s. However 40% drop in charging efficiency was observed for a mass flow rate of 0.04 kg/s
- The temperature change of the storage material shows a decrease in the load-bearing capacity of the storage material.
- The maximum tolerable pressure of the storage material during the initial cycle was ~ 60 KN and after 8 cycles its compressive strength decreased by 50%. However, thermal cracks was slower.

- No cracks were found during the first few cycles, but after the 7th cycle thermal cracks starts at a slower rate.

In Chapter 7 parametric optimization has been done along techno economic of TES system for CSP applications. Based on the analysis carried out following conclusions are summarized.

- Correlation developed to calculate thermocline thickness is found to be in reasonable agreement for the D/L ratio greater than 1.
- The optimal parameter for minimum thermocline thickness is D/L ratio 1.4, mass flow rate 9 kg/s, void fraction 0.4, pebbles diameter 0.06, lower thermal diffusivity of pebbles, and higher thermal diffusivity of HTF.
- Specific cost is not the correct indicator of techno-economic analysis. The normalized cost of the thermal energy storage system (NCOTES) can be taken to evaluate the various alternatives of the TES system.

The thermocline model presented in this work showed a good agreement between numerical and experimental results with suitable boundary conditions. However, the wall effect with variable void fraction during charging and discharging of the tank is not considered in the numerical model, and that needs to be addressed in the future. Since the thermocline thickness is a broad parameter for studying the thermocline behavior of tanks. Therefore, the use of empirical correlation to determine the thermocline thickness is strongly recommended for the initial investigation of TES tank design.

Future studies will involve thermodynamic modeling of TES tank by considering wall effects with variable pebbles diameter. However, to investigate the influence of variable temperature, a realistic approach will be used in the experimental setup by integrating the system with a solar receiver and a parabolic trough collector.

REFERENCES

- Advances in Thermal Energy Storage Systems: Methods and Applications - Google Books. (n.d.).
- Agalit, H., Zari, N., Maalmi, M., & Maaroufi, M. (2015). Numerical investigations of high temperature packed bed TES systems used in hybrid solar tower power plants. *Solar Energy*, *122*, 603–616. <https://doi.org/10.1016/j.solener.2015.09.032>
- Aghaei, M., Kumar, N. M., Eskandari, A., Ahmed, H., de Oliveira, A. K. V., & Chopra, S. S. (2020). Solar PV systems design and monitoring. *Photovoltaic Solar Energy Conversion*, 117–145. <https://doi.org/10.1016/b978-0-12-819610-6.00005-3>
- Ahmed, N., Elfeky, K. E., Lu, L., & Wang, Q. W. (2019). Thermal and economic evaluation of thermocline combined sensible-latent heat thermal energy storage system for medium temperature applications. *Energy Conversion and Management*, *189*, 14–23. <https://doi.org/10.1016/j.enconman.2019.03.040>
- Almendros-Ibáñez, J. A., Fernández-Torrijos, M., Díaz-Heras, M., Belmonte, J. F., & Sobrino, C. (2019). A review of solar thermal energy storage in beds of particles: Packed and fluidized beds. *Solar Energy*, *192*(January), 193–237. <https://doi.org/10.1016/j.solener.2018.05.047>
- Alptekin, E., & Ezan, M. A. (2020). Performance investigations on a sensible heat thermal energy storage tank with a solar collector under variable climatic conditions. *Applied Thermal Engineering*, *164*, 114423. <https://doi.org/10.1016/j.applthermaleng.2019.114423>
- Aneke, M., & Wang, M. (2016). Energy storage technologies and real life applications – A state of the art review. *Applied Energy*, *179*, 350–377. <https://doi.org/10.1016/j.apenergy.2016.06.097>
- Araújo, A. K. A., & Medina T., G. I. (2018). Analysis of the effects of climatic conditions, loading level and operating temperature on the heat losses of two-tank thermal storage systems in CSP. *Solar Energy*, *176*(September),

- 358–369. <https://doi.org/10.1016/j.solener.2018.10.020>
- Baghapour, B., Rouhani, M., Sharafian, A., Kalhori, S. B., & Bahrami, M. (2018a). A pressure drop study for packed bed adsorption thermal energy storage. *Applied Thermal Engineering*, *138*, 731–739. <https://doi.org/https://doi.org/10.1016/j.applthermaleng.2018.03.098>
- Baghapour, B., Rouhani, M., Sharafian, A., Kalhori, S. B., & Bahrami, M. (2018b). A pressure drop study for packed bed adsorption thermal energy storage. *Applied Thermal Engineering*, *138*, 731–739. <https://doi.org/https://doi.org/10.1016/j.applthermaleng.2018.03.098>
- Barlev, D., Vidu, R., & Stroeve, P. (2011). Innovation in concentrated solar power. *Solar Energy Materials and Solar Cells*, *95*(10), 2703–2725. <https://doi.org/10.1016/j.solmat.2011.05.020>
- Bayón, R., Rivas, E., & Rojas, E. (2014). Study of thermocline tank performance in dynamic processes and stand-by periods with an analytical function. *Energy Procedia*, *49*, 725–734. <https://doi.org/10.1016/j.egypro.2014.03.078>
- Bayón, R., & Rojas, E. (2013). Simulation of thermocline storage for solar thermal power plants: From dimensionless results to prototypes and real-size tanks. *International Journal of Heat and Mass Transfer*, *60*(1), 713–721. <https://doi.org/10.1016/j.ijheatmasstransfer.2013.01.047>
- Bell, S., Steinberg, T., & Will, G. (2019). Corrosion mechanisms in molten salt thermal energy storage for concentrating solar power. *Renewable and Sustainable Energy Reviews*, *114*(November 2018), 109328. <https://doi.org/10.1016/j.rser.2019.109328>
- Bijarniya, J. P., Sudhakar, K., & Baredar, P. (2016). Concentrated solar power technology in India: A review. *Renewable and Sustainable Energy Reviews*, *63*, 593–603. <https://doi.org/10.1016/j.rser.2016.05.064>
- Boretti, A., Castelletto, S., & Al-Zubaidy, S. (2019). Concentrating solar power tower technology: Present status and outlook. *Nonlinear Engineering*, *8*(1), 10–31. <https://doi.org/10.1515/nleng-2017-0171>
- Bruch, A., Fourmigué, J. F., & Couturier, R. (2014). Experimental and numerical investigation of a pilot-scale thermal oil packed bed thermal

-
- storage system for CSP power plant. *Solar Energy*, *105*, 116–125.
<https://doi.org/10.1016/j.solener.2014.03.019>
- Bruch, A., Fourmigue, J. F., Couturier, R., & Molina, S. (2014). Experimental and numerical investigation of stability of packed bed thermal energy storage for CSP power plant. *Energy Procedia*, *49*, 743–751.
<https://doi.org/10.1016/j.egypro.2014.03.080>
- Buonomano, A., Calise, F., & Palombo, A. (2018). Solar heating and cooling systems by absorption and adsorption chillers driven by stationary and concentrating photovoltaic/thermal solar collectors: Modelling and simulation. *Renewable and Sustainable Energy Reviews*, *81*, 1112–1146.
<https://doi.org/10.1016/j.rser.2017.07.056>
- Cabello Núñez, F., López Sanz, J., & Zaversky, F. (2019). Analysis of steel making slag pebbles as filler material for thermocline tanks in a hybrid thermal energy storage system. *Solar Energy*, *188*(February), 1221–1231.
<https://doi.org/10.1016/j.solener.2019.07.036>
- Cabeza, L. F., Martorell, I., Miró, L., Fernández, A. I., & Barreneche, C. (2015). *Introduction to thermal energy storage (TES) systems. Advances in Thermal Energy Storage Systems: Methods and Applications*. Woodhead Publishing Limited. <https://doi.org/10.1533/9781782420965.1>
- Chang, Z. S., Li, X., Xu, C., Chang, C., & Wang, Z. F. (2015). The Design and Numerical Study of a 2MWh Molten Salt Thermocline Tank. *Energy Procedia*, *69*, 779–789. <https://doi.org/10.1016/j.egypro.2015.03.094>
- Cocco, D., & Serra, F. (2015). Performance comparison of two-tank direct and thermocline thermal energy storage systems for 1 MWe class concentrating solar power plants. *Energy*, *81*, 526–536.
<https://doi.org/https://doi.org/10.1016/j.energy.2014.12.067>
- Concentrated solar power (CSP) in India: An outlook to 2024 – HELIOSCSP. (n.d.). Retrieved July 13, 2020, from <http://helioscsp.com/concentrated-solar-power-csp-in-india-an-outlook-to-2024/>
- Concentrating solar power – Tracking Power – Analysis - IEA. (n.d.). Retrieved June 3, 2020, from <https://www.iea.org/reports/tracking-power-2019/concentrating-solar-power>

- Crandall, D. M., & Thacher, E. F. (2004). Segmented thermal storage, 77(May 2003), 435–440. <https://doi.org/10.1016/j.solener.2003.08.011>
- Doretti, L., Martelletto, F., & Mancin, S. (2019). A simplified analytical approach for concrete sensible thermal energy storages simulation. *Journal of Energy Storage*, 22(January), 68–79. <https://doi.org/10.1016/j.est.2019.01.029>
- du Plessis, J. P., & Woudberg, S. (2008). Pore-scale derivation of the Ergun equation to enhance its adaptability and generalization. *Chemical Engineering Science*, 63(9), 2576–2586. <https://doi.org/10.1016/j.ces.2008.02.017>
- Elouali, A., Kousksou, T., El Rhafiki, T., Hamdaoui, S., Mahdaoui, M., Allouhi, A., & Zeraouli, Y. (2019). Physical models for packed bed: Sensible heat storage systems. *Journal of Energy Storage*, 23(January), 69–78. <https://doi.org/10.1016/j.est.2019.03.004>
- ELSihiy, Els. S., Liao, Z., Xu, C., & Du, X. (2021). Dynamic characteristics of solid packed-bed thermocline tank using molten-salt as a heat transfer fluid. *International Journal of Heat and Mass Transfer*, 165, 120677. <https://doi.org/10.1016/j.ijheatmasstransfer.2020.120677>
- Energy Storage – Analysis - IEA. (n.d.).
- Erdim, E., Akgiray, Ö., & Demir, I. (2015). A revisit of pressure drop-flow rate correlations for packed beds of spheres. *Powder Technology*, 283, 488–504. <https://doi.org/10.1016/j.powtec.2015.06.017>
- Ergun, S., & Orning, A. A. (1949). Fluid Flow through Randomly Packed Columns and Fluidized Beds. *Industrial & Engineering Chemistry*, 41(6), 1179–1184. <https://doi.org/10.1021/ie50474a011>
- Erregueragui, Z., Boutammachte, N., & Bouatem, A. (2016). Packed-bed Thermal Energy Storage Analysis : Quartzite and Palm- Oil Performance. *Energy Procedia*, 99(March), 370–379. <https://doi.org/10.1016/j.egypro.2016.10.127>
- Esence, T., Bruch, A., Molina, S., Stutz, B., & Fourmigué, J. F. (2017). A review on experience feedback and numerical modeling of packed-bed thermal energy storage systems. *Solar Energy*, 153, 628–654.

- <https://doi.org/10.1016/j.solener.2017.03.032>
- Ethod, M. (2012). IMPROVED PERFORMANCE OF HEAT EXCHANGER OVER SEGMENTAL BUFFLE HEAT EXCHANGER USING KERN'S, 5(1), 29–39.
- Fernández-Torrijos, M., Sobrino, C., & Almendros-Ibáñez, J. A. (2017). Simplified model of a dual-media molten-salt thermocline tank with a multiple layer wall. *Solar Energy*, 151, 146–161. <https://doi.org/10.1016/j.solener.2017.04.072>
- Filali Baba, Y., Al Mers, A., & Ajdad, H. (2020). Dimensionless model based on dual phase approach for predicting thermal performance of thermocline energy storage system: Towards a new approach for thermocline thermal optimization. *Renewable Energy*, 153, 440–455. <https://doi.org/10.1016/j.renene.2020.01.102>
- Flueckiger, S. M., Iverson, B. D., Garimella, S. V., & Pacheco, J. E. (2014). System-level simulation of a solar power tower plant with thermocline thermal energy storage. *Applied Energy*, 113, 86–96. <https://doi.org/10.1016/j.apenergy.2013.07.004>
- Gajbhiye, P., Salunkhe, N., Kedare, S., & Bose, M. (2018). Experimental investigation of single media thermocline storage with eccentrically mounted vertical porous flow distributor. *Solar Energy*, 162(December 2017), 28–35. <https://doi.org/10.1016/j.solener.2017.12.062>
- Galione, P. A., Pérez-Segarra, C. D., Rodríguez, I., Torras, S., & Rigola, J. (2015). Multi-layered solid-PCM thermocline thermal storage for CSP. Numerical evaluation of its application in a 50MWe plant. *Solar Energy*, 119, 134–150. <https://doi.org/10.1016/j.solener.2015.06.029>
- Gautam, A., & Saini, R. P. (2020). A review on technical, applications and economic aspect of packed bed solar thermal energy storage system. *Journal of Energy Storage*, 27(October 2019), 101046. <https://doi.org/10.1016/j.est.2019.101046>
- Geissbühler, L., Kolman, M., Zanganeh, G., Haselbacher, A., & Steinfeld, A. (2016). Analysis of industrial-scale high-temperature combined sensible/latent thermal energy storage. *Applied Thermal Engineering*, 101.

- <https://doi.org/10.1016/j.applthermaleng.2015.12.031>
- Geissbühler, L., Mathur, A., Mularczyk, A., & Haselbacher, A. (2019). An assessment of thermocline-control methods for packed-bed thermal-energy storage in CSP plants , Part 1 : Method descriptions. *Solar Energy*, *178*(December 2018), 341–350. <https://doi.org/10.1016/j.solener.2018.12.015>
- Global energy use projected to nearly double by 2050 - Energy Live News. (n.d.). Retrieved May 15, 2021, from <https://www.energylivenews.com/2020/01/08/global-energy-use-projected-to-nearly-double-by-2050/>
- González, I., Pérez-segarra, C. D., Lehmkuhl, O., Torras, S., & Oliva, A. (2016). Thermo-mechanical parametric analysis of packed-bed thermocline energy storage tanks, *179*, 1106–1122. <https://doi.org/10.1016/j.apenergy.2016.06.124>
- Grirate, H., Agalit, H., Zari, N., Elmchaouri, A., Molina, S., & Couturier, R. (2016). Experimental and numerical investigation of potential filler materials for thermal oil thermocline storage. *Solar Energy*, *131*, 260–274. <https://doi.org/10.1016/j.solener.2016.02.035>
- Guillot, S., Faik, A., Rakhmatullin, A., Lambert, J., Veron, E., Echegut, P., ... Py, X. (2012). Corrosion effects between molten salts and thermal storage material for concentrated solar power plants. *Applied Energy*, *94*, 174–181. <https://doi.org/10.1016/j.apenergy.2011.12.057>
- Guo, Z., Sun, Z., Zhang, N., Ding, M., & Wen, J. (2017). Experimental characterization of pressure drop in slender packed bed ($1 < D/d < 3$). *Chemical Engineering Science*, *173*, 578–587. <https://doi.org/10.1016/j.ces.2017.08.022>
- Haller, M. Y., Cruickshank, C. A., Streicher, W., Harrison, S. J., Andersen, E., & Furbo, S. (2009). Methods to determine stratification efficiency of thermal energy storage processes - Review and theoretical comparison. *Solar Energy*, *83*(10), 1847–1860. <https://doi.org/10.1016/j.solener.2009.06.019>
- Hoffmann, J., Fasquelle, T., Goetz, V., & Py, X. (2016). A thermocline thermal

- energy storage system with filler materials for concentrated solar power plants : Experimental data and numerical model sensitivity to different experimental tank scales, *100*, 753–761. <https://doi.org/10.1016/j.applthermaleng.2016.01.110>
- Islam, R., Bhuiyan, A. B. M. N., & Ullah, M. W. (2017). An Overview of Concentrated Solar Power (CSP) Technologies and its Opportunities in Bangladesh. *ECCE 2017 - International Conference on Electrical, Computer and Communication Engineering*, (October 2019), 844–849. <https://doi.org/10.1109/ECACE.2017.7913020>
- Ismail, K. A. R., & Jr, R. S. (1999). A parametric study on possible fixed bed models for pcm and sensible heat storage, *19*.
- Johnson, E., Bates, L., Dower, A., Bueno, P. C., & Anderson, R. (2020). Thermal energy storage with supercritical carbon dioxide in a packed bed : Modeling charge-discharge cycles. *The Journal of Supercritical Fluids*, *137*(December 2017), 57–65. <https://doi.org/10.1016/j.supflu.2018.03.009>
- Kaguei, S., Shiozawa, B., & Wakao, N. (1976). Dispersion-concentric packed bed heat. *Chemical Engineering Science*, *32*(8), 507–513.
- Kalaiselvam, S., & R. Parameshwaran. (2014). Applications of Thermal Energy Storage Systems Introduction to thermal energy storage (TES) systems.
- Koller, M., Hofmann, R., & Walter, H. (2019). MILP model for a packed bed sensible thermal energy storage. *Computers and Chemical Engineering*, *125*, 40–53. <https://doi.org/10.1016/j.compchemeng.2019.03.007>
- Kuravi, S., Trahan, J., Goswami, D. Y., Rahman, M. M., & Stefanakos, E. K. (2013). Thermal energy storage technologies and systems for concentrating solar power plants. *Progress in Energy and Combustion Science*, *39*(4), 285–319. <https://doi.org/10.1016/j.pecs.2013.02.001>
- Kusch-Brandt. (2019). *Urban Renewable Energy on the Upswing: A Spotlight on Renewable Energy in Cities in REN21's "Renewables 2019 Global Status Report."* *Resources* (Vol. 8). <https://doi.org/10.3390/resources8030139>
- Laing, D., & Zunft, S. (2015). *Using concrete and other solid storage media in thermal energy storage (TES) systems. Advances in Thermal Energy*

-
- Storage Systems: Methods and Applications*. Woodhead Publishing Limited. <https://doi.org/10.1533/9781782420965.1.65>
- Languri, E. M., & Cunningham, G. (2019). Thermal Energy Storage Systems. *Lecture Notes in Energy*, 70, 169–176. https://doi.org/10.1007/978-3-030-05636-0_9
- Lew, J. T. Van, Li, P., & Stephens, J. (2011). Analysis of Heat Storage and Delivery of a Thermocline Tank, (May). <https://doi.org/10.1115/1.4003685>
- Li, L., & Ma, W. (2011). Experimental Study on the Effective Particle Diameter of a Packed Bed with Non-Spherical Particles. *Transport in Porous Media*, 89(1), 35–48. <https://doi.org/10.1007/s11242-011-9757-2>
- Li, P., Lew, J. Van, Chan, C., Karaki, W., Stephens, J., & Brien, J. E. O. (2012). Similarity and generalized analysis of efficiencies of thermal energy storage systems. *Renewable Energy*, 39(1), 388–402. <https://doi.org/10.1016/j.renene.2011.08.032>
- Li, S., Li, Y., Zhang, X., & Wen, C. (2013). Experimental study on the discharging performance of solar storage tanks with different inlet structures. *International Journal of Low-Carbon Technologies*, 8(3), 203–209. <https://doi.org/10.1093/ijlct/cts023>
- Li, X., Wu, S., Wang, Y., & Xie, L. (2018). Experimental investigation and thermodynamic modeling of an innovative molten salt for thermal energy storage (TES). *Applied Energy*, 212(July 2017), 516–526. <https://doi.org/10.1016/j.apenergy.2017.12.069>
- Liu, M., Steven Tay, N. H., Bell, S., Belusko, M., Jacob, R., Will, G., ... Bruno, F. (2016). Review on concentrating solar power plants and new developments in high temperature thermal energy storage technologies. *Renewable and Sustainable Energy Reviews*, 53, 1411–1432. <https://doi.org/10.1016/j.rser.2015.09.026>
- Lu, J., Yu, T., Ding, J., & Yuan, Y. (2015). Thermal storage performance of molten salt thermocline system with packed phase change bed. *Energy Conversion and Management*, 102, 267–274. <https://doi.org/10.1016/j.enconman.2014.10.049>

- Lugolole, R., Mawire, A., Okello, D., Lentswe, K. A., Nyeinga, K., & Shobo, A. B. (2019). Experimental analyses of sensible heat thermal energy storage systems during discharging. *Sustainable Energy Technologies and Assessments*, 35(February), 117–130. <https://doi.org/10.1016/j.seta.2019.06.007>
- Marcot, Q., & Kunwer, R. (2019). Numerical analysis of phase change material (PCM) for concentrated solar power (CSP) application. *International Journal of Ambient Energy*, 0(0), 1–9. <https://doi.org/10.1080/01430750.2019.1611633>
- Mayerhofer, M., Govaerts, J., Parmentier, N., Jeanmart, H., & Helsen, L. (2011). Experimental investigation of pressure drop in packed beds of irregular shaped wood particles. *Powder Technology*, 205(1–3), 30–35. <https://doi.org/10.1016/j.powtec.2010.08.006>
- Mctigue, J. D., Markides, C. N., & White, A. J. (2018). Performance response of packed-bed thermal storage to cycle duration perturbations. *Journal of Energy Storage*, 19(July), 379–392. <https://doi.org/10.1016/j.est.2018.08.016>
- Mctigue, J. D., & White, A. J. (2020). Segmented packed beds for improved thermal energy storage performance, 10(Oses 2015), 1498–1505. <https://doi.org/10.1049/iet-rpg.2016.0031>
- Media, P. (2019). Teach Second Law of Thermodynamics via Analysis.
- Mehari, A., Xu, Z. Y., & Wang, R. Z. (2020). Thermal energy storage using absorption cycle and system: A comprehensive review, 206(December 2019). <https://doi.org/10.1016/j.enconman.2020.112482>
- Mehta, D., & Hawley, M. C. (1969). Wall effect in packed columns. *Industrial and Engineering Chemistry Process Design and Development*, 8(2), 280–282. <https://doi.org/10.1021/i260030a021>
- Members, R. E. N. (2020). *Renewables 2020 global status report 2020*.
- Mira-hern, C., & Flueckiger, S. M. (2015). Comparative Analysis of Single- and Dual-Media Thermocline Tanks for Thermal Energy Storage in Concentrating Solar Power Plants, 137(June). <https://doi.org/10.1115/1.4029453>

- Modi, A., & Pérez-Segarra, C. D. (2014). Thermocline thermal storage systems for concentrated solar power plants: One-dimensional numerical model and comparative analysis. *Solar Energy*, *100*, 84–93. <https://doi.org/10.1016/j.solener.2013.11.033>
- Module Price Index – pv magazine International. (n.d.).
- Moser, M., Trieb, F., & Fichter, T. (2013). Potential of concentrating solar power plants for the combined production of water and electricity in MENA countries. *Journal of Sustainable Development of Energy, Water and Environment Systems*, *1*(2), 122–140. <https://doi.org/10.13044/j.sdewes.2013.01.0009>
- Mostafavi, S. S., Taylor, R. A., Nithyanandam, K., & Shafiei, A. (2017). Annual comparative performance and cost analysis of high temperature , sensible thermal energy storage systems integrated with a concentrated solar power plant. *Solar Energy*, *153*, 153–172. <https://doi.org/10.1016/j.solener.2017.05.044>
- Nandi, B. R., Bandyopadhyay, S., & Banerjee, R. (2018). Numerical modeling and analysis of dual medium thermocline thermal energy storage. *Journal of Energy Storage*, *16*, 218–230. <https://doi.org/10.1016/j.est.2018.01.020>
- Nations, U., Programme, D., & Nations, U. (1973). *Energy, the Environment and Human Health*. <https://doi.org/10.2105/ajph.64.12.1166-b>
- Niedermeier, K., Marocco, L., Flesch, J., Mohan, G., Coventry, J., & Wetzel, T. (2018). Performance of molten sodium vs. molten salts in a packed bed thermal energy storage. *Applied Thermal Engineering*, *141*, 368–377. <https://doi.org/10.1016/j.applthermaleng.2018.05.080>
- Nithyanandam, K., & Pitchumani, R. (2014). Cost and performance analysis of concentrating solar power systems with integrated latent thermal energy storage. *Energy*, *64*, 793–810. <https://doi.org/10.1016/j.energy.2013.10.095>
- Nunes, V. M. B., Queirós, C. S., Lourenço, M. J. V., Santos, F. J. V., & Nieto de Castro, C. A. (2016a). Molten salts as engineering fluids – A review: Part I. Molten alkali nitrates. *Applied Energy*, *183*, 603–611. <https://doi.org/10.1016/j.apenergy.2016.09.003>

- Nunes, V. M. B., Queirós, C. S., Lourenço, M. J. V., Santos, F. J. V., & Nieto de Castro, C. A. (2016b). Molten salts as engineering fluids – A review: Part I. Molten alkali nitrates. *Applied Energy*, *183*, 603–611. <https://doi.org/10.1016/j.apenergy.2016.09.003>
- O'Rourke, S., Kim, P., & Polavarapu, H. (2009). Solar photovoltaic industry: looking through the storm. *Global Markets Research*, (January 2009).
- Odenthal, C., Steinmann, W. D., & Zunft, S. (2020). Analysis of a horizontal flow closed loop thermal energy storage system in pilot scale for high temperature applications – Part II: Numerical investigation. *Applied Energy*, *263*(September 2019), 114576. <https://doi.org/10.1016/j.apenergy.2020.114576>
- Of, P. (2016). A ANALYSIS AND OPTIMISATION OF.
- Oró, E., Castell, A., Chiu, J., Martin, V., & Cabeza, L. F. (2013). Stratification analysis in packed bed thermal energy storage systems. *Applied Energy*, *109*, 476–487. <https://doi.org/10.1016/j.apenergy.2012.12.082>
- Ozahi, E., Gundogdu, M. Y., & Carpinlioglu, M. Ö. (2008). A modification on Ergun's correlation for use in cylindrical packed beds with non-spherical particles. *Advanced Powder Technology*, *19*(4), 369–381. <https://doi.org/10.1163/156855208X314985>
- Pacheco, J. E., Showalter, S. K., & Kolb, W. J. (2013). Development of a Molten-Salt Thermocline Thermal Storage System for Parabolic Trough, *124*(May 2002). <https://doi.org/10.1115/1.1464123>
- Palacios, A., Barreneche, C., Navarro, M. E., & Ding, Y. (2019). Thermal energy storage technologies for concentrated solar power – A review from a materials perspective. *Renewable Energy*. <https://doi.org/10.1016/j.renene.2019.10.127>
- Partopour, B., & Dixon, A. G. (2017). An integrated workflow for resolved-particle packed bed models with complex particle shapes. *Powder Technology*, *322*, 258–272. <https://doi.org/10.1016/j.powtec.2017.09.009>
- Peiró, G., Prieto, C., Gasia, J., Jové, A., Miró, L., & Cabeza, L. F. (2018). Two-tank molten salts thermal energy storage system for solar power plants at pilot plant scale: Lessons learnt and recommendations for its design, start-

- up and operation. *Renewable Energy*, 121, 236–248.
<https://doi.org/10.1016/j.renene.2018.01.026>
- Pelay, U., Luo, L., Fan, Y., Stitou, D., & Rood, M. (2017). Thermal energy storage systems for concentrated solar power plants. *Renewable and Sustainable Energy Reviews*, 79(March), 82–100.
<https://doi.org/10.1016/j.rser.2017.03.139>
- Pitz-Paal, R. (2020). Concentrating solar power. *Future Energy: Improved, Sustainable and Clean Options for Our Planet*, 413–430.
<https://doi.org/10.1016/B978-0-08-102886-5.00019-0>
- Pizzolato, A., Donato, F., Verda, V., Santarelli, M., & Sciacovelli, A. (2017). *CSP plants with thermocline thermal energy storage and integrated steam generator – Techno-economic modeling and design optimization*. *Energy* (Vol. 139). Elsevier B.V. <https://doi.org/10.1016/j.energy.2017.07.160>
- Power, C. S. (n.d.). <Csp_Roadmap.Pdf>.
- Prieto, C., Gasia, J., Cabeza, L. F., Prieto, C., Gasia, J., & Cabeza, F. (2018). Accepted Manuscript. <https://doi.org/10.1016/j.renene.2018.01.026>
- Purohit, I., Purohit, P., & Shekhar, S. (2013). Evaluating the potential of concentrating solar power generation in Northwestern India. *Energy Policy*, 62(August), 157–175. <https://doi.org/10.1016/j.enpol.2013.06.069>
- Ravi, C., Rao, C., Niyas, H., & Muthukumar, P. (2017). Performance Tests on Lab–scale Sensible Heat Storage Prototypes. *Applied Thermal Engineering*. <https://doi.org/10.1016/j.applthermaleng.2017.10.085>
- Reddy, K. S., Jawahar, V., Sivakumar, S., & Mallick, T. K. (2017). Performance investigation of single-tank thermocline storage systems for CSP plants. *Solar Energy*, 144, 740–749.
<https://doi.org/10.1016/j.solener.2017.02.012>
- Rong, L. W., Zhou, Z. Y., & Yu, A. B. (2015). Lattice-Boltzmann simulation of fluid flow through packed beds of uniform ellipsoids. *Powder Technology*, 285, 146–156. <https://doi.org/10.1016/j.powtec.2015.06.047>
- Santos, J. J. C. S., Palacio, J. C. E., Reyes, A. M. M., Carvalho, M., Freire, A. J. R., & Barone, M. A. (2018). Concentrating Solar Power. *Advances in Renewable Energies and Power Technologies*, 1(2), 373–402.

- <https://doi.org/10.1016/B978-0-12-812959-3.00012-5>
- Sarbu, I. (2018). A Comprehensive Review of Thermal Energy Storage. <https://doi.org/10.3390/su10010191>
- Schumann, T. E. W. (1929). Heat transfer: A liquid flowing through a porous prism. *Journal of the Franklin Institute*, 208(3), 405–416. [https://doi.org/10.1016/S0016-0032\(29\)91186-8](https://doi.org/10.1016/S0016-0032(29)91186-8)
- Shouman, E. R., & Khattab, N. M. (2015). Future economic of concentrating solar power (CSP) for electricity generation in Egypt. *Renewable and Sustainable Energy Reviews*, 41, 1119–1127. <https://doi.org/10.1016/j.rser.2014.08.067>
- Singh, H., Saini, R. P., & Saini, J. S. (2010). A review on packed bed solar energy storage systems. *Renewable and Sustainable Energy Reviews*, 14(3), 1059–1069. <https://doi.org/10.1016/j.rser.2009.10.022>
- Solar Heating & Cooling | SEIA. (n.d.).
- States, U., States, U., & Southwest, T. (2001). Power : Energy from Mirrors.
- States, U., Storage, T. E., Tes, T., & Fluid, H. T. (2011). 3 [13]., 32(4), 269–270. <https://doi.org/10.1007/s11669-011-9904-z>
- Stekli, J., Irwin, L., & Pitchumani, R. (2013). Technical Challenges and Opportunities for Concentrating Solar Power With Thermal Energy Storage. *Journal of Thermal Science and Engineering Applications*, 5(2), 021011. <https://doi.org/10.1115/1.4024143>
- Stephanie Weckend, Andreas Wade, & Garvin Heath. (2016). *End of Life Management Solar PV Panels*.
- Thabet, A., & Straatman, A. G. (2018). The development and numerical modelling of a Representative Elemental Volume for packed sand. *Chemical Engineering Science*, 187, 117–126. <https://doi.org/10.1016/j.ces.2018.04.054>
- Thermal Energy Storage - Overview and basic principles. (n.d.).
- Tian, Y., & Zhao, C. Y. (2013). A review of solar collectors and thermal energy storage in solar thermal applications. *Applied Energy*, 104, 538–553. <https://doi.org/10.1016/j.apenergy.2012.11.051>
- Torras, S., Pérez-Segarra, C. D., Rodríguez, I., Rigola, J., & Oliva, A. (2015).

- Parametric Study of Two-tank TES Systems for CSP Plants. *Energy Procedia*, 69, 1049–1058. <https://doi.org/10.1016/j.egypro.2015.03.206>
- Ushak, S., Fernández, A. G., & Grageda, M. (2015). *Using molten salts and other liquid sensible storage media in thermal energy storage (TES) systems. Advances in Thermal Energy Storage Systems: Methods and Applications.* Woodhead Publishing Limited. <https://doi.org/10.1533/9781782420965.1.49>
- Vigneshwaran, K., Sodhi, G. S., Muthukumar, P., Guha, A., & Senthilmurugan, S. (2019). Experimental and numerical investigations on high temperature cast steel based sensible heat storage system. *Applied Energy*, 251(December 2018), 113322. <https://doi.org/10.1016/j.apenergy.2019.113322>
- Wang, L., Yang, Z., & Duan, Y. (2015). Influence of flow distribution on the thermal performance of dual-media thermocline energy storage systems. *Applied Energy*, 142, 283–292. <https://doi.org/10.1016/j.apenergy.2014.12.024>
- Wang, Q. W., Luo, L. Q., Chen, Q. Y., & Zeng, M. (2015). An Experimental Study of Shell-and-Tube Heat Exchangers, 129(October 2007), 1425–1431. <https://doi.org/10.1115/1.2754878>
- Wang, Z. (2019). Chapter 6 - Thermal Storage Systems. *Design of Solar Thermal Power Plants*, (1), 387–415. <https://doi.org/10.1201/9781315137025-12>
- Webb, R. L. (1994). *Principles of enhanced heat transfer.* [https://doi.org/10.1016/0301-9322\(95\)90005-5](https://doi.org/10.1016/0301-9322(95)90005-5)
- Wu, M., Li, M., Xu, C., He, Y., & Tao, W. (2014). The impact of concrete structure on the thermal performance of the dual-media thermocline thermal storage tank using concrete as the solid medium. *Applied Energy*, 113, 1363–1371. <https://doi.org/10.1016/j.apenergy.2013.08.044>
- Xu, B., Li, P., & Chan, C. (2015). Application of phase change materials for thermal energy storage in concentrated solar thermal power plants: A review to recent developments. *Applied Energy*, 160, 286–307. <https://doi.org/10.1016/j.apenergy.2015.09.016>

- Xu, C., Wang, Z., He, Y., Li, X., & Bai, F. (2012). Sensitivity analysis of the numerical study on the thermal performance of a packed-bed molten salt thermocline thermal storage system. *Applied Energy*, 92, 65–75. <https://doi.org/10.1016/j.apenergy.2011.11.002>
- Yang, X., & Cai, Z. (2019). An analysis of a packed bed thermal energy storage system using sensible heat and phase change materials. *International Journal of Heat and Mass Transfer*, 144, 118651. <https://doi.org/10.1016/j.ijheatmasstransfer.2019.118651>
- Yildiz, L. (2018). *Fossil Fuels. Comprehensive Energy Systems* (Vol. 1–5). <https://doi.org/10.1016/B978-0-12-809597-3.00111-5>
- Zanganeh, G., Pedretti, A., Zavattoni, S., Barbato, M., & Steinfeld, A. (2012). Packed-bed thermal storage for concentrated solar power – Pilot-scale demonstration and industrial-scale design. *Solar Energy*, 86(10), 3084–3098. <https://doi.org/10.1016/j.solener.2012.07.019>
- Zaversky, F., García-Barberena, J., Sánchez, M., & Astrain, D. (2013). Transient molten salt two-tank thermal storage modeling for CSP performance simulations. *Solar Energy*, 93, 294–311. <https://doi.org/10.1016/j.solener.2013.02.034>
- Zhang, H. L., Baeyens, J., Degreè, J., & Cacères, G. (2013). Concentrated solar power plants: Review and design methodology. *Renewable and Sustainable Energy Reviews*, 22, 466–481. <https://doi.org/10.1016/j.rser.2013.01.032>
- Zhao, B., Cheng, M., Liu, C., & Dai, Z. (2017). An efficient tank size estimation strategy for packed-bed thermocline thermal energy storage systems for concentrated solar power. *Solar Energy*, 153, 104–114. <https://doi.org/10.1016/j.solener.2017.05.057>
- Zheng, X., Shi, R., Wang, Y., You, S., Zhang, H., Xia, J., & Wei, S. (2019). Mathematical modeling and performance analysis of an integrated solar heating and cooling system driven by parabolic trough collector and double-effect absorption chiller. *Energy and Buildings*, 202, 109400. <https://doi.org/10.1016/j.enbuild.2019.109400>
- Zhu, Y., Yuan, Y., Zhang, C., Xie, M., & Tan, H. (2019). Numerical study on

heat transfer enhancement of thermal energy storage systems considering radiation of molten salt. *Solar Energy*, 183(December 2018), 337–344. <https://doi.org/10.1016/j.solener.2019.03.044>

Ram Kunwer

B.Tech. Mechanical Engineering
M.Tech Industrial Tribology
PhD Mechanical Engineering (Pursuing)

Areas of Interest: Solar Thermal, Heat Exchanger, Heat Transfer
Phone: 7817808881

Email: ramkunwer085@gmail.com, rkunwer@ddn.upes.ac.in

Current Affiliation

Assistant Professor (selection Grade)
Mechanical Engineering, SOE
University of petroleum and Energy Studies
Dehradun, Uttarakhand



Academic Record

Course	School/College	Year of Passing	Division	Marks (%)
PhD (Pursuing)	University of Petroleum and Energy Studies, Dehradun	2016-pursuing	First class (Course work)	72
M.Tech (Industrial Tribology)	Indian Institute of Technology, Delhi	2012	First Class	84.29
B.Tech(Mechanical Engineering)	Krishna Institute of Engineering and Technology	2010	First class	66.00

Publications from PhD

Kunwer, R., Pandey, S., & Bhurat, S. S. (2020). Comparison of selected shell and tube heat exchangers with segmental and helical baffles. *Thermal Science and Engineering Progress*, 100712. <https://doi.org/10.1016/j.tsep.2020.100712>

Kunwer, R., & Pandey, S. (2021). Analysis and optimization of packed bed thermocline energy storage tank for CSP power plant. *International Journal of Ambient Energy*, (just-accepted), 1–25.

Kunwer, R., Pandey, S., & Pandey, G. (2021). Characteristic analysis of thermal energy storage system using synthetic oil as a heat transfer fluid: techno-economic modeling and LAB scale demonstration. *Energy Sources, Part A: Recovery, Utilization, and Environmental Effects*, 1–17.

Publications and Patent

Marcot, Q., & Kunwer, R. (2019). Numerical analysis of phase change material (PCM) for concentrated solar power (CSP) application.

International Journal of Ambient Energy.
<https://doi.org/10.1080/01430750.2019.1611633>

- Jaunet, P., Kunwer, R., & Raghav, G. (2019). Numerical analysis of thermal energy storage system using packed-bed. *Energy Sources, Part A: Recovery, Utilization and Environmental Effects*.
<https://doi.org/10.1080/15567036.2019.1652372>
- Shukla, P., Kunwer, R., & Bhurat, S. S. (2018). Design Optimization of an Automotive Fuel Tank for the Minimization of Evaporative Losses of Gasoline Due to Thermal Conduction: Experimental & Analytical Approach. *Chemical Engineering Transactions*, 71, 1393–1398.
- Kunwer, R., Shukla, P., & Bhurat, S. S. (2018). Noise and Acoustic Emission Monitoring of Gear. *International Journal of Applied Engineering Research*, 13(6), 7–12.
- Bhurat, S. S., & Kunwer, R. (2018). Magnetization of Diesel fuel for Compression Ignition Engine to Enhance Efficiency and Emissions, 13(6), 341–347.
- Kunwer, R., Pandey, S., & Bhurat, S. S. (2020). Comparison of selected shell and tube heat exchangers with segmental and helical baffles. *Thermal Science and Engineering Progress*, 100712.
<https://doi.org/10.1016/j.tsep.2020.100712>
- Kunwer, R., & Pandey, S. (2021). Analysis and optimization of packed bed thermocline energy storage tank for CSP power plant. *International Journal of Ambient Energy*, (just-accepted), 1–25.
- Kunwer, R., Pandey, S., & Pandey, G. (2021). Characteristic analysis of thermal energy storage system using synthetic oil as a heat transfer fluid: techno-economic modeling and LAB scale demonstration. *Energy Sources, Part A: Recovery, Utilization, and Environmental Effects*, 1–17.
- Kunwer, R., & Bhurat, S. S. (2021). Thermal characterization of phase change materials (PCM) for heating applications. *Materials Today: Proceedings*.
- Bhurat, S., Pandey, S., Chintala, V., Sharma, S., & Kunwer, R. (2021). Influence of Compression Ratio and Exhaust Gas Recirculation on Light-Duty Diesel Engine. *Current Advances in Mechanical Engineering: Select Proceedings of ICRAMERD 2020*, 493.
- Pandey, S., Bhurat, S. S., & Kunwer, R. (2021). Investigation of fumigation of ethanol and exhaust gas recirculation on combustion and emission characteristics of partially premixed charge compression-ignition engine.

Energy Sources, Part A: Recovery, Utilization, and Environmental Effects, 1–15.

Patent: Electric Power Loader for moving payloads, Mansas Jaiswal, Abhinav Dhaka, Swapnil Bhurat, Dr. Ajay Kumar, **Ram Kunwer**, University of petroleum and Energy Studies, Patent No. 202011009945, Published (2020)

Professional Experience

Current Teaching at engineering level as Senior Scale Assistant Professor in Mechanical Department of UPES, Dehradun (March 2016 to Till date)

Past • Three and half years of experience in Teaching at engineering level at Lovely Professional university, Jalandhar (From August 2012 to March 2016

Personal Details

Name Ram Kunwer

Sex Male

Nationality Indian

Marital Married

Status

Address 185, Silver Height Residency, Jalvayu Vihar, Pondha Premnagar
248007

I do hereby declare that above particulars of information and facts stated are true, correct and complete to the best of my knowledge and belief.

Ram Kunwer

Thesis

ORIGINALITY REPORT

9%

SIMILARITY INDEX

7%

INTERNET SOURCES

5%

PUBLICATIONS

3%

STUDENT PAPERS

PRIMARY SOURCES

1

Submitted to University of Petroleum and Energy Studies

Student Paper

1%

2

eprints.nottingham.ac.uk

Internet Source

<1%

3

J.A. Almendros-Ibáñez, M. Fernández-Torrijos, M. Díaz-Heras, J.F. Belmonte, C. Sobrino. "A review of solar thermal energy storage in beds of particles: Packed and fluidized beds", Solar Energy, 2019

Publication

<1%

4

Wolf-Dieter Steinmann. "Thermal Energy Storage for Medium and High Temperatures", Springer Science and Business Media LLC, 2022

Publication

<1%

5

S. Saeed Mostafavi Tehrani, Robert A. Taylor, Karthik Nithyanandam, Ardalan Shafiei Ghazani. "Annual comparative performance and cost analysis of high temperature, sensible thermal energy storage systems

<1%